

CELL BIOLOGICAL AND FUNCTIONAL ANALYSIS OF A
MUTATION IN THE K_{ATP} CHANNEL THAT CAUSES
FAMILIAL HYPERINSULINISM

by

Etienne Cartier

A DISSERTATION

Presented to the Neurosciences Program
and the Oregon Health and Sciences University
School of Medicine
in partial fulfillment of
the requirements for the degree of
Doctor of Philosophy
May 2004

School of Medicine
Oregon Health Sciences University

CERTIFICATE OF APPROVAL

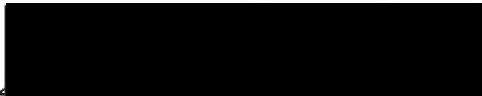
This is certify that the Ph.D. thesis titled:

"Cell Biological and Functional Analysis of a Mutation
in the KATP Channel that causes Familial Hyperinsulinism"

by

Etienne Cartier

has been approved



Professor in charge of thesis



Member



Member



Member

TABLE OF CONTENTS

Acknowledgments	iii
Abstract	iv
Introduction	1
Chapter 1	51
Abstract	52
Introduction	53
Material and Methods	55
Results	57
Discussion	67
Chapter 2	71
Abstract	72
Introduction	73
Experimental Procedures	76
Results	79
Discussion	88
Chapter 3	101
Abstract	102
Introduction	103
Experimental Procedures	106
Results	109
Discussion	134
Summary and Conclusions	141
Appendix	149
References	155

LIST OF FIGURES and TABLES

Figure 1	3
Figure 2	4
Figure 3	8
Figure 4	14
Figure 5	22
Figure 6	23
Figure 7	25
Table I	26
Table II	28
Figure 8	36
Figure 9	59
Figure 10	61
Figure 11	65
Figure 12	66
Figure 13	80
Figure 14	82
Figure 15	84
Figure 16	89
Figure 17	91
Figure 18	92
Figure 19	94
Figure 20AB	111-112
Figure 21AB	115-116
Figure 21C	118
Figure 22	119
Figure 23AB	122-123
Figure 24ABC	126-127
Figure 25AB	130
Figure 25C	132
Figure 26	133
Figure 27	150

Acknowledgments

First of all, I have to acknowledge my advisor Show-Ling that has taught me how to think in a focused and systematic way. She has showed me how to become an independent scientist and I will be always thankful for that. I really admire her capacity to do multiple unrelated tasks and excelling in all of them. She has a brilliant intelligence and she is extremely hard worker. I am very much proud to have been her first graduate student.

I also want to acknowledge all the people in my lab, Satoko, Yu-Wen, Fei-Fei, and Chia-Wei. All of them, hard workers and wonderful persons. Fei-Fei helped me doing a significant number of experiments in Chapter 3 without hesitation.

Erin Jobst edited drafts of this dissertation without asking anything in return. Thanks Erin!

Finally, I have to recognize my sister Nicole that has been always a huge emotional support from far, far away. Also, I have to acknowledge my friend Gonzalo-‘Chupacabras’ Torres and his beautiful family. A family that has become also mine.

ABSTRACT

The pancreatic ATP-sensitive potassium (K_{ATP}) channel regulates insulin secretion by linking metabolic changes to the β -cell membrane potential. K_{ATP} channels are oligomeric complexes composed by the sulfonylurea receptor 1 (SUR1) and the inward rectifier Kir6.2. K_{ATP} channel biogenesis is delineated by a number of ER quality control mechanisms. Among those, a tripeptide RKR retention signal present in both subunits produces retention of unassembled subunits. Loss of functional K_{ATP} channels because of mutations in either the SUR1 or Kir6.2 channel subunit causes persistent hyperinsulinemic hypoglycemia of infancy (HI). We investigated the molecular mechanism by which a single phenylalanine deletion in SUR1 (Δ F1388) causes HI. Previous studies have shown that co-expression of Δ F1388 SUR1 with Kir6.2 results in no channel activity. We demonstrated here that the lack of functional expression is due to failure of the mutant channel to traffic to the cell surface. Inactivation of the RKR retention signal in Δ F1388 and its co-expression with Kir6.2, produces partial surface expression of the mutant channel. Moreover, mutant channels were active. Nevertheless, compared with wild-type channels, the mutant channels have reduced ATP sensitivity and do not respond to stimulation by MgADP or diazoxide. Therefore, SUR1 Δ F1388 leads to defects in both trafficking and MgADP response of K_{ATP} channels. Subsequently, we investigated the biochemical features of Phe-1388 that control the proper trafficking and function of K_{ATP} channels by substituting the residue with all other 19 amino acids. We found that while surface expression is largely dependent on hydrophobicity, channel response to MgADP is governed by multiple factors and involves the detailed architecture of the amino acid side chain. Remarkably, replacing Phe-1388 by leucine profoundly

alters the physiological and pharmacological properties of the channel. The F1388L-SUR1 channel has increased sensitivity to MgADP and metabolic inhibition, decreased sensitivity to glibenclamide, and responds to both diazoxide and pinacidil. Thus, structural features in SUR1 required for proper channel function are distinct from those required for correct protein trafficking. The mutant Δ F1388 is rapidly degraded in the ER showing monophasic kinetics. Moreover, wild-type K_{ATP} channel subunits are also degraded in the ER but featuring biphasic kinetics. K_{ATP} channel biogenesis appears to be inefficient: ~70% of the channel subunits are rapidly degraded by this ER mechanism, and only ~30% acquires metabolic stability and can be incorporated into channel complexes which eventually reach the plasma membrane. By contrast, inhibition of proteasome function slows down the turnover of all wild-type and mutant subunits and leads to their accumulation as deglycosylated and/or polyubiquitinated species. Under this condition, the undegraded K_{ATP} channel subunits are found in perinuclear inclusions that can be co-immunostained with aggresome markers such as ubiquitin and vimentin. These results suggest that the ubiquitin-proteasome pathway is involved in the degradation of K_{ATP} channels under both normal and pathological conditions.

INTRODUCTION

Introduction

ATP-sensitive potassium (K_{ATP}) channels were first discovered in cardiac myocytes and were later found in many other tissues, including pancreatic β -cells [1, 2], skeletal muscle, smooth muscle, brain, pituitary and kidney. By linking the cell metabolic state to the plasma membrane potential, K_{ATP} channels regulate a variety of cellular functions. Activation of K_{ATP} channels leads to shortening of the cardiac action potential, relaxation of vascular smooth muscle, and inhibition of both insulin and neurotransmitter release. They also play a role in K^+ recycling in renal epithelia, seizure protection, and cytoprotection in cardiac and brain ischemia. K_{ATP} channels are essentially voltage independent, but intracellular nucleotides, particularly ATP (which inhibits channel activity) and Mg^{2+} ADP (which stimulates channel activity) modulate them. Overall, K_{ATP} channel activity is regulated by the $[ATP]/[ADP]$ ratio (the cell metabolic state), which provides a mean of linking electrical activity of a cell to its metabolic rate [3-7].

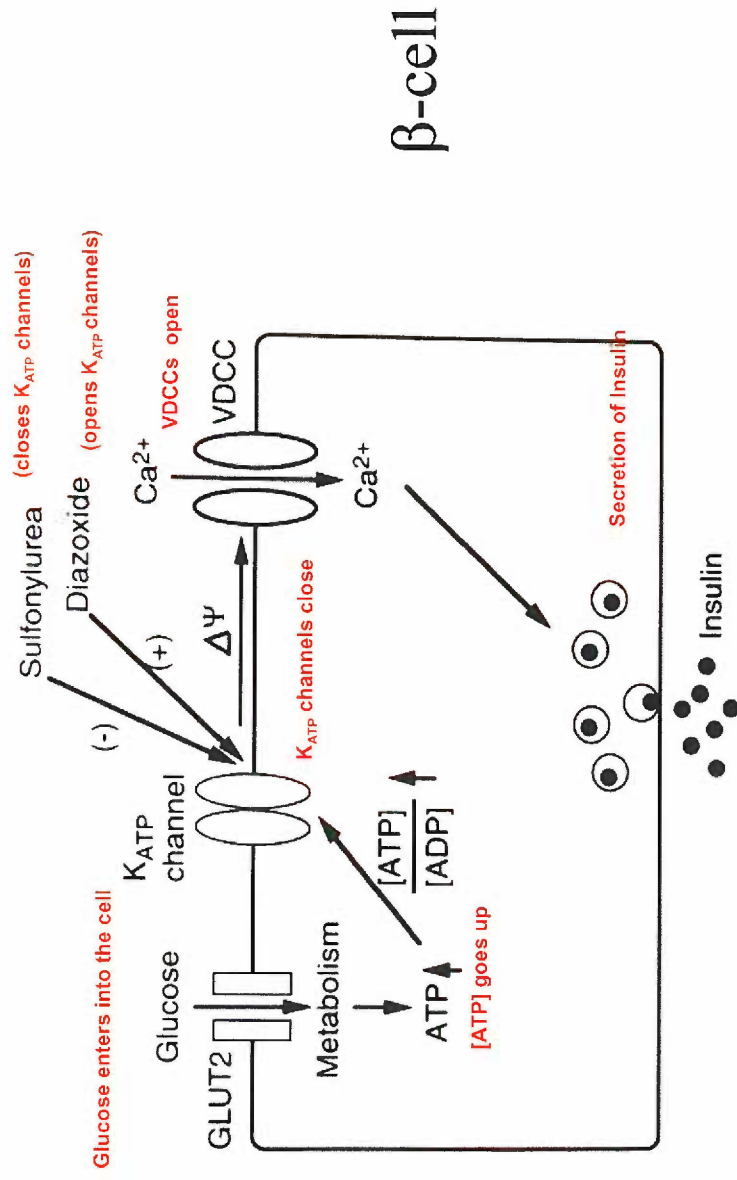
The functional roles of K_{ATP} channels have been best-characterized in pancreatic β -cells [2-7]. Since the discovery of the K_{ATP} channels in pancreatic β -cells, the model of glucose-induced insulin secretion has generally been accepted. Glucose is transported through the glucose transporter GLUT2, and the subsequent metabolism of glucose produces ATP. The increase in the ATP/ADP ratio closes the K_{ATP} channels, which depolarizes the β -cell membrane and leads to the opening of the voltage-dependent calcium channels (VDCC), allowing calcium influx. The rise in intracellular calcium concentration in the β -cell triggers insulin granule exocytosis [7]. Therefore, the K_{ATP} channels are key molecules in the regulation of glucose-induced insulin secretion. Accordingly, pharmacological agents that modulate the activity of K_{ATP} channels are

effective in treating certain insulin secretion disorders. For example, sulfonylureas, a class of drugs commonly used in the treatment of non-insulin-dependent diabetes mellitus (NIDDM), induce insulin release by inhibiting K_{ATP} channels. In contrast, potassium channel openers (KCOs), inhibit insulin secretion by activating K_{ATP} channels (Figure 1).

Human mutations of pancreatic K_{ATP} channels that lead to loss of channel function are linked to a pathological condition known as Persistent Hyperinsulinemic Hypoglycemia of Infancy (HI). HI is an inherited disorder of glucose metabolism evident in newborns and infants. It is mainly characterized by inappropriately high insulin levels in the presence of low levels of blood glucose, and it is the most common cause of persistent and recurrent hypoglycemia in infancy [3-7].

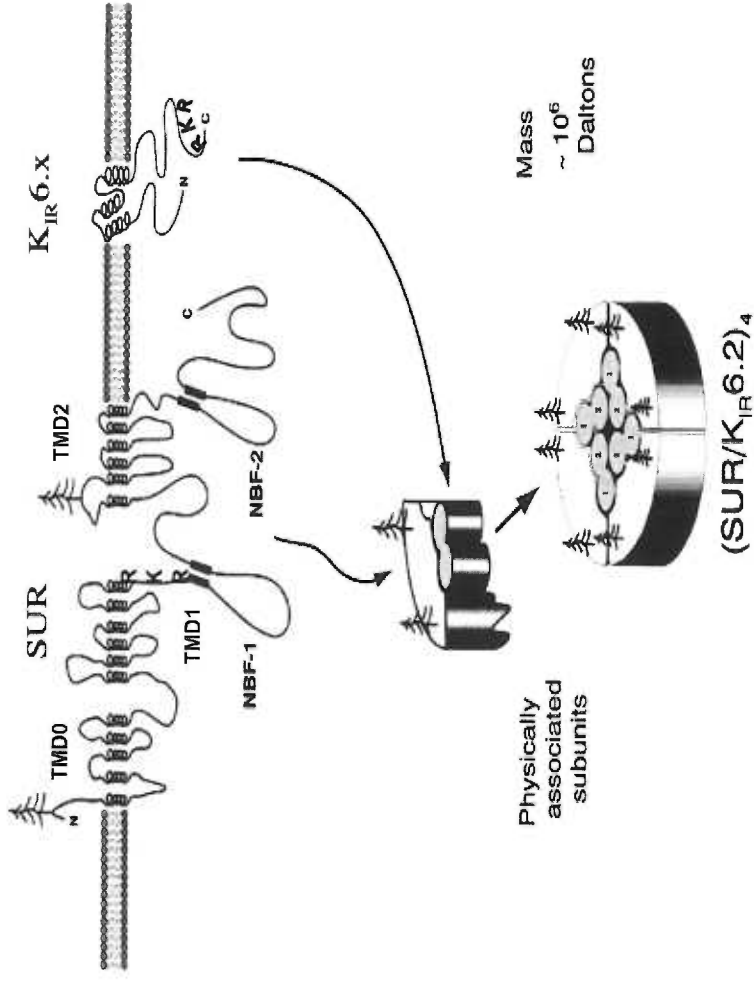
The K_{ATP} channel is an octameric complex of two distinct types of protein subunits (Figure 2). The pore is formed from four Kir6 subunits, each of which is associated with a much larger regulatory sulfonylurea receptor (SUR) subunit. Kir6 belongs to the inward-rectifying K^+ channel family and each Kir6 subunit has two transmembrane domains connected by a pore loop. In contrast, SUR is a member of the ATP-binding cassette (ABC) transporter super-family. Each SUR subunit has multiple transmembrane domains and two large intracellular loops that contain consensus sequences for nucleotide binding and hydrolysis, known as the (two) nucleotide binding folds (NBFs). Both NBFs are capable of binding and hydrolyzing $Mg^{2+}ATP$, but NBF2 seems to have a significantly higher $Mg^{2+}ATP$ hydrolytic activity. This SUR enzymatic behavior is essential in the gating regulation of K_{ATP} channels because it links the control of the membrane potential with metabolic sensors through phosphotransfer reactions [3-7].

Glucose-induced insulin secretion via K_{ATP} channels



A model for glucose-induced insulin secretion via the K_{ATP} channels in pancreatic β -cells. The K_{ATP} channels are thought to be ATP and ADP sensors that couple glucose metabolism to electrical activity, to stimulate insulin secretion. Sulfonylureas such as tolbutamide and glibenclamide stimulate insulin secretion by inhibiting the K_{ATP} channels, and diazoxide inhibits insulin secretion by activating the channels. GLUT2: glucose transporter 2, VDCC: voltage-dependent calcium channel (modified from Seino S. Ann. Review of Physiol (1999) Vol. 61, pp. 337-362).

K_{ATP} channel subunits and assembly



K_{ATP} channel subunits and assembly. The sulfonylurea receptor (SUR) assembles with the inward rectifier Kir6. SUR has 17 transmembrane segments grouped in three domains: TMD0, TMD1 and TMD2. It has two glycosylation sites. The Nucleotide Binding Folds (NBF's) face the intracellular side and are known as NBF1 and NBF2. The RKR retention signal is shown on both subunits. The Kir6 subunit has two transmembrane domains, a pore loop, and a N- and C-terminus facing the intracellular side. Both subunits oligomerize in octamers forming K_{ATP} channels. The SUR subunit has the binding sites for sulfonylureas, KCOs, and Mg²⁺-nucleotides. The Kir6 subunit possesses the binding sites for ATP and PIP2 (Modified from Bryan J and Aguilar-Bryan L. Biochim Biophys Acta. 1999 Dec 6;1461(2):285-303).

FIGURE 2

K_{ATP} channels in different tissues are composed of different Kir and SUR subunits. In most cases, Kir6.2 acts as the pore-forming subunit, but in some smooth muscles it is likely that Kir6.1 serves this role [8]. Two different genes encoding SUR1 [9] and SUR2 [10] have been identified and alternative splicing of SUR2 mRNA creates further diversity. One important splice site in SUR2 lies distal to NBF2 and alters the 42 amino acids at the C-terminus. These splice variants are known as SUR2A [10] and SUR2B [11], and the alternatively spliced region in SUR2B is actually more similar to SUR1 (74 % identity) than to SUR2A (33% identity). There is evidence that SUR1 serves as the regulatory subunit of the K_{ATP} channel in pancreatic β -cells and some type of neurons. SUR2A plays a similar role in cardiac and skeletal muscle, whereas SUR2B serves this function in smooth muscle and some neurons [3-7].

K_{ATP} channels reach the plasma membrane as octamers. This is due to the presence of an endoplasmic reticulum (ER) Arginine-Lysine-Arginine retention motif (RKR) on each subunit that prevents their surface expression in the absence of proper assembly. This ensures that only fully functional octameric complexes reach the plasma membrane in all tissues in which they are expressed [12].

Molecular Structure and Assembly of K_{ATP} channels

The inwardly-rectifying potassium channel subfamily Kir6.

Since the isolation by expression cloning of the Kir channel family members, ROMK1 (Kir 1.1a), IRK (Kir2.1), and GIRK (Kir3.1), seven subfamilies (Kir1.0-7.0) have been identified, based on their degree of identity [13] [14]. Inward rectification refers to the ability of an ion channel to allow greater influx than efflux of ions. In the

case of Kir channels, inward rectification is caused by cytoplasmic ions such as polyamines and Mg^{+2} , which plug the conduction pathway on depolarization thereby impeding the outward flow of K^+ . Different subfamilies show different rectification strengths; for example, Kir3 channels are strongly rectifying, whereas Kir6 are weakly rectifying [14].

Using a Kir3.1 cDNA probe, the first Kir6 to be cloned was Kir6.1 [8]. This channel is a 424-amino acid protein that is ubiquitously expressed. An isoform of Kir6.1 was subsequently cloned, which was identified as Kir6.2. It is composed of 390 amino acids, sharing 71% identity with Kir6.1. Kir6.2 is strongly, but not exclusively, expressed in insulin-secreting cell lines. The identification of Kir6.2, along with SUR1, allowed reconstitution of K_{ATP} channel currents for the first time [15].

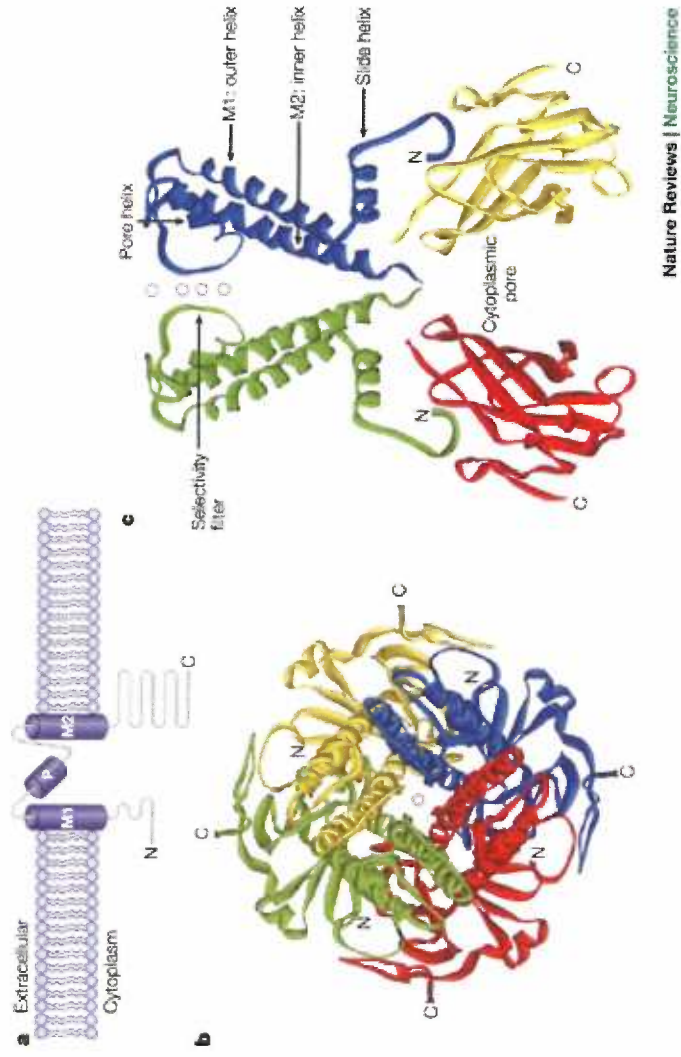
Kir channels are tetramers, with each subunit having two transmembrane (TM) segments called M1 and M2, a pore loop (P), and amino (N-) and carboxy (C-) terminal cytoplasmic domains. Recently, high-resolution structures of two Kir channels have been reported: (1) the closed conformation of KirBac1.1, a bacterial ion channel closely related to eukaryotic Kir channels [16], and (2) the cytoplasmic domain of the mammalian Kir3.1 channel [17].

Architecture. The overall architecture of Kir channels can be simply divided between membrane and cytoplasmic domains. In the KirBac [16] and KcsA structures [18], the outer (M1) and inner (M2) helices compose the transmembrane domains that are connected by the pore loop. M2 lines the pore of the channel and makes contact with M1. The four M2 helices together form an ‘inverted teepee’ in a closed channel

conformation. The pore loop contains the descending *pore helix* and the ascending K⁺ channel *signature* sequence (TXGYG or TXGFG) that forms the K⁺ selectivity filter. The KirBac structure includes an additional helix, the '*slide helix*', which runs parallel to the cytoplasmic face of the membrane (Figure 3) [14, 16]. Besides the M1 and M2 transmembrane domains, there is a large cytoplasmic domain, constituting two-thirds of the Kir channel amino acid sequence. This region of the channel is crucial for Kir6 channel modulation by its specific intracellular regulators, such as ATP, PIP₂, and perhaps the SUR subunit as well. The cytoplasmic domain seems to be composed of several β -sheets, with some of them forming a wall containing many polar and charged residues that surround a large pore ~ 32 Å in length and 7-15 Å in diameter. At the C-terminal end of the structure, an α -helix projects into the cytoplasm [14, 16, 17]. Interestingly, the N- and C- termini interact through two parallel β -strands. Based on the crystallized cytoplasmic domain structure, it has been proposed that the ATP and PIP₂ binding sites in Kir6.2 localize on the external surface of its cytoplasmic domain. These ATP and PIP₂ 'patches' may reside very close to each other overlapping some critical residues for binding of both ligands [19].

Ion selectivity, permeation and gating. The selectivity filter confers selectivity for K⁺. In all K⁺ channel crystal structures resolved so far, the selectivity filter is formed by mainchain carbonyl oxygens of the P-loop conserved K⁺ channel signature sequence (residues TXGFG for Kir6)[20]. In most Kir channels, a salt-bridge between conserved charged residues in adjacent subunits has been proposed to anchor and stabilize the K⁺ channel signature sequence [21].

Kir structure



Nature Reviews | Neuroscience

a | Schematic drawing of a Kir channel subunit. Each subunit comprises two transmembrane helices (M1 and M2), a pore-forming region containing the pore-helix (P), and a cytoplasmic domain formed by the amino (N) and carboxy (C) termini. **b** | View of the tetrameric structure of the KirBac1.1 channel from the extracellular side. Monomers are individually coloured red, green, yellow and blue. A K⁺ ion (white) indicates the conduction pathway. **c** | Side view of the KirBac1.1 structure showing the transmembrane domain of two subunits (green and blue) and the C-terminal domains of their neighbouring subunits (red and yellow). White spheres represent K⁺ ions in the selectivity filter. (Modified from Bichet D, Haass F and Jan LY. *Nature Reviews Neuroscience* 4, 957-967 (2003))

Although Kir6 channels are rectifiers, their rectification properties are weak, a property that is correlated with the affinity of the channel for blocking cations (i.e. cytoplasmic Mg^{2+} ions and polyamines). In strong rectifier channels, such as Kir2 and Kir3, the residues responsible for interacting with blocking cations are localized along the M2 helix as well as the cytoplasmic domains. Despite such differences, Kir6 shares a common molecular mechanism with other Kir channels to control ion flow ('or gating'). Two locations for the intrinsic gate have been proposed: the bundle crossing and the selectivity filter.

The gate at the bundle crossing is composed by of M2 transmembrane helices crossing each other at a point that is close to the intracellular surface of the membrane. This bundle crossing seems to be narrow enough to restrict the passage of hydrated K^+ ions. In addition, hydrophobic residues that line the pore in this region create an unfavorable environment for K^+ ions. Evidence also indicates that the M2 helices may move to open the channel. These movements may include M2 rotation and tilting relative to the central axis of the channel as well as M2 bending movements. These actions would determine bundle crossing widening during channel opening. The selectivity filter and the outer pore of Kir channels may also undergo conformational changes during gating.

Single channel recordings have demonstrated that SUR1/Kir6.2 channels, as well as other Kir channels, display a characteristic 'bursting' pattern in which the channel rapidly 'flickers' between open and closed states. Evidence indicates that these short open and closed states, termed intra-burst, may correspond to stochastic movements at the Kir6.2 selectivity filter, known as fast gating. Silent interburst intervals define the duration of the burst. The transition between a burst and an interburst state seems to be

mediated by the bundle crossing of Kir6.2, due to movements of its transmembrane helices. The rate of this transition may be mediated by SUR, in a process known as slow gating. The importance of SUR1 regulating these transitions is reflected by the fact that the open probability of Kir6.2 (truncated) is ~0.15 in the absence of SUR whereas the open probability increases to ~0.65 with the expression of SUR1.

The sulfonylurea receptor SUR and reconstitution of $I_{K_{ATP}}$.

The structure of the sulfonylurea receptor was revealed by the cloning of a sulfonylurea receptor (SUR1) from cDNA libraries of insulin-secreting cell lines. Hamster SUR1 was the first sequence to be revealed as a 1582 amino acid, 177-kDa protein with two potential glycosylation sites localized at the N-terminus and at the extracellular loop between TM12-13 (TMD2) [9]. Human SUR1, a 1581 amino acid protein, has 96% identity with hamster SUR1. SUR1 belongs to the ABC transporter super-family as well as the cystic fibrosis transmembrane conductance regulator (CFTR), P-glycoprotein (P-gp), and multidrug-resistance-associated protein (MRP) [22]. Therefore, these transporter proteins share a basic structure of multiple transmembrane domains and two nucleotide binding folds (NBFs). Topologically, SUR has 17 transmembrane segments (TMs) distributed in three transmembrane domains (TMDs) known as TMD0, TMD1 and TMD2, each one containing five, six and six TMs respectively. Nucleotide Binding Folds 1 and 2 (NBF1 and NBF2) are located in the loop between TMD1 and TMD2 and the C-terminus, respectively (Figure 1) [23]. As previously mentioned, SUR2A and SUR2B also share a similar topology to that of SUR1 [10].

SUR interacts with Kir6.2 in two different ways. First, its NBFs bind Mg^{2+} nucleotides, activating and regulating Kir6.2 gating—that is, they play a physiological role. Second, SUR1 assembly with Kir6.2 allows K_{ATP} channels to be expressed at the cell surface—thus, they also play a role in trafficking.

Co-expression of Kir6.2 and SUR1 in COS-1 cells reconstitutes weakly inward-rectifying K^+ -channel currents that have a unitary conductance of approximately 76pS in the presence of symmetrical (140mM) K^+ [8]. ATP inhibits the reconstituted channel activity with half-maximal inhibition (K_i) at approximately 10 μ M in the presence of Mg^{2+} . The currents are blocked by glibenclimide (nM concentrations) and are stimulated by the channel opener diazoxide (μ M), an exclusive β -cell K_{ATP} channel agonist. The K^+ currents from reconstituted SUR1 and Kir6.2 have features characteristic of K_{ATP} channels in native β -cells, suggesting that pancreatic β -cell-type K_{ATP} channels also consist of the two subunits, Kir6.2 and SUR1 [8].

The association of SUR1 and Kir6.2 has been established in several ways. First, they form 950kDa octameric complexes that can be isolated, using sucrose gradient centrifugation. This is compatible with a tetramer of SUR1/Kir6.2 (4 x 176,000 (SUR1) + 4 x 45,000 (Kir6.2) = 880,000), with additional mass attributed to glycosylation [24]. Also, studies on the interaction between SUR1 and Kir6.2 indicate that the N-terminus and the M1 transmembrane domain of Kir6.2 are important in conferring assembly with the transmembrane domains of SUR. These findings are compatible with the facts that M1 does not directly contribute to the ion-conducting pathway and is exposed to the lipid membrane environment. Thus, the Kir6.2 N-terminus and M2 interaction with transmembrane domains of SUR suggests a mechanism by which an ABC protein might

assemble with and regulate gating of a Kir [25]. Finally, a recent study has established that SUR1 TMD0 is strongly associated with Kir6.2 and modulates its trafficking and gating. These results are interesting since TMD0 is only found in certain members of the ABC protein superfamily. It has been speculated that TMD0 might represent an evolutionary advantage serving a specialized purpose such as regulating the function of a potassium channel [26].

Physiology of K_{ATP} channels

Regulation of Kir6.2 by nucleotides and PIP_2

K_{ATP} channels are activated by Mg^{2+} -nucleotides and inhibited by intracellular nucleotides such as ATP and ADP [27]. The inhibitory effects of nucleotides are mediated via the pore-forming subunit Kir6.2, whereas their excitatory effects are conferred through SUR. At the same time, membrane lipids such as PIP_2 can compete for a putatively overlapping ATP/ PIP_2 binding site on Kir6.2, antagonizing nucleotide inhibition and, in this way, activating K_{ATP} channels [4-7].

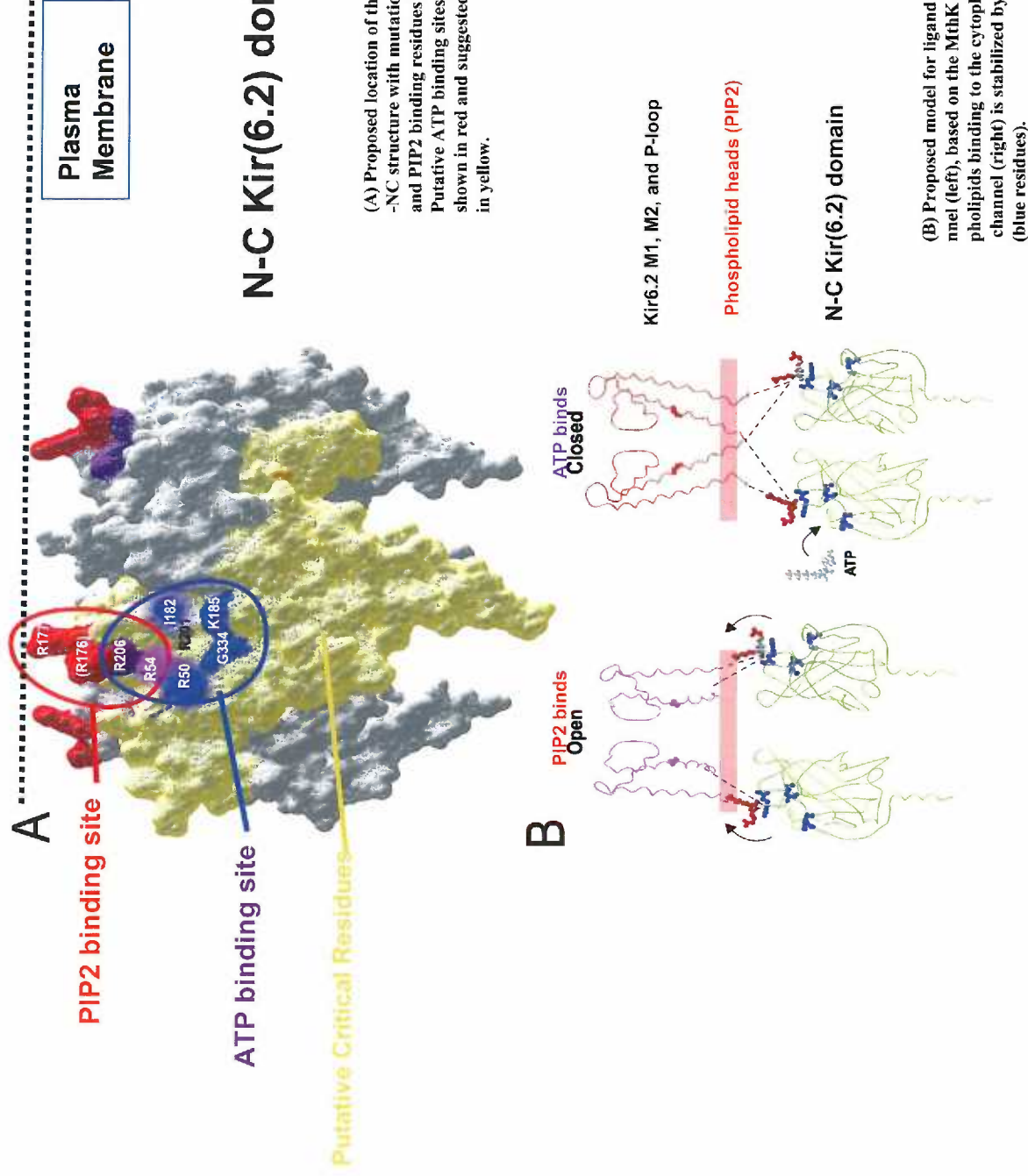
ATP inhibition. The preeminence of the Kir 6.2 subunit in the ATP inhibitory response has been established by studying truncated forms of Kir6.2 (Kir6.2 Δ C26 or Kir6.2 Δ C36) that can generate functional channels independently of SUR1 [28]. These truncated forms of Kir6.2 retain intrinsic ATP sensitivity ($K_i \sim 100\mu M$), but are unable to respond to Mg^{2+} ADP. These results demonstrated that the primary ATP-inhibitory site is located on Kir6.2. Moreover, sulfonylureas and KCOs do not affect Kir6.2 Δ C26 currents, demonstrating that their effects are exerted through the SUR subunit. It is interesting that

SUR1, but not SUR2, enhances the sensitivity of Kir6.2 for ATP (from $K_i \sim 100\mu\text{M}$ to $K_i \sim 10\mu\text{M}$) [28]. More studies are needed to clarify this point.

Further studies have established that ATP's adenine moiety and its β -phosphate are critical for K_{ATP} channel inhibition. Site-directed mutagenesis studies on Kir 6.2 have determined that ATP inhibition is dependent on residues in both the N- (~70 amino acids) and C- termini (8) (~220 amino acids) of the channel [29, 30]. This is not totally unexpected, since Kir6.2 N- and C- termini are physically associated, a feature that appears to be common to all inward rectifiers [31]. Moreover, the recently described crystal structure of a bacterial Kir channel (KirBac1.1) [16] and the cytoplasmic pore of GIRK1 [17] have confirmed many of these mutational studies. Those studies have led to the proposal of an ATP binding patch at the cytoplasmic domain, which is composed of residues from N- and C- termini of Kir6.2 [19]. Since there is an ATP binding site located on each subunit, four separate ATP binding sites per channel are thus established. Interestingly, the model predicts that PIP_2 -interacting residues are localized in an overlapping patch sharing some of these residues with the ATP binding patch [19] (Figure 4).

Most, but not all, of the ATP binding residues are located in the C-terminus. Among the most prominent binding residues are R50 [32] [33] and K185 [34] localized at the Kir6.2 N- and C-termini respectively. Both R50 and K185 affect ATP binding and Kir6.2 channel activity without affecting single-channel kinetics. A recent report using cysteine-scanning mutagenesis and charged thiol reagents has established that these two residues probably interact directly with ATP [30]. R50 interacts primarily with the γ -phosphate of ATP, whereas K185 interacts specifically with the β -phosphate [30].

Kir6.2 gating by ATP and PIP2



(A) Proposed location of the ligand binding domains of Kir6.2. The Kir3.1 -NC structure with mutations of residues corresponding to putative ATP- and PIP2 binding residues in Kir6.2 is shown as space filling representation. Putative ATP binding sites, shown in blue; putative PIP2 binding sites are shown in red and suggested unresolved missing critical residues are shown in yellow.

(B) Proposed model for ligand gating in Kir6.2 channels. The open channel (left), based on the MthK structure, is stabilized by membrane phospholipids binding to the cytoplasmic domain (red residues). The closed channel (right) is stabilized by ATP binding to the cytoplasmic domain (blue residues).

(Modified from Enkvetchakul D, Nichols CG. : J Gen Physiol. 2003 Nov;122(5):471-80).

These residues lie in close proximity to a hydrophobic pocket that accommodates the adenosine moiety. Accordingly, the adenine ring of ATP sits in a pseudohydrophobic pocket lined by a number of amino acids, including the well-characterized C-terminus residue I182 [35] [36]. Once mutated, I182 decreases channel sensitivity to ATP inhibition by >1,000-fold. In addition, G334 also seems important in conferring ATP binding and response, since mutation of G334 to D decreases ATP sensitivity by 1,000-fold [36]. Finally, the two most interesting residues, also present in the ATP binding patch, are the N-terminus R54 [37] and the C-terminus R201 [38]. Substitutions of R201 to A or R54 to A affect both ATP and PIP₂ interaction, reducing sensitivity to both ligands. This is consistent with a model in which each ligand interacts with possibly overlapping sites on the same cytoplasmic domain to stabilize either closed (ATP) or open (PIP₂) states [19, 39] [40, 41].

PIP₂ activation. Hilgemann et al. [42] showed that phospholipids such as PIP₂ and PIP are important regulators of ion transporters and channels. These authors demonstrated that in excised membrane patches from cardiac myocytes, the functional integrity of the Na⁺/Ca²⁺ exchanger as well as the K_{ATP} channel requires the presence of PIP₂. Removal of this phospholipid through phospholipase C resulted in a loss of channel or transporter activity, or ‘run-down’, which could be reversed with PIP₂ and PIP.

In line with these results, the observed run down of K_{ATP} channel activity with cloned subunits in excised patches could also be reversed by application of PIPs [43] [44] [45]. Surprisingly, PIPs not only restored activity of the channels but they also changed

the inhibition by ATP quite dramatically. Following patch excision, channels were inhibited by low μM ATP, whereas mM ATP concentrations were required for channel inhibition after PIP_2 was applied to inside-out patches. Prolonged exposure to PIP_2 rendered channels completely insensitive to 1 mM ATP. This K_{ATP} channel shift from an ATP-sensitive state to a ATP-insensitive state was rendered gradually, suggesting this resulted from a progressive reduction in binding of ATP to the channel [43] [44] [45]. This is not totally surprising, since further studies have demonstrated that the Kir6.2 C-terminus forms a nucleotide and phospholipid modulated channel gate on which ATP and phospholipids compete for binding [43].

What are the molecular determinants that define the PIP_2 and Kir6.2 interaction?

For the phospholipid, two properties have been found to be important. The first is the negatively charged head group of the phospholipids [43]. While PIP_3 and PIP exert an effect similar to PIP_2 , no shift in ATP sensitivity was observed with the dephosphorylated PI that lacks negative charges on the inositol ring. The second requirement for the phospholipid is insertion into the plasma membrane, which is mediated by the lipid tail of the PIPs. Accordingly, PIPs are only effective when inserted into the inner leaflet of the membrane bilayer. The effects of PIP_2 on channel activity have also been demonstrated in intact cells where PIP_2 and PIP_3 levels can be increased by the activity of PIP kinase that phosphorylates PIP [46]. Conversely, PIP_2 and PIP_3 levels can be decreased by the action of phospholipase C, activated by P_2Y_2 receptors. In this way, K_{ATP} channel activity might be regulated physiologically by the local concentration of PIPs [44].

The PIP₂ binding domain in the Kir 6.2 subunit has been partially characterized, and it is composed of residues located at the N- and C- termini of Kir6.2. Potential PIP₂-interacting residues (N-terminus: R54; C-terminus: R176, R177, R201, R206, R222) [38] [47, 48] are located in a patch that overlaps the ATP-binding domain. These residues are on the top surface of the Kir6.2 putative cytoplasmic domain, where they would be expected to be directly opposing lipid headgroups (Figure 4) [19]. The overlap of the ATP-binding sites and the PIP₂-interacting sites is consistent with the apparent competition of the two ligands for the same state but without perfect exclusion of one ligand by the other.

Mechanism of action: how does ligand binding gate Kir6.2? The crystallization of a bacterial Kir channel and the cytoplasmic domain of Kir3.1 provide snapshots of the putative structures of the gating modules in Kir channels. The demonstration of four separated ligand-binding domains per channel supports a tetrameric subunit model of gating. Based on the crystalized GIRK-NC domain [17], the orientation of the M1/2 helices, and the spatial orientation of domains relative to one another, Nichols et al. [19] have proposed that ligand-gating of the Kir6.2 channel occurs by “pinching” of the permeation pathway at the M2 helix bundle crossing. The cytoplasmic domain plays a central role in this proposed model. Interaction of certain residues (54, 176, 177, 201, 206) with PIP₂ may “pull” the cytoplasmic domain toward the membrane, thereby stabilizing the open state of the channel. Conversely, interaction of a set of residues (50, 54, 182, 185, 201, 206, 334) overlapping with ATP, will destabilize or exclude the

membrane interaction, 'pulling' the cytoplasmic domain away from the membrane, thereby stabilizing the closed state [19].

K_{ATP} channel activation by Mg²⁺-nucleotides: the role of SUR

Nucleotide Binding Fold cooperative function. The NBFs in SUR are not important for channel inhibition by ATP, but they are essential for channel activation by Mg²⁺ADP. They bind Mg²⁺ADP and also bind and hydrolyze Mg²⁺ATP, producing Mg²⁺ADP as result. Each NBF contains three motifs that are important for this process: a Walker A (W_A) motif, a Walker B motif (W_B) and a linker region. A conserved, positively-charged lysine residue in the W_A motif is involved in coordinating the negative charge of the phosphate tail of ATP. A negatively-charged aspartate residue in the W_B motif is believed to coordinate the Mg²⁺ ion of Mg²⁺ATP. The linker (LSGGQ) does not appear to be determinant in nucleotide binding but seems to be essential in transducing nucleotide binding into channel activation [27].

Electrophysiological studies [49-51] have shown that mutating the W_A lysine, W_B aspartate, or the linker sequence on either NBF of SUR1 has three consequences: (1) Mg²⁺ADP-induced activation is generally abolished; (2) response to the channel opener diazoxide is diminished or abolished; (3) the sensitivity of the channels to ATP-mediated inhibition is slightly enhanced. These data indicate that the stimulatory effect of Mg²⁺ADP involves the NBFs of SUR1. The increase in ATP-sensitivity suggests that Mg²⁺ATP also has a stimulatory effect on channel activity that may be mediated by its hydrolysis, which is normally masked by the inhibitory effect of the nucleotide. The

response to diazoxide is Mg-nucleotide dependent, and its abolition correlates well with K_{ATP} channel insensitivity to Mg-nucleotides as a result of NBF mutations. Mutations on the linker region may affect the transduction step linking nucleotide binding, the hydrolysis in SUR1, or both to activation of Kir 6.2 [49-51].

Binding studies indicate that both NBFs act in cooperation, but they show different binding preferences depending on the specific NBF. NBF1 appears to bind preferentially to ATP, whereas NBF2 seems to bind mainly Mg^{2+} ADP [52-54]. Ueda et al. [55-57] have demonstrated that there are some nucleotide-binding properties that are similar among all the SUR subtypes: 1) NBF1 is a Mg^{2+} -independent ATP and ADP binding site; 2) NBF2 is a Mg^{2+} -dependent ATP and ADP binding site; 3) the analogue 8-azido-ATP binds to NBF1 very stably; 4) the binding of Mg^{2+} ATP and Mg^{2+} ADP to NBF2 stabilizes 8-azido-ATP binding at NBF1; and 5) NBF2 has ATPase activity, whereas NBF1 has little or no ATPase activity.

Functional and binding analysis of SUR1 subunits with an HI missense mutation (R1420C that is localized on NBF2) have also demonstrated that functional cooperation between NBFs is lost when the structural and binding properties of NBF2 are compromised [52]. The mutation lowers the affinities of NBF2 for ATP and ADP and impairs the ability of Mg^{2+} ATP and Mg^{2+} ADP to stabilize ATP binding at NBF1. These results suggest that the R1420C mutation not only decreases the nucleotide-binding affinity of NBF2 but also impedes the transduction of a conformational change at NBF2 and thereby its ability to stabilize ATP binding at NBF1 [52].

Biochemical studies have demonstrated that the ATPase activity of NBFs is critical for the ability of SUR to confer channel sensitivity to nucleotide stimulation [58-

60]. The ATPase activity has been characterized in fusion proteins containing NBF1 and NBF2 of the cardiac SUR2A isoform. There, NBF2 hydrolyzes ATP in the presence of Mg^{2+} with a twofold higher rate compared to NBF1. Mutations affecting its Walker A or B motifs reduce its activity, producing channels with increased sensitivity to ATP, which correlates well with electrophysiological studies. The ATPase is dependent on cooperative interaction between both NBFs since NBF2 enzymatic activity relies on NBF1's ATP binding capacity[58-60].

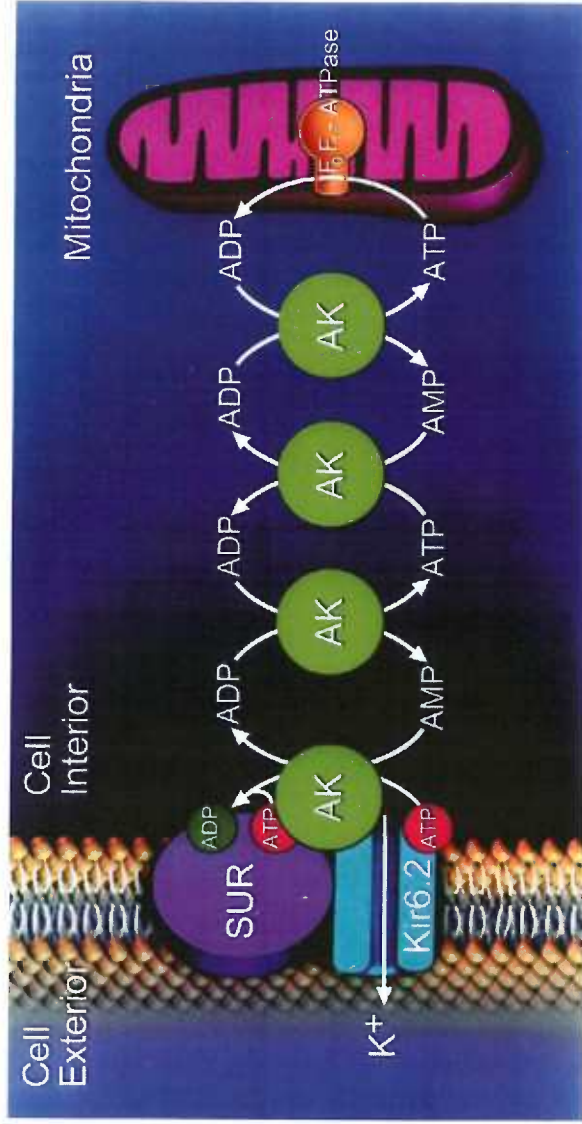
The ATPase activity of NBFs may be regulated by its association with phosphotransfer enzymes such as creatine kinase (CK) that can interact with SUR-NBFs. Moreover, studies have demonstrated that the creatine kinase/creatine phosphate system might remove ADP from NBF2 after ATP hydrolysis and for that reason may regulate K_{ATP} channel activity. In this way, K_{ATP} channel complexes may function as an ATPase that would regulate nucleotide-dependent channel gating [61-63].

Based on these and other findings, Terzic et al. [61-63] have proposed a biochemical model for K_{ATP} channel regulation in cardiac myocytes. K_{ATP} channels may be associated with a set of phospho-enzymes such as adenylate kinase (AK), creatine kinase (CK), and pyruvate kinase (PK) that may directly mediate nucleotide exchange on the NBFs. These phospho-enzymes would link metabolic signals from mitochondria with K_{ATP} channel activity at the plasma membrane through cytosolic phosphotransfer reactions. Under this model, concurrent action of AK, CK and PK could contribute to regulation of the ATP-ADP exchange rates at the channel site, thereby modulating the equilibrium between open and closed channel states. The AK-catalyzed phosphotransfer system would promote K_{ATP} channel opening primarily by accelerating conversion of

ATP to ADP, whereas CK and PK/glycolytic systems would predominantly facilitate conversion of ADP to ATP and channel closure. The open-closed transition that governs K_{ATP} channel behavior would thus be regulated through competitive interactions between the AK system on the one hand and the CK/PK/glycolytic system on the other (Fig. 5 and Fig. 6).

Mg²⁺ADP activation mechanism. A question that is not well answered yet is how Mg^{2+} ADP activates K_{ATP} channels and counteracts the inhibitory effect of ATP. Shyng et al. have proposed that SUR1 acts as a ‘hypersensitivity switch’ to modulate ATP sensitivity of channel activity. This is based on the observation that SUR1 co-expression shifts the Kir6.2 ATP sensitivity from a half-maximal inhibition of $\sim 100\mu M$ to $\sim 10\mu M$; in this way, SUR1 appears to sensitize the channel to ATP. Nucleotide hydrolysis at the SUR1 NBFs may uncouple this sensitizing effect, increasing channel activity at intermediate ATP concentrations. Thus, Mg^{2+} ADP binding would stabilize the activated, or uncoupled, state [51].

Adenyl Kinase (AK) phosphotransfer pathway and regulation of K_{ATP} channels



AK phosphotransfer communicates mitochondria-generated signals to K_{ATP} channels. AK molecules form a phosphorelay network connecting mitochondria with the cell membrane. Under hypoxic stress, mitochondrial F_1F_0 -ATPase consumes cellular ATP generating ADP, which is delivered to the K_{ATP} channel through the chain of sequential AK-catalyzed phosphotransfer reactions. The inwardly rectifying potassium channel (Kir6.2) and the SUR are the pore-forming and regulatory subunits of the K_{ATP} channel complex (Modified from Carrasco et al. Proc Natl Acad Sci U S A. 2001; 98 (13): 7623-7628)

SUR ATPase Cycle Associated with closure and opening of K_{ATP} Channels

A "bird's eye view" of the hetero-octameric K_{ATP} channel complex, composed of four Kir6.2 pore-forming and four SUR regulatory subunits, undergoing conformational transitions during the ATPase cycle. Distinct transitional states during ATP hydrolysis are shown. Removal of ADP by creatine kinase facilitates ATPase cycling, providing cross-talk between the intrinsic channel catalytic activity and cellular enzymatic pathways. High intracellular levels of creatine phosphate support ADP to ATP conversion at the channel site and promote initiation of the ATPase cycle keeping K_{ATP} channels closed. A drop of intracellular creatine phosphate, as it occurs under metabolic stress, reduces the ability of creatine kinase to scavenge ADP. This would facilitate stabilization of the MgADP-bound posthydrolytic conformation and K_{ATP} channel opening. For simplicity of this scheme, the ATPase activity is presented as a collective property of the SUR module without ascribing specific functions to individual nucleotide binding domains. It should be noted, however, that in addition to NBD2, an ATPase activity has been measured at NBD1, albeit at a much lesser rate, and moreover cooperative interaction between the two nucleotide binding domains in regulating K_{ATP} channel gating has been proposed (modified from Zingman L. et al. Neuron, Vol 31, 233-245, 2001)

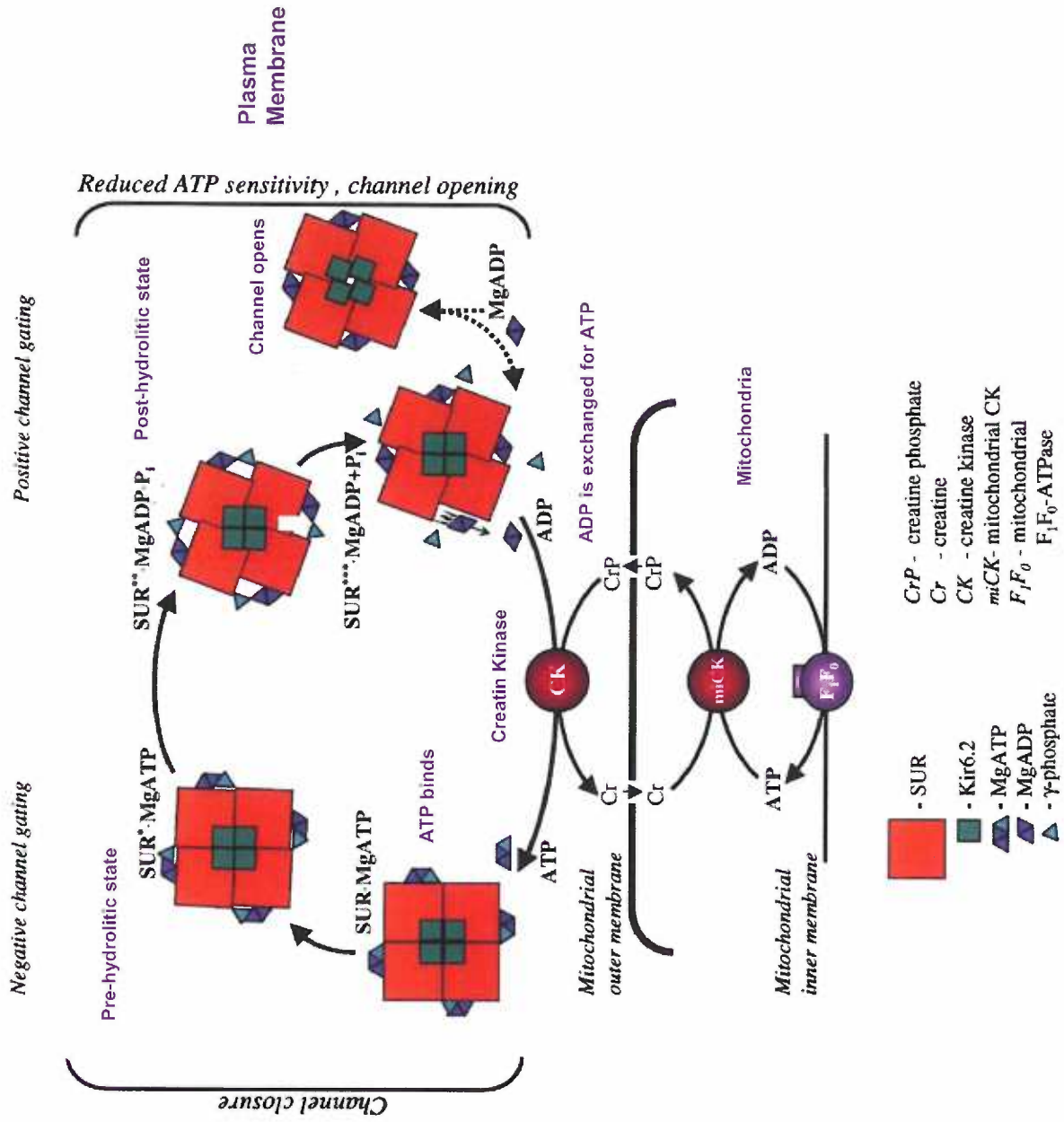


FIGURE 6

Pharmacology of K_{ATP} channels: Sulfonylureas and K_{ATP} Channel Openers.

Pharmacological control of pancreatic K_{ATP} channels is critically important in the treatment of insulin disorders like type II Diabetes Mellitus (DMII) and Familial Hyperinsulinism (HI). The SUR1 subunit is the primary target for most of these drugs, which belong to two main groups: the sulfonylureas and the K_{ATP} channel openers (KCOs). Sulfonylureas inhibit K_{ATP} channels, promoting insulin secretion. Thus, sulfonylureas are used in the treatment of DMII. In contrast, KCOs activate K_{ATP} channels, attenuating insulin secretion. KCOs are used in the treatment of HI.

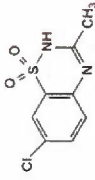
Closing K_{ATP} Channels: Sulfonylureas

The inhibition of K_{ATP} channels in pancreatic β -cells by tolbutamide or glibenclamide has been the pharmacological basis for treatment of DMII for almost 60 years. These drugs bind the SUR receptors with different affinities depending on the SUR receptor sub-type. The K_d values for binding to the SUR1 receptor in pancreatic β -cells and in brain are in the low μ M range for tolbutamide and in the low nM range for glibenclamide (known as the *high-affinity site*). The estimated K_d values for sulfonylurea binding to SUR2 receptors are typically about a thousand-fold weaker than those for SUR1 [64] [65] (Figure 7).

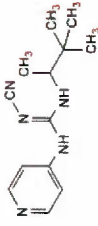
K_{ATP} channel pharmacology

Potassium Channel Openers

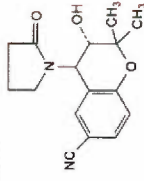
Diazoxide



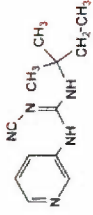
Pinacidil



Cromakalim



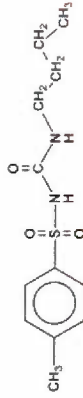
P1075



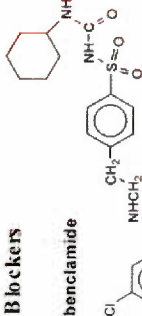
KCOs

Potassium Channel Blockers

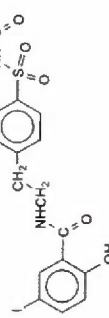
Tolbutamide



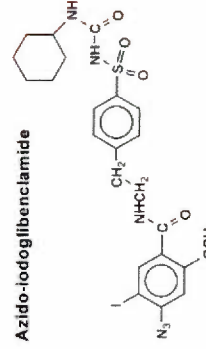
Glibenclamide



Iodoglibenclamide



Azido-iodoglibenclamide



Sulfonylureas

Two pharmacological criteria have been used to define and classify K_{ATP} channels. A diverse group of compounds, referred to as potassium channel openers or KCOs, increase the mean open time, while sulfonylureas like tolbutamide and glibenclamide reduce channel activity. It is generally possible to distinguish two types of K_{ATP} channels based on their sensitivity to sulfonylureas. The β-cell/neuroendocrine/neuronal type channel is 100- to 1000-fold more sensitive than the SUR2 channels, as expected from the higher affinity of SUR1 for sulfonylureas [dissociation constants (K_{Ds}) in the nanomolar range]. Similarly, there are differences in response to KCOs, with the SUR1 and SUR2B channels responding better to diazoxide than cardiac channels. The differential sensitivity of the SUR2B channels to pinacidil allows them to be discriminated from the SUR2A channels. The binding sites for both sulfonylureas and KCOs reside on SUR (Modified from Aguilar-Bryan L and Bryan J (1999) Endocrine Reviews 20 (2): 101-135).

FIGURE 7

TABLE I

<i>K_{ATP}</i> ch. Type → <i>Sulfonylurea</i> →	SUR1/Kir6.2* IC ₅₀ Glibenc / Tolbut	SUR2A/Kir6.2* IC ₅₀ Glibenc / Tolbut	SUR2B/Kir6.2* IC ₅₀ Glibenc / Tolbut
IC ₅₀ channel activation for each sulfonylurea	<10nM / ~2 μM	1.2μM / 1.4mM	~1μM / < mM

* Recombinant

In recordings from K_{ATP} channels, sulfonylureas do not block the open pore of the K_{ATP} channel, nor do they affect unitary conductance or intraburst kinetics. Instead, sulfonylureas shorten the mean burst duration and lengthen the intervals between bursts, placing channels in long-lived interburst closed-states. This inhibition seems to be mediated by binding of sulfonylureas to the *high-affinity site* that lies on SUR1 (IC₅₀ ~5-10 μM for tolbutamide). The *high-affinity site* is only present when SUR1 is co-expressed with Kir6.2. There is also a so-called *low-affinity site* (IC₅₀ >1.5 mM for tolbutamide) that has no known physiological relevance and it is independent of SUR1 [64] [65].

Sulfonylurea binding site. The high-affinity inhibition by sulfonylureas seen in the β-cell channels can be explained by a two-step process. In excised patches, in the *absence* of stimulation by Mg-nucleotides, tolbutamide reduces channel activity by approximately 50-60%. This inhibition involves the N-terminus of Kir6.2 since deletion of 5 amino acids from Kir6.2 reduces the effect of tolbutamide. In addition, deletion of ten or more residues essentially eliminates the inhibitory effect. These results suggest a mechanism in

which the binding of tolbutamide to SUR1 determines a conformational change that prolongs closed channel conformations and involves the N-terminus of Kir 6.2 [66] [67].

The second effect of tolbutamide is the elimination of the stimulatory effect of Mg^{2+} -nucleotides. Normally, this stimulatory effect antagonizes the inhibitory action of ATP on the Kir6.2 subunit. Therefore, disrupting nucleotide stimulation reveals the ATP inhibitory action. This becomes additive with the direct tolbutamide inhibitory effect. Consequently, K_{ATP} channel activity in excised patches is inhibited >90% when saturating concentrations of tolbutamide (200 μ M) are combined with the presence of Mg^{2+} nucleotides [66] [67].

The SUR1 domain that is necessary for high affinity tolbutamide inhibition has been identified. The SUR1 transmembrane domains 12-17 segment (TMD2) is sufficient to confer inhibition by tolbutamide. A more detailed study has narrowed the binding site to TMs 14-16 of SUR1 (1035-1277 residues) and to a critical residue, S1237, that--once mutated--abolishes inhibition and binding of sulfonylureas to SUR1. This is consistent with the idea that the transmembrane regions, rather than the NBFs, contain the sulfonylurea high-affinity binding site [66] [67].

Mechanism of action. Sulfonylurea binding to TMD2-SUR1 appears to have an allosteric influence affecting binding of Mg^{2+} -nucleotides to the SUR1-NBFs. A mechanism has been proposed in which sulfonylureas would bind the SUR1-TMD2 domain, inducing a conformational change irrespective of whether Mg^{2+} and/or nucleotides are present. This conformational switch uses the N-terminus of Kir 6.2 to stabilize a long-lived closed state and also disrupts the Mg^{2+} nucleotide-induced

stimulatory action of SUR1 on Kir6.2. This stimulatory signal normally antagonizes the inhibitory action of intracellular nucleotides on Kir6.2. Impairment of nucleotide stimulation reveals the inhibitory action of intracellular nucleotides. This model accounts for the increased efficacy of sulfonylureas on SUR1/Kir6.2 channels in vivo [66] [67] [68].

Opening K_{ATP} Channels: Potassium Channel Openers

K_{ATP} channel openers (KCOs) are a structurally diverse group of drugs with broad spectrum of potential therapeutic applications. These drugs interact with K_{ATP} channels in numerous tissues and increase their activity, thereby hyperpolarizing the plasma membrane and reducing electrical excitability. The most commonly studied K_{ATP} channel openers are diazoxide, pinacidil, cromakalim, minoxidil sulfate and nicorandil (Figure 7) [69] [70]. Clinically diazoxide is used to suppress excessive insulin secretion, minoxidil sulfate is used topically to stimulate hair growth, and nicorandil is a new drug that is increasingly being used for the treatment of angina.

TABLE II.

<i>K_{ATP} ch. Type</i> →	SUR1/Kir6.2¶ IC ₅₀	SUR2A/Kir6.2¶ IC ₅₀	SUR2B/Kir6.2¶ IC ₅₀
<i>KCO ligand</i> →	Diaz/Pinac/Cromk	Diaz/Pinac/Cromk	Diaz/Pinac/Cromk
IC ₅₀ channel activation for each KCO	60µM/↑µM/↑µM	No /30µM /30µM	58µM/0.68µM/3.1µM*

¶ Recombinant

*levcromakalim

Native K_{ATP} channels from different tissues display varying sensitivities to K_{ATP} channel openers. In the presence of cytosolic $Mg^{2+}ATP$, β -cell K_{ATP} channels are activated by diazoxide, but are unaffected by pinacidil, cromakalim or nicorandil. In contrast, pinacidil, cromakalim and nicorandil, (but not diazoxide) activate cardiac K_{ATP} channels. Smooth-muscle K_{ATP} channels are activated by diazoxide, pinacidil, cromakalim and nicorandil. Since truncated forms of Kir 6.2 expressed at the plasma membrane are insensitive to KCOs, the differential tissue sensitivity to K_{ATP} channels openers is probably attributed to the different types of SURs that comprise β -cell (SUR1), cardiac (SUR2A) and smooth muscle (SUR2B) K_{ATP} channels. This implies that the SUR subunit is the primary target of KCOs [69] [70] [71].

KCOs binding site. The ability of pinacidil to interact with K_{ATP} channels that contain SUR2, but not SUR1, has been exploited to identify the regions of SUR that are involved in the binding of K_{ATP} channels openers. Chimeric molecules based on either SUR1 or SUR2 have been analyzed for binding of the labeled pinacidil-analogue [3H] P1075, or they have been co-expressed with Kir6.2 to assess the ability of pinacidil to enhance channel activity. The [3H] P1075 pinacidil-analogue binds with high affinity to SUR2A ($K_d \sim 10$ nM) and SUR2B ($K_d \sim 46$ nM). However, it does not bind to SUR1 with high affinity ($K_d = \sim 1$ mM) [69].

Uhde et al. [72] have demonstrated that high-affinity [3H] P1075 binding and K_{ATP} channel activation can be conferred on SUR1 by the replacement of certain domains within TMD2 (TMs 12-17) with the homologous region of SUR2B. Conversely, the analogue sensitivity of SUR2B was abolished when those domains (TMs16-17 and

intracellular between TMs 13-14) were replaced with those of SUR1. Swapping these regions between SUR1 and SUR2B subunits did not affect high affinity sulfonylurea binding for SUR1, demonstrating that high sulfonylurea and KCO affinity can coexist in the same SUR molecule.

Using differently labeled analogues and chimeras between the isoforms SUR1 and SUR2A, the main binding site for KCOs has been localized on TMD2 of SUR. Moreover, additional domains (SUR C-terminus, TMD1, and NBF1), present in SUR1 and SUR2B, may contribute to their exclusive sensitivity to diazoxide [73].

A more detailed study, using a cromakalim (KCO agonist) analog, identified two SUR residues that are intimately involved with the responsiveness of K_{ATP} channels to KCOs. The two residues may form part of a binding pocket able to accommodate openers of different chemical classes. These residues, named residues I and II, are located within the last transmembrane helix (TM 17) of SUR at positions Leu¹²⁴⁹ and Thr¹²⁵³ of SUR 2A and at the aligned positions Thr¹²⁸⁶ and Met¹²⁹⁰ of SUR1 [74].

Mechanism of action. The binding of KCOs and activation of K_{ATP} channels is Mg^{2+} -nucleotide dependent [71]. Non-hydrolysable ATP-analogues and mutations that compromise the nucleotide binding or ATPase capacity of the SUR-NBFs markedly affect, or abolish, KCOs binding and K_{ATP} channel activation.

The confirmation of ATPase activity on the SUR-NBFs has produced a more detailed characterization of the mechanism of these drugs. It has been demonstrated that low concentrations of KCOs promote ATPase activity [59]. Nevertheless, at higher concentrations, KCOs reduced ATPase activity, possibly through stabilization of

Mg²⁺ADP at the NBFs. Further studies confirmed that channel openers bind and stabilize the SUR post-hydrolytic conformation (Mg²⁺ADP Pi ~ SUR bound), thereby promoting K_{ATP} channel activation [59].

Consistent with these data, Gribble et al. [70] have proposed that the presence of Mg²⁺ATP slows the rate of drug dissociation. The Mg²⁺-nucleotide binding/hydrolysis at NBFs might be transmitted via the SUR intracellular loops to the TMD2 KCOs-binding site(s), thereby resulting in a SUR conformational change from a KCO-low affinity to a KCO-high affinity conformer.

K_{ATP} channel mutations and HI

Persistent hyperinsulinemic hypoglycemia of infancy (HI) is an inherited disorder of glucose metabolism that presents in newborns and in infants. It is mainly characterized by inappropriately high insulin levels, in the presence of low glucose levels; it is the most common cause of persistent and recurrent hypoglycemia in infancy. Incidence of the disease is estimated to be ~1:50,000 live births, but in some areas of high consanguinity, it is as high as 1:3,000 [75]. The clinical phenotype is variable but the disease can be a major cause of severe mental retardation and epilepsy if not treated properly [6, 75]. In most cases, symptoms of hypoglycemia appear almost immediately after birth, but others show mild hypoglycemia weeks or months after birth. A biochemical diagnosis is based on abnormally high insulin levels in the presence of persisting hypoglycemia, low ketone bodies, increased glucose requirements to maintain normo-glycemia and a glucagon test that shows an increased glycemic response due to increased glycogen in the liver.

The K_{ATP} channel opener diazoxide administered together with other drugs and hormones is the mainstay of medical management of HI. However, some patients fail to respond to medical treatment, necessitating surgical removal of up to 95% of the pancreas to avoid permanent neurological damage. In a follow-up study on patients who were treated clinically, it has been shown that although patients appear to go into remission, the β -cell defect remains and a significant number of these individuals become diabetic when they reach puberty. Over the last five years, rapid advances have been made in determining the molecular genetics of HI. Although some mutations are in genes encoding metabolic enzymes (glucokinase, glutamate dehydrogenase), the majority of causal mutations that have been uncovered are in genes encoding the K_{ATP} channel. Still, the molecular basis remains to be established in $\geq 50\%$ of all cases [6, 75].

The recessive form of HI may be a channelopathy, a suggestion first indicated by the mapping of the SUR1 and Kir 6.2 clustered genes to the short arm of chromosome 11 (11p15.1). A number of groups traced the genetic locus of HI to the same region. HI-associated SUR1 mutations were rapidly identified, and more than 50 HI mutations have now been recognized in the SUR1 and Kir6.2 genes [6, 75]. Most K_{ATP} channel defects resulting from HI mutations were divided into two major functional categories: 1) defects of expressed channel properties, and 2) defects in cell-surface expression. The first mutation shown to alter K_{ATP} channel properties was an HI-associated missense mutation (G1479R) in the NBF2 of SUR1 [76]. Recombinant channels encoded by this mutation behave essentially normally with respect to single channel conductance and ATP sensitivity in inside-out membrane patches. However, these channels do not respond to stimulation by MgADP, rendering the channels physiologically nonfunctional, because

they cannot open in response to a rise in [ADP] after glucose deprivation. As a result, β -cells remain depolarized, and insulin secretion continues [76]. Reduced sensitivity to stimulation by MgADP is a defect of channels generated by a number of HI-associated SUR1 mutations, including F591L, T1139M, R1215Q, G1382, and E1506K, among others [51].

The second functional category of mutations in K_{ATP} subunits causing HI is the reduced, or absent surface expression of channels. Most of these defects correspond to clinically severe HI cases. This is clear for mutations that cause large truncation of SUR or Kir6.2 proteins. Only a few mutations that produce HI have been identified in the Kir 6.2 gene. One of them is a point mutation L147P [77], localized in the Kir6.2 P-loop. This mutation is associated with a severe and drug-resistant form of HI in one patient of Iranian origin. *In vitro*, the mutation does not produce functional channels and does not seem to be able to associate with SUR1. A similar situation has been observed with the point mutant W91R [6], detected in a newborn of Palestinian origin, which has also been localized in the Kir6.2 P-loop. This mutation caused severe HI that required pancreatectomy. A non-sense Kir 6.2 mutation, Y12X, was detected in a patient from a Palestinian family. It involved truncation of the protein after 12 amino acids. When Y12X was engineered into Kir6.2, it did not form a functional channel when coexpressed with wild-type SUR1 [78].

A mutation in exon 35 of SUR1 causes a frame shift after R1437, resulting in a protein with an additional 23 extraneous amino acids and deletion of NBF2. When coexpressed with Kir6.2 in COS cells, the mutant SUR1 fails to generate active channels. A possible explanation is that truncation of NBF2 might cause defective trafficking of the

channel complex, because it also removes an anterograde traffic signal encoded in the C-terminus [79]. Nevertheless, direct proof of a trafficking defect is lacking. Moreover, a reported SUR1 splice variant that introduced a frame shift after amino acid 1,330 generated K_{ATP} currents in *Xenopus* oocytes [80]. In this case, NBF2 is also completely absent, but there is an addition of 25 novel amino acids after residue 1,300. The discrepancy between the two cases may be due to the nature of the additional amino acids introduced by the frame shift, but it is also possible that the requirements for trafficking and surface expression are different in *Xenopus* oocytes and mammalian cells [75].

Animal Models. Generation of transgenic mice models of HI by manipulation of the SUR1 and the Kir6.2 genes has achieved relative success. Miki et al. [81] first generated transgenic mice expressing a dominant-negative mutant Kir6.2 (Kir6.2 [G132S]) in pancreatic β -cells. K_{ATP} currents are significantly reduced in isolated β -cells, and both resting membrane potential and basal intracellular calcium concentration are consequently higher than those in control mice. Neonatal transgenic mice exhibit relatively high levels of serum insulin despite hypoglycemia, resembling HI in humans, but the transgenic mice rapidly develop hyperglycemia with reduced glucose-induced insulin secretion. Histologically, transgenic mice islets reveal enhanced apoptosis and a marked decrease in the number of β -cells in adult mice.

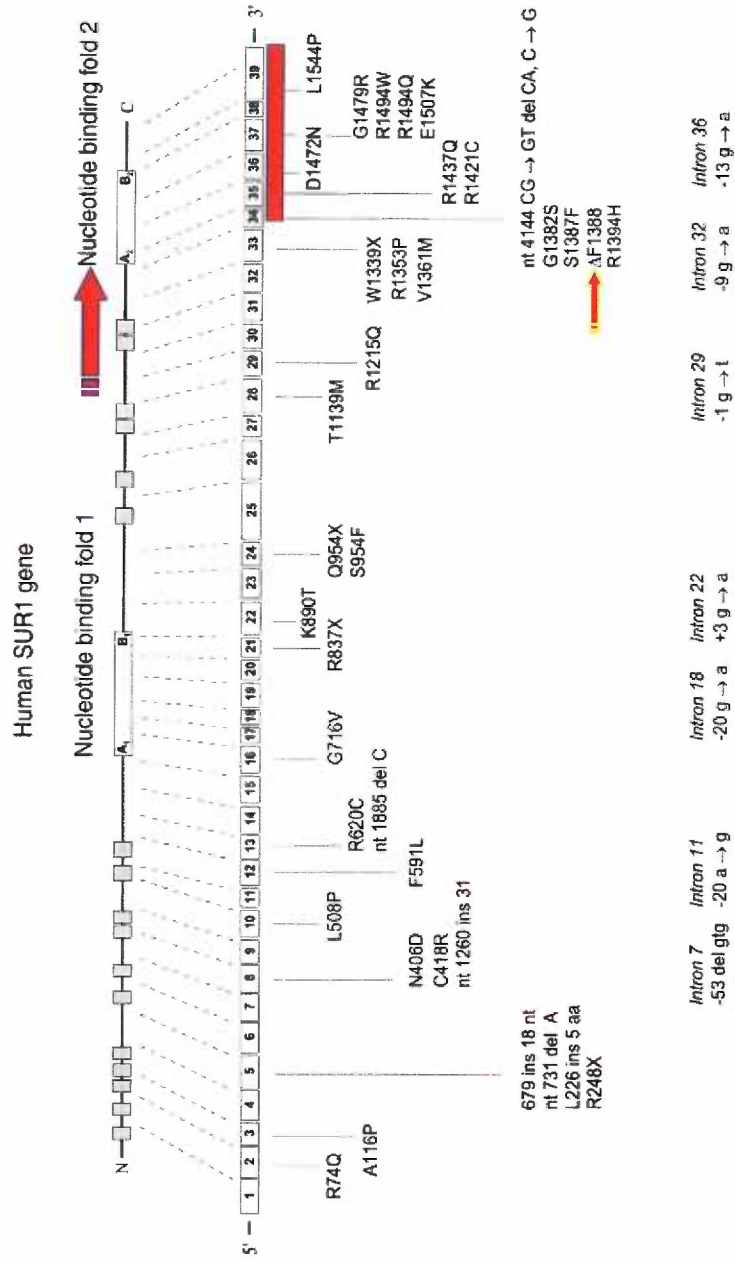
Knocking out the Kir6.2 gene generated animals completely lacking K_{ATP} channels in β -cells of homozygous (Kir6.2 $-/-$) mice [82]. As expected, β -cell $[Ca^{2+}]_i$ and membrane potentials are elevated. The mice also show a transient hypoglycemia, no glucose-dependent insulin secretion, and older animals are glucose intolerant. Moreover, glucose

tolerance is apparently normal in young mice, and insulin tolerance is actually enhanced, possibly a consequence of reduced K_{ATP} channel activity in skeletal muscle cells.

Seghers et al. produced SUR1 knockout (SUR $-/-$) mice [83], generating β -cells also lacking of K_{ATP} channels. Transgenic mice first-phase insulin release is almost completely abolished, the second-phase insulin release is reduced, and adult SUR $-/-$ mice glucose levels are normal. Nevertheless, SUR $-/-$ mice show statistically significant hypoglycemia during fasting, consistent with an inability to ‘turn off’ insulin release. Frank hypoglycemia and hyperinsulinemia are really observed only in the 1st day of SUR1 $-/-$ mice, and by day 5, the situation is reversed to hyperglycemic phenotype.

Although these various knockout animals reiterate the cellular phenotypes (i.e., abolition of K_{ATP} channels and elevated $[Ca^{2+}]_i$) that are expected to underlie HI, in no case is persistent hyperinsulinemia observed. Moreover, there is a rapid reversal of any transient neonatal hypoglycemia to a hyperglycemic, diabetic, phenotype. The reasons for the lack of correlation between the mouse phenotypes with HI in humans are not entirely clear. Although temporally uncorrelated, there is evidence that HI patients may cross over to a diabetic phenotype in later life. Conceivably, β -cell death, coupled with a decreased glucose-dependent insulin release may underlie a later onset of diabetes.

Human SUR1 gene mutations



Hypotheses about the molecular mechanism of a HI mutation.

Many SUR1 HI mutations affect different regions of SUR1 by unknown molecular mechanisms [6]. As shown in Figure 8, mutations spread along the SUR1 molecule but they are particularly concentrated around the NBFs sequences in general and in the NBF2 sequence in particular. Among those HI mutations present in the NBF2 is $\Delta F1388$ [84]. This mutation is responsible for ~20% of the incidence of HI in Ashkenazi Jews. The $\Delta F1388$ mutation resembles the CFTR $\Delta F508$ mutation [85], which accounts for the majority of cystic fibrosis cases. $\Delta F508$ is localized in the NBF1 of CFTR, causing ER retention, degradation and lack of cell-surface CFTR channel expression [85-87]. SUR1 $\Delta F1388$ might therefore render disease by a similar mechanism.

If this hypothesis can be demonstrated, it opens a number of questions and hypotheses. First, is it possible to introduce molecular manipulations in order to overcome the trafficking defect? Second, what is structurally important in the SUR1 F1388 site that makes K_{ATP} channels behave in certain way when the mutation is present? Third, if the SUR1 $\Delta F1388$ mutant can cause mistrafficking, does that render them more susceptible to degradation? These are the primary questions that I will address in this thesis.

In order to learn how mutations might affect K_{ATP} channel trafficking and, as a consequence, K_{ATP} channel cell-surface expression, it is important to understand the mechanisms that control trafficking. The following sections review current understanding of the trafficking regulation of K_{ATP} channels.

Quality control and trafficking of ion channels

General Mechanisms: Folding and Retention

As the first station of the secretory pathway, the ER is where membrane proteins are synthesized, folded and assembled[88-90]. In mammalian cells, proteins are translocated into the ER co-translationally and folding starts at the same time a protein is being translated and translocated through the translocon[91-93]. Post-translational folding takes place after the completed chain has been released from the ribosome and the translocon complex. In this way, proteins acquire their secondary and tertiary structures. While still in the ER, many proteins also proceed to assembly into homo- or hetero-oligomers (e.g. octameric K_{ATP} channels[24, 94, 95]).

It is well established that a protein's three-dimensional structure and its oligomeric state control not only its functional properties, but also its intracellular targeting and life-span. Misfolded, misassembled, and unassembled polypeptides are generally retained in the ER and eventually degraded. These properties of the ER provide *quality control* (QC) in the secretory pathway[88-90]. The ER quality control is a retention-based system: properly folded and assembled conformations are not detected and therefore free to leave the ER compartment. Thus, when proteins exit the ER, they are not only sorted away from resident ER proteins, but also from conformant variants of themselves. Proteins in their export-competent form usually correspond to the compactly folded native conformation that has undergone correct co- and posttranslational processing. For most oligomeric proteins, a correct quaternary structure is also required.

Chaperones and folding enzymes that reside in the ER lumen in high concentrations participate directly in all stages of protein folding [88-90].

What are the general protein molecular properties that determine ER retention?

It remains largely unclear which molecular cues direct folding sensors to unfolded conformers. Nevertheless, some information is available. Among other factors, chaperones are involved in protein retention. Chaperones recognize specific hydrophobic surface patches (UDP-Glucosyltransferase), heptapeptides that have aliphatic amino-acid chains in alternating positions (BiP), exposure of free cysteines (protein disulfide isomerase), and the trimming state of the glycan moiety of glycoproteins (calnexin/calreticulin). During normal protein biogenesis, these features are only transiently exposed, resulting in association of newly synthesized proteins with QC elements[88-90].

The association between newly-formed proteins and QC elements may become prolonged if the normal kinetics of protein folding is altered by a disrupting factor, such as a mutation, that changes the native protein structure. A number of mutations that affect protein trafficking have been identified. The best-studied is the CFTR $\Delta F508$ mutation, which accounts for a large percentage of all cystic fibrosis cases. The $\Delta F508$ mutation determines a kinetic impairment in the normal folding pathway of CFTR. Consequently, CFTR $\Delta F508$ is retained in the ER and degraded [86, 87, 96, 97].

The presence of a strict QC system in the ER is important. ER quality control ensures that proteins are not dispatched to terminal compartments when they are incompletely folded and potentially damaging to the cell. It is essential that non-

functional or partially- functional ion channels, transporters and receptors do not reach the plasma membrane, where their presence could be toxic [88-90].

Trafficking signals in K_{ATP} channels: Retrieval and Export signals.

ER quality control can be far more specific for certain groups of proteins such as ion channels and membrane receptors [98]. This specificity goes beyond the sole recognition of the common set of protein structural features that are exposed during the folding process. A critical point for this specificity is the existence of ER trafficking signals, recognized by special receptors that may be exposed or hidden on the final protein structure [88, 89].

On K_{ATP} channels, correct trafficking and cell-surface expression are under the control of a tripeptide ER-retention/retrieval signal, RKR, present in both the SUR1 and Kir6.2 subunits. This retention signal is shielded only after the complete assembly of octameric K_{ATP} channels [98, 99]. This signal causes ER retention of Kir6 tetramers, SUR1 monomers, and other partial complexes with fewer than eight subunits. In this way, the ER quality control impairs the export of unassembled channels [99].

In contrast to the well-known C-terminal dilysine motif [100], which is restricted to the distal C-terminus of membrane proteins, RKR is position-independent [12]. Nevertheless, the RKR motif is capable of binding the COP I vesicle coat that initiates retrieval. Interestingly, this interaction between RKR/COP I can be competed by 14-3-3 dimers. This association of RKR/14-3-3 seems to be related to the oligomeric state of the subunits containing the RKR signal and it may regulate forward K_{ATP} channel trafficking [101-103].

Similar arginine-based motifs (RXR motifs) also function as ER retention/retrieval signals during the assembly of the GABA_B receptor [104] and the NMDA receptor [105, 106]. Removal of four arginine-based motifs has also been reported to cause surface expression of a misfolded Δ F508 cystic fibrosis transmembrane conductance regulator (CFTR) mutant channel, which is otherwise retained in the ER by the quality control machinery [107]. Thus, the RXR motif may be used to monitor both the folding (CFTR) and the assembly (K_{ATP}, GABA_B, NMDA receptors) of membrane proteins [98].

A similar checkpoint exists during the assembly of the high voltage-activated calcium channels (VGCC) [108] and AMPA receptors [109, 110]. In the case of the VGCC, an ER retention/retrieval signal is present in the cytoplasmic loop linking the first two transmembrane domains of the pore-forming α 1 subunit. Its coassembly with the auxiliary β subunit shields this signal in the α 1 subunit, allowing the channel complex to reach the cell membrane [108]. In the case of the tetrameric AMPA receptor, RNA editing at Arg607 on the GluR2 subunit regulates channel ER retention and assembly. Reversion of GluR2-Arg607 to Gln (R607Q) results in rapid release from the ER and elevated cell surface expression of GluR2 [109, 110].

Other arginine-related ER retention signals have recently been identified on kainate receptors. Disruption of this motif results in ER exit and surface expression of KA2 and GluR5-2b receptors [111, 112] [113]. In the pentameric nicotinic receptor channels, a transmembrane retention signal has been found in all subunits. Like the RKR motif in K_{ATP} channels, the signal seems to be critical in assuring proper assembly and

subunit stoichiometry to the nicotinic receptor [114]. In this way, the ER quality control impairs export of unassembled nicotinic channels.

ER export signals. Exit of proteins from the ER occurs at the ER exit sites. These are small membrane clusters contiguous with the ER membrane and coated with the COPII coat [115-118]. Importantly, incompletely folded cargo proteins and ER chaperones are generally excluded from exit sites [119]. Therefore, the exit sites function as an intrinsic part of the ER QC system. Cargo concentration at these exit sites can be mediated by ER export signals, which can interact directly with COPII coat or through a cargo receptor [101] [115-118].

One of the first described export signals was the DXE motif, which was found on the vesicular stomatitis virus glycoprotein [120]. This di-acidic sequence is also found in many other membrane proteins such as the Kir 2.1 potassium channel. Studies on Kir 2.1 potassium channels revealed the existence of a FCYENE motif as an ER export signal. Significantly, when fused to several unrelated proteins, FCYENE promoted ER export and boosted the steady-state surface density of these membrane proteins. The FCYENE motif was the first export signal described in ion channels. Similar but distinct ER export signals are present in other Kir family members, including Kir 1.1, Kir 3.2A, and Kir 3.4 [98, 121, 122].

Different types of ER export signals have also been identified. A K_{ATP} channel ER export signal has been identified within the C-terminus of SUR1. Deletion of as few as 7 amino acids from the C-terminus of SUR1 markedly reduces surface expression of the K_{ATP} channels [123]. In this particular case, it would be intriguing to determine if the

SUR1 C-terminus interacts with COP II or with some other protein that may escort K_{ATP} channels to the ER exit sites. Interestingly, although both Kir6.2 and SUR1 have retention signals, it is only SUR that possesses an export signal a condition that is necessary to ensure total cell-surface expression of K_{ATP} channels [123].

Additional ER export signals have been described in NMDA [105, 124] and kainate receptors [111, 112] [113] and in voltage-gated potassium channels [125] [126]. In the NMDA receptor, a di-valine motif localized at the end-C-terminus, binds to COP II and determines ER export [101, 124]. In the kainate receptor, the motif is localized in the C-terminus of GluR6. It is arranged as a 7 amino-acid stretch of predominantly basic residues (CQRRLKH) [111, 112] [113]. In the Kv1.4 potassium channel, the C-terminal VXXSL also acts as an export signal [124].

Regulation of ER to Golgi Transport. The presence of retention/retrieval signals and ER export signals in channels raises the possibility that transport of proteins destined to the cell surface from the ER to the Golgi might be regulated.

Indeed, there is some recent evidence that links neuronal activity with trafficking regulation at the ER/Golgi level. Neuronal activity seems to regulate synaptic accumulation and ER export of NMDA receptors. This is due to mRNA splicing that is capable of switching between two NMDAR variants that have different capabilities of forward trafficking. These findings define a pathway underlying trafficking regulation at the ER/Golgi level [124].

ER/Golgi trafficking also seems to be regulated by phosphorylation. In KCNK3 potassium channels, phosphorylation on the C-terminus allows exclusive binding of the

14-3-3 protein that suppresses the COP I coat binding on the N-terminus. This 14-3-3/KCNK3-channel interaction allows forward transport through the secretory pathway [103]. In this way, phosphorylation targets the channel for forward trafficking, when it would otherwise be retrieved back to the ER.

Phosphorylation might also play a role in suppressing ER forward trafficking of NMDA receptor subunits. This occurs via protein kinase C acting through the RXR retention signal present in some of the splicing variants of NMDA-NR1 subunits [106, 127].

These studies open the possibility that ER export and surface expression of K_{ATP} channels, for which trafficking is also controlled by RXR retention motifs, may be regulated by channel activity.

Inefficient processing of some membrane proteins.

Once a protein has reached the export-competent conformation, it leaves the ER for the Golgi apparatus, where many proteins acquire their final mature form (i.e. full glycosylation). After processing in the Golgi, the protein is ready to be sorted, and it is either secreted or expressed at the plasma membrane as a functional protein [128, 129]. However, this entire process can be inefficient, with only a small fraction of the initially synthesized product achieving the export-competent conformation, while the rest is retained in the ER and eventually degraded [130]. This inefficiency is related to an ineffective folding process that prevents the protein from reaching the export-competent (or degradation-resistant) conformation inside the ER [46]. In other cases, interaction between oligomers is a critical factor that determines efficient exportation out of the ER[131]⁵⁴.

Integral membrane proteins are unique cases because they contain folded domains on both sides of the ER membrane. These domains associate with luminal as well as cytosolic folding factors. The CFTR and mutant CFTR- Δ F508 are two membrane proteins that have been extensively studied for their quality-control properties [96]. The biogenesis of CFTR exemplifies the inefficient processing of some membrane proteins. In this case, the wild type (wt) channel is synthesized as a core-glycosylated precursor, but only 25-30% of the initially synthesized protein is correctly folded into a degradation-resistant form inside the ER and exported to the Golgi. Once inside the Golgi, the protein matures into a complex-glycosylated polypeptide. The remaining 70% of the CFTR is retained in the ER and rapidly degraded through the proteasome pathway [85, 86, 96, 132]. In contrast, the CFTR mutant Δ F508 cannot be exported and most of it is rapidly degraded through the cytosolic proteasomes [86, 132].

The wt δ -opioid receptor is another example of inefficient biogenesis [133-135]²⁴⁻²⁶. This protein is synthesized as a core-glycosylated precursor that is converted to a fully mature receptor in the Golgi apparatus. Less than 50% of the precursor is processed to the fully glycosylated protein, suggesting that only a fraction of the synthesized receptors attain the properly folded conformation that allows exit from the ER. Opioid receptors that fail to be exported become targets for ubiquitination and proteasomal degradation [133-135]. The NMDA receptors, which are heteromultimeric ion channels composed of two different kinds of subunits, are also a case of inefficient biogenesis. In this case, NR1 and NR2 subunits are assembled and expressed at the cell surface. Nevertheless, a significant fraction of NR1 subunits stay in an unassembled

form. The unassembled fraction of NR1 subunits cannot reach the plasma membrane and they are rapidly degraded [136].

Retention and degradation of incorrectly folded proteins entering the secretory pathway may not be restricted to products of mutated genes. For instance, Schubert et al. have proposed that as much as 30% of newly synthesized proteins in various cell types never attain their correct native structure. These incorrectly folded proteins, called defective ribosomal products (DRiPs), were found to be ubiquitinated and degraded by the cytosolic proteasomes[130].

Degradation

ER-terminal retained products are most commonly targeted for degradation. The main component of this ER-related degradation process is the ubiquitin-proteasome system localized in the cytosol and nucleus outside the ER. In order to reach the cytosolic proteasome, membrane proteins must be retro-transported and dislocated from the ER through a reprogrammed translocon, deglycosylated, ubiquitinated, and finally degraded.

Ubiquitin is a protein that when covalently added to other proteins targets them for recognition and destruction by the 26S proteasomes. Conjugation of ubiquitin proceeds via a three-step mechanism. Initially, the ubiquitin-activating enzyme, *E1*, ligates and activates the ubiquitin molecule. Once ubiquitin is activated by *E1*, it is taken by one of the several *E2* enzymes (ubiquitin-conjugating enzymes) and transferred to the substrate (e.g. a misfolded protein) that is specifically bound to an ubiquitin-protein ligase, *E3*. The *E3* ligase gives specificity, and facilitates and catalyzes covalent attachment of ubiquitin to a specific substrate. The first moiety is usually transferred to

an ϵ -NH₂ group of an internal Lys residue of a targeted protein. In successive reactions, a polyubiquitin chain is synthesized by transfer of additional activated ubiquitin moieties to an internal Lys residue of the previously conjugated ubiquitin molecule (normally K48 of ubiquitin), resulting in the generation of chains of ubiquitin generally referred to as polyubiquitin. In many cases, protein polyubiquitination generates high molecular weight (HMW) detergent-insoluble aggregates.

The Proteasome is a large 26S multicatalytic protease that degrades polyubiquitinated proteins into small peptides. The proteasome can be separated into two subcomplexes: a 20S particle, which carries the catalytic activity of the proteasome and a regulatory 19S particle. The 20S complex is barrel-shaped and consists of four stacked rings, and the catalytic sites are localized inside the barrel. Each extremity of the 20S complex is capped by a 19S particle, which has several functions. The 19S particle recognizes ubiquitinated proteins and changes the conformation of the 20S particle to create a channel through which substrates can be inserted into the proteolytic interior chamber. Finally, because a folded protein may be unable to fit into the channel, the 19S particle unfolds the polypeptide chain and inserts it into the 20S particle [137].

When the proteasome is experimentally altered by either proteasome inhibition or saturated by overexpression of a mutant protein, proteins tend to form aggregates that cannot be degraded and these accumulate as a large perinuclear inclusion that colocalizes with the intermediate filament vimentin proximal to the centrosome. These inclusions are also enriched with proteasome components and chaperones. The inclusions have been characterized as a novel cellular organelle called “*aggresomes*” [138].

Strong evidence exists that cell-surface expression of certain membrane proteins can be regulated by the rate of degradation through the proteasome pathway. This seems to be the case for connexin 43 (Cx43), a gap junction protein. In this case, proteasome inhibition is able to up-regulate gap junctions. Stabilization of connexins under such conditions could facilitate cell-to-cell transfer of metabolites and signaling molecules [139].

Aquaporin-1 is another example. In this case, AQP-1 can be up-regulated by decreasing the basal ubiquitination upon exposure to hypertonic medium, which retards its degradation rate [140].

Concluding Remarks

The questions that I will address in this thesis are delimited by the SUR1 mutation, $\Delta F1388$, which renders K_{ATP} channels non-functional and is associated with HI. The $\Delta F1388$ mutation is located in the NBF2 of SUR1 and resembles the well-known $\Delta F508$ mutation of CFTR.

A first set of questions will try to address the cell biological aspects of the $\Delta F1388$ mutation. *Are the $\Delta F1388$ mutant channels able to reach the plasma membrane?* If the mutant channels cannot reach the plasma membrane, other related questions may be addressed as follows. *Are the $\Delta F1388$ mutant channels retained in a compartment of the secretory pathway?* And, if the mutant channels are retained, *are they prone to degradation?*

A second group of questions will address the structural basis of the F1388 site that once mutated, renders non-functional K_{ATP} channels. *What is structurally important*

in the SUR1 F1388 site? And, what is the physicochemical basis for the ability of F1388 to promote the functional expression of K_{ATP} channels?

As was mentioned before, the $\Delta F1388$ mutation is coupled to Hyperinsulinism (HI). Consequently, the answers to the formulated questions are important for a better understanding of the molecular mechanism of HI caused by the $\Delta F1388$ mutation. Moreover, determining some of the biological differences between the $\Delta F1388$ mutant and the wild type K_{ATP} channels makes it possible to establish the significance of the F1388 residue in the functionality and biogenesis of the K_{ATP} channels.

CHAPTER ONE

Defective trafficking and function of K_{ATP} channels caused by a sulfonylurea receptor 1 mutation associated with persistent hyperinsulinemic hypoglycemia of infancy

Etienne A. Cartier^{*}, Lisa R. Conti[†], Carol A. Vandenberg[†], and Show-Ling Shyng^{*}

^{*} Center for Research on Occupational and Environmental Toxicology, Oregon Health Sciences University, Portland, OR 97201; and [†] Department of Molecular, Cellular, and Developmental Biology and the Neuroscience Research Institute, University of California, Santa Barbara, CA 93106

Abstract

The ATP-sensitive potassium channel (K_{ATP}) regulates insulin secretion in pancreatic β cells. Loss of functional K_{ATP} channels because of mutations in either the SUR1 or Kir6.2 channel subunit causes persistent hyperinsulinemic hypoglycemia of infancy (PHHI). We investigated the molecular mechanism by which a single phenylalanine deletion in SUR1 (Δ F1388) causes PHHI. Previous studies have shown that coexpression of Δ F1388 SUR1 with Kir6.2 results in no channel activity. We demonstrate here that the lack of functional expression is due to failure of the mutant channel to traffic to the cell surface. Trafficking of K_{ATP} channels requires that the endoplasmic reticulum-retention signal, RKR, present in both SUR1 and Kir6.2, be shielded during channel assembly. To ask whether Δ F1388 SUR1 forms functional channels with Kir6.2, we inactivated the RKR signal in Δ F1388 SUR1 by mutation to AAA (F1388 SUR1_{AAA}). Inactivation of similar endoplasmic reticulum-retention signals in the cystic fibrosis transmembrane conductance regulator has been shown to partially overcome the trafficking defect of a cystic fibrosis transmembrane conductance regulator mutation, Δ F508. We found that

coexpression of Δ F1388 SUR1_{AAA} with Kir6.2 led to partial surface expression of the mutant channel. Moreover, mutant channels were active. Compared with wild-type channels, the mutant channels have reduced ATP sensitivity and do not respond to stimulation by MgADP or diazoxide. The RKR \rightarrow AAA mutation alone has no effect on channel properties. Our results establish defective trafficking of K_{ATP} channels as a molecular basis of PHHI and show that F1388 in SUR1 is critical for normal trafficking and function of K_{ATP} channels.

Introduction

ATP-sensitive potassium channels (K_{ATP}) couple metabolic signals to cell excitability. They play important roles in many tissues, including regulation of insulin secretion, control of vascular tone, and protection of neurons and muscles from ischemia [141-143]. K_{ATP} channels are octameric complexes composed of four sulfonylurea receptors (SUR.x) and four inward rectifier potassium channels Kir6.x [15, 24, 144, 145]. They are regulated by intracellular ATP and ADP. ATP inhibits channel activity whereas ADP, in the presence of Mg²⁺, antagonizes the inhibitory effect of ATP and stimulates channel activity [146]. These gating properties are crucial for the ability of the channel to sense metabolic changes in cells. Thus, in pancreatic β cells, the [ATP]/[ADP] ratio increases in response to increases in blood glucose levels, leading to K_{ATP} channel closure, membrane depolarization, activation of voltage-gated Ca²⁺ channels, and insulin release. Conversely, when blood glucose levels are low, the [ATP]/[ADP] ratio decreases, K_{ATP} channels open, and insulin secretion ceases.

Persistent hyperinsulinemic hypoglycemia of infancy (PHHI) is a neonatal metabolic disease characterized by inappropriate insulin hypersecretion and profound hypoglycemia [147, 148]. Genetic studies have identified 50 PHHI mutations in the K_{ATP} channel genes [149, 150]. Among these, some introduce premature stop codons that result in nonfunctional truncated proteins [78, 151], and some result in channels that are unable to respond to stimulation by MgADP [52, 76, 152]. Mutant channels in the latter group, although they are active in excised membrane patches and exhibit normal sensitivity to ATP inhibition, are unable to open in intact cells upon glucose starvation because of reduced or lack of response to MgADP [52, 76, 152]. Patients bearing these mutations also have poor responses to diazoxide, a potassium channel opener commonly used to treat PHHI, because the same mutations cause parallel decreases in channel response to diazoxide [76, 152]. Despite our progress in understanding how certain mutations cause excessive insulin secretion, the molecular defects of K_{ATP} channels caused by many PHHI mutations in the channel genes remain unknown.

Correct trafficking and cell surface expression of K_{ATP} channels is under the control of a tripeptide endoplasmic reticulum (ER)-retention signal, RKR, present in both the SUR1 and Kir6.2 subunits [12]. When expressed independently, the two proteins are retained in the ER because of exposure of the RKR signal. Removal of this retention signal allows the proteins to escape the ER quality control mechanism and express on the cell surface [12, 28]. Under normal conditions, SUR1 and Kir6.2 associate with one another to form an octameric channel complex. This association is proposed to shield the ER-retention signal and permit the channel complex to traffic to the cell surface. An anterograde trafficking signal involving the C terminus of SUR1 also has been identified [123].

Deletion of as few as 7 aa from the C terminus of SUR1 markedly reduces surface expression of K_{ATP} channels [123]. Although defective trafficking of K_{ATP} channels has been proposed as a potential mechanism by which mutations in the SUR1 and Kir6.2 genes can cause PHHI [84, 123, 153, 154], direct evidence is still lacking. We show here that a previously identified PHHI mutation in SUR1, F1388 [84], causes defective trafficking and lack of surface expression of K_{ATP} channels. The study provides evidence that defective K_{ATP} channel trafficking is a molecular basis of PHHI. Moreover, we show that the trafficking defect caused by the Δ F1388 SUR1 mutation can be partially overcome by inactivation of the RKR ER-retention signal in SUR1. The resulting mutant channel, although it is fully active in the absence of ATP, has decreased ATP sensitivity and does not respond to stimulation by MgADP or diazoxide.

Material and Methods

Molecular Biology. FLAG epitope (DYKDDDDK) was inserted at the N terminus of the hamster SUR1 cDNA by sequential overlap extension PCR. Constructs containing point mutations were prepared by using the QuickChange site-directed mutagenesis kit (Stratagene). Epitope tag and mutations were confirmed by DNA sequencing. All SUR1 and SUR1-Kir6.2 fusion constructs were in pECE vector, and mouse Kir6.2 cDNA was in pCMV6b vector [76].

Immunofluorescence Staining. COSm6 cells were plated in 6-well tissue culture plates, transfected with Lipofectamine (GIBCO/BRL) or Fugene (Roche) according to the manufacturer's directions, and analyzed 48 h posttransfection. For cell surface staining,

COSm6 cells transiently transfected with various FLAG-tagged SUR1 constructs (with or without Kir6.2) were incubated with anti-FLAG M2 mouse mAb (diluted to 10 μ g/ml in OptiMEM containing 1% BSA; Sigma) for 1 h at 4°C. The cells were washed with ice-cold PBS and incubated with Cy3-conjugated donkey anti-mouse secondary antibodies (Jackson ImmunoResearch) for 30 min at 4°C. After 3 \times 5-min washes in ice-cold PBS, cells were viewed immediately by using a Leica fluorescent microscope. For total cellular staining of FLAG-tagged SUR1, cells were fixed with cold (-20° C) methanol for 5 min. Fixed cells were incubated with the anti-FLAG M2 mAb (10 μ g/ml in PBS containing 1% BSA) at room temperature for 1 h, washed in PBS, incubated with Cy3-conjugated donkey anti-mouse secondary antibodies for 30 min at room temperature, and washed again in PBS before viewing.

Immunoblotting. COS1 cells were plated onto 35-mm culture dishes and transiently transfected with FLAG-tagged SUR1 constructs in the presence or absence of Kir6.2 by using Fugene. Cells coexpressing SUR1 and Kir6.2 were transfected with 0.6 μ g SUR1 and 0.1 μ g Kir6.2 per 35-mm dish; cells expressing SUR1 alone were transfected with 1 μ g SUR1 per 35-mm dish. Cells were lysed 48 h posttransfection in 20 mM HEPES, pH 7.0/5 mM EDTA/150 mM NaCl/1% Nonidet P-40 with Complete protease inhibitors (Roche). Proteins in the cell lysates were separated by SDS/PAGE (10%), transferred to nitrocellulose, analyzed by M2 anti-FLAG antibody (Sigma) followed by horseradish peroxidase-conjugated anti-mouse secondary antibodies (Amersham Pharmacia), and visualized by chemiluminescence (Super Signal West Femto; Pierce).

Patch-Clamp Recordings. COSm6 cells were transfected by using Lipofectamine or Fugene and plated onto coverslips. The cDNA for the green fluorescent protein was cotransfected with SUR1 and Kir6.2 to facilitate identification of positively transfected cells. Patch-clamp recordings were made 36-72 h posttransfection. All experiments were performed at room temperature as described ([145], [76, 152], [51]). Micropipettes were pulled from thin-walled glass (WPI Instruments, Waltham, MA) on a horizontal puller (Sutter Instruments, Novato, CA). Electrode resistance was typically 0.5-1 M Ω when filled with K-INT solution (below). Inside-out patches were voltage-clamped with an Axopatch 1D amplifier (Axon Instruments, Foster City, CA). The standard bath (intracellular) and pipette (extracellular) solution (K-INT) had the following composition: 140 mM KCl/10 mM K-Hepes/1 mM K-EGTA, pH 7.3. ATP was added as the potassium salt. All currents were measured at a membrane potential of -50 mV (pipette voltage = $+50$ mV), and inward currents at this voltage are shown as upward deflections. Data were analyzed by using PCLAMP 7 software (Axon Instruments). Off-line analysis was performed by using Microsoft EXCEL programs. Data were presented as mean \pm SEM. Microsoft SOLVER was used to fit ATP-dose-response curves by a least-squares algorithm.

Results

Δ F1388 SUR1 Prevents Trafficking of K_{ATP} Channels to the Cell Surface. Previous studies have demonstrated that Δ F1388 SUR1, when coexpressed with Kir6.2 in COS cells, resulted in no K_{ATP} channel activity [84, 152]. The lack of functional expression

could be due to lack of channel expression on the cell surface or dysfunction of properly assembled and targeted channels. To distinguish these possibilities, we first determined whether the Δ F1388 SUR1 mutant protein is expressed on the cell surface.

To track the expression of SUR1, the N terminus of the protein was tagged with a FLAG epitope. The N terminus of SUR1 is predicted to lie on the extracellular face of the plasma membrane (Fig. 9; refs.[155] and [156]), allowing access to anti-FLAG antibodies without permeabilizing cells. The FLAG-tagged SUR1, when coexpressed with Kir6.2, gives rise to channels with properties indistinguishable from the untagged channels (not shown). Cell surface expression of wild-type and Δ F1388 SUR1 was monitored by immunofluorescent labeling of the FLAG epitope. Labeling was performed with living cells at 4°C to prevent endocytosis of the antibodies, which might give rise to intracellular staining. Although clear fluorescent signal in the plasma membrane of cells coexpressing FLAG-tagged wild-type SUR1 (FLAG-WT SUR1) and Kir6.2 was observed, no signal was detected in cells expressing FLAG-tagged Δ F1388 SUR1 (FLAG- Δ F1388 SUR1) and Kir6.2 (Fig. 10A *Upper*). The lack of surface expression of FLAG- Δ F1388 SUR1 is not due to poor transfection efficiency of the mutant SUR1 construct or lack of biosynthesis of the mutant protein. Staining of cells fixed and permeabilized with methanol shows that the percentage of cells expressing FLAG- Δ F1388 SUR1 is comparable to that of cells expressing FLAG-WT SUR1 (17.06 ± 1.03 vs. $17.01 \pm 1.30\%$; $n = 8$). There is, however, a clear difference in the staining pattern. Whereas FLAG- Δ F1388 SUR1 shows strong perinuclear staining that is consistent with accumulation of the protein in the ER, FLAG-WT SUR1 has less perinuclear and more membranous staining (Fig. 10B). Immunoblot analysis of SUR1 (Fig.10C) showed that

the total steady-state protein levels are similar for all SUR1 constructs. The wild-type SUR1 was resolved into two major bands when coexpressed with Kir6.2. These two bands correspond to the mature complex glycosylation and immature core glycosylation forms reported previously [24] [12] [156]. In contrast, the $\Delta F1388$ SUR1 was detected as a single lower band whether or not Kir6.2 was coexpressed, consistent with the mutant protein being trapped in the ER. Although faint surface staining was observed in cells expressing FLAG- $\Delta F1388_{AAA}$ (see below), no mature, complex glycosylated band was detected for this construct by immunoblotting. This may reflect differences in the sensitivity of the two procedures in detecting surface SUR1.

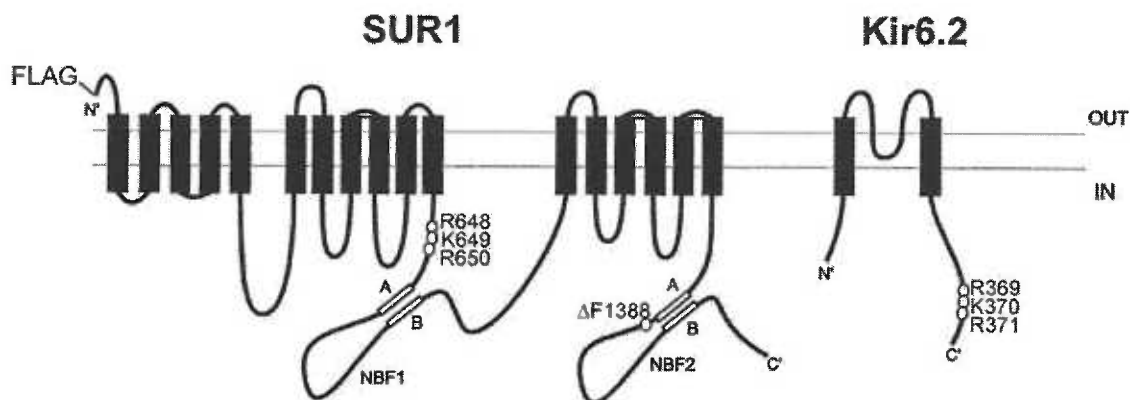


Figure 9. Location of the $\Delta F1388$ mutation and the RKR ER-retention signals in SUR1 and Kir6.2. The topology of SUR1 shown is by Tuszny et al. The $\Delta F1388$ mutation is in the NBF2. The RKR motif in SUR1 is in cytoplasmic segment right before the first nucleotide binding fold (NBF1). The RKR motif in Kir6.2 is near the C-terminus [12].

Inactivation of the RKR Motif in SUR1 Allows Partial Expression of Δ F1388 Mutant Channels. Although Δ F1388 SUR1 causes failure of K_{ATP} channels to traffic to the cell surface, it still may form functional channels with Kir6.2. If so, molecular or pharmacological manipulations that can overcome the trafficking defect may have therapeutic values. Both SUR1 and Kir6.2 contain a RKR ER-retention signal that prevents the individual subunit from exiting the ER in the absence of the other subunit. Upon proper assembly of the two subunits, the ER-retention signals become shielded to allow trafficking of the channel complex to the plasma membrane [12]. Similar arginine-framed ER-retention signals have been identified in cystic fibrosis transmembrane conductance regulator (CFTR) [157]. Inactivation of these arginine-framed ER-retention signals in CFTR can partially overcome the trafficking defect caused by a cystic fibrosis-associated CFTR mutation F508 [157]. We asked whether similar manipulations in SUR1 could overcome the trafficking defect caused by the Δ F1388 mutation.

The RKR motif in SUR1 is located in a cytoplasmic loop between the putative 11th transmembrane domain and the first nucleotide-binding fold (Fig. 9). When we inactivated the RKR signal sequence in FLAG- Δ F1388 SUR1 by mutating it to AAA (FLAG- Δ F1388 SUR1_{AAA}), we observed surface labeling in cells cotransfected with FLAG- Δ F1388 SUR1_{AAA} and Kir6.2 (Fig. 10A *Upper*). However, the fluorescent signal was clearly weaker compared with that of cells expressing FLAG-WT SUR1 or FLAG-SUR1_{AAA} channels (Fig. 10A *Upper*), suggesting that inactivation of the RKR signal only partially overcomes the trafficking defect. Similarly, cells transfected with FLAG- Δ F1388 SUR1_{AAA} alone also showed surface expression level that is lower than cells transfected with FLAG-WT SUR1_{AAA} alone (Fig. 10A *Lower*).

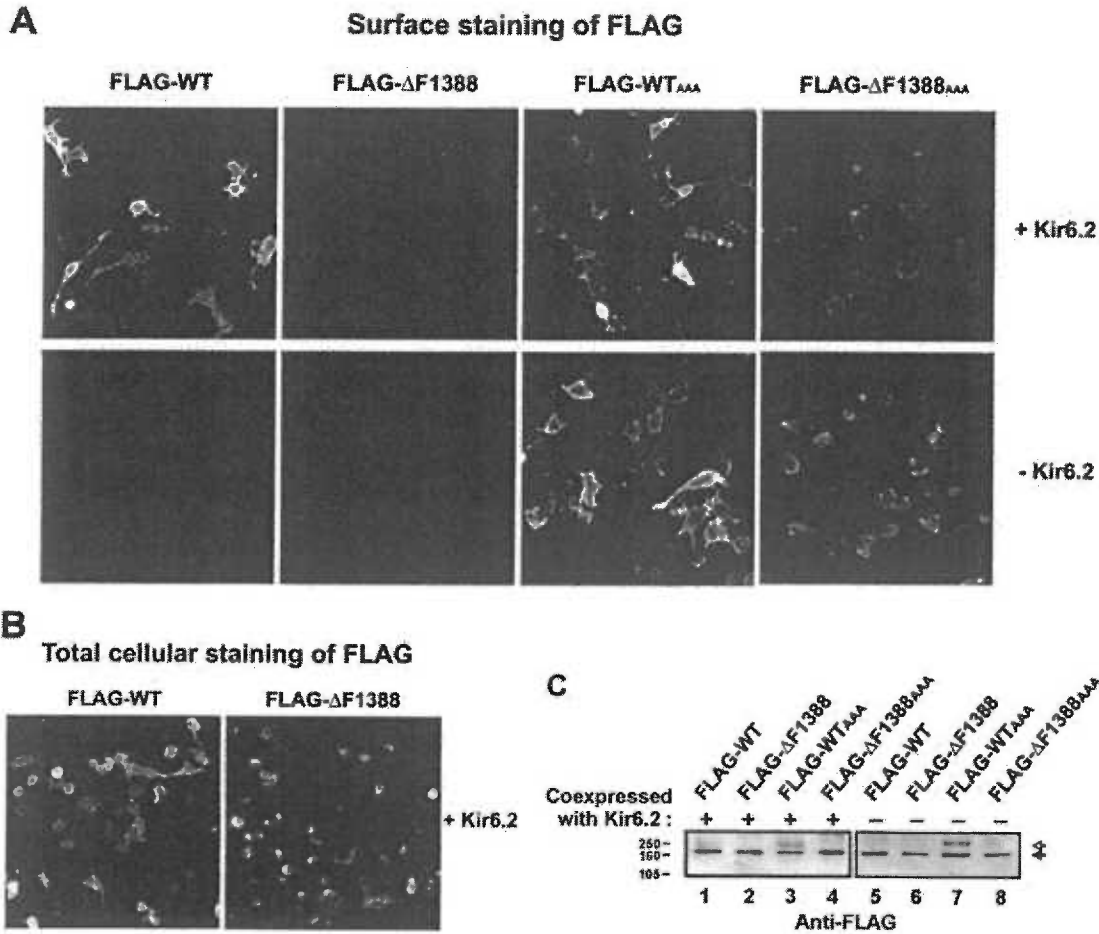


Fig. 10. Lack of surface expression of F1388 SUR1 mutant K_{ATP} channels. (A) COSm6 cells transiently transfected with FLAG-wild type (WT) SUR1, FLAG-F1388 SUR1, or FLAG-F1388 SUR1_{AAA}, in the presence (Upper) or absence (Lower) of Kir6.2, were immunostained for the FLAG epitope. When coexpressed with Kir6.2, surface staining was clearly observed with FLAG-WT SUR1 but not with FLAG-F1388 SUR1. Mutating the RKR sequence to AAA in SUR1 (FLAG-F1388_{AAA} SUR1) partially overcomes the trafficking defect caused by the F1388 mutation and allows surface expression of the mutant protein both in the presence (Upper) and in the absence (Lower) of Kir6.2. (B) COSm6 cells transiently expressing Kir6.2 and FLAG-WT SUR1 or FLAG-F1388 SUR1 were fixed with methanol and immunostained for the FLAG epitope. The FLAG-WT SUR1 and the FLAG-F1388 SUR1 showed equivalent levels of staining, suggesting the wild type and the mutant protein are expressed at similar levels. A strong perinuclear staining pattern indicative of ER accumulation was observed with FLAG-F1388 SUR1, whereas less perinuclear and more membrane staining was seen with FLAG-WT SUR1. (C) FLAG-WT, FLAG-F1388, FLAG-WT_{AAA}, and FLAG-F1388_{AAA} SUR1 constructs were expressed in the presence or absence of Kir6.2 and detected by immunoblotting with antibody to the FLAG tag. Solid arrow indicates core glycosylated SUR1; open arrow denotes complex glycosylated SUR1 seen with FLAG-WT coexpressed with Kir6.2 (lane 1) and FLAG-WT_{AAA} (lanes 3 and 7). Molecular mass markers (kDa) are indicated at left. Note that the amount of DNA used for transfection in the two blots were different (see *Materials and Methods*), so intensities of bands cannot be compared between blots.

ΔF1388 SUR1_{AAA} and Kir6.2 Form K_{ATP} Channels with Altered Physiological Properties. Surface expression of FLAG-ΔF1388 SUR1_{AAA} allowed us to analyze the interaction between the mutant SUR1 and Kir6.2 at the functional level by patch-clamp recordings. Potassium currents that were readily inhibited by ATP were recorded from cells coexpressing FLAG-ΔF1388 SUR1_{AAA} and WT Kir6.2 (Fig. 11B), demonstrating that the mutant SUR1 can form functional channels with Kir6.2. Comparison of K_{ATP} current densities from cells coexpressing Kir6.2 and WT SUR1, SUR1_{AAA}, or ΔF1388 SUR1_{AAA} by using inside-out patch-clamp recordings shows that the expression level of ΔF1388 SUR1_{AAA} mutant channels is $16.8 \pm 4.9\%$ ($n = 35$) that of WT channels. Mutation of RKR to AAA alone (SUR1_{AAA} channels) caused an increase in the level of expression ($162.1 \pm 23.2\%$ that of WT channels, $n = 37$), consistent with that reported by Zerangue *et al.* [12].

A number of PHHI-associated SUR1 mutations located in the second nucleotide-binding fold (NBF2) of the protein have been shown to cause reduced K_{ATP} channel response to MgADP and diazoxide [52, 76, 152]. Because F1388 is also in NBF2 of SUR1, we examined in detail the physiological properties of FLAG-ΔF1388 SUR1_{AAA} channels. Channel open probability (P_o) was estimated by using noise analysis [158]. There is no significant difference between the P_o of WT channels (0.46 ± 0.01 , $n = 5$) and the P_o of ΔF1388 SUR1_{AAA} channels (0.47 ± 0.05 , $n = 7$). ATP dose-response experiments showed that FLAG-ΔF1388 SUR1_{AAA} mutant channels have reduced sensitivity to ATP inhibition, with a half-maximal inhibitory concentration, $K_{1/2}$, of $37 \mu\text{M}$ (Fig. 11A), whereas FLAG-SUR1_{AAA} channels have ATP sensitivity ($K_{1/2}$ of $9 \mu\text{M}$) similar to that of

WT channels ($\approx 10 \mu\text{M}$; ref. [158]). In WT channels, MgADP antagonizes the inhibitory effects of ATP and stimulates channel activity. However, this stimulatory effect is completely absent in FLAG- $\Delta\text{F1388 SUR1}_{\text{AAA}}$ mutant channels (Fig. 11B). The mutant channel also lacks response to diazoxide (Fig. 11C). The lack of response is not due to the RKR-to-AAA mutation because FLAG-SUR1_{AAA} channels have a normal response to MgADP (Fig. 11B) and diazoxide (Fig. 11C).

The stimulatory effect of MgADP on K_{ATP} channel activity is conferred by the SUR1 subunit ([76], [28], [49], [51]). Channels formed by $\Delta\text{C25 Kir6.2}$ (a mutant Kir6.2 in which the C-terminal 25 aa including the RKR signal have been removed; refs. [12] and [28] in the absence of SUR1 have reduced ATP sensitivity ($K_{1/2} \sim 100 \mu\text{M}$) and do not respond to MgADP or diazoxide [28] [19]. One can argue that the altered ATP sensitivity and MgADP response we observed with the $\Delta\text{F1388 SUR1}_{\text{AAA}}$ mutant channel is a result of weak association between the mutant SUR1 and Kir6.2 or even temporary dissociation between the two subunits after reaching cell surface. In this scenario, although $\Delta\text{F1388 SUR1}_{\text{AAA}}$ can assemble with Kir6.2 and traffic to the cell surface, the interaction between the two subunits is so weak that there is little or no "functional" coupling between the two subunits. To test this possibility, we used a $\Delta\text{F1388 SUR1}_{\text{AAA}}$ -Kir6.2 fusion construct in which $\Delta\text{F1388 SUR1}_{\text{AAA}}$ was physically linked to Kir6.2 through a hexaglycine linker [24, 144, 145] to force physical association between the two subunits and to ensure an octameric channel stoichiometry. Analysis of channels formed by the mutant fusion protein shows that similar to channels formed by expressing $\Delta\text{F1388 SUR1}_{\text{AAA}}$ and Kir6.2 as individual subunits, channels formed by the mutant fusion protein also fail to respond to MgADP stimulation (Fig. 12). In contrast, SUR1_{AAA}-Kir6.2 fusion channels

have a positive response to stimulation by MgADP (Fig. 4). These results provide convincing evidence that the $\Delta F1388$ mutation not only causes defective trafficking of the channel complex, it also affects sensitivity of the channel to ATP, MgADP, and diazoxide.

Figure 11

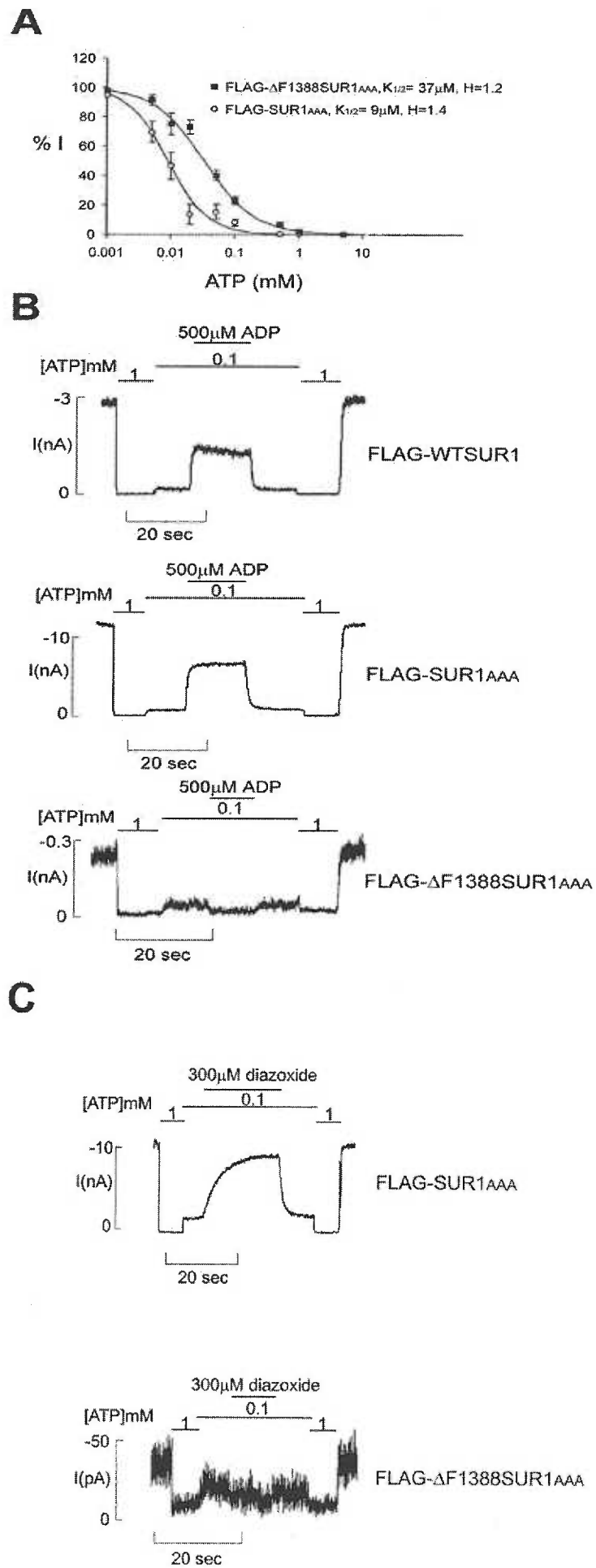




Fig. 11. FLAG- F1388 SUR1_{AAA} mutant channels have reduced ATP sensitivity and do not respond to MgADP or diazoxide. (A) Dose-response curves of FLAG-SUR1_{AAA} and FLAG- F1388 SUR1_{AAA} channels to ATP inhibition. The $K_{1/2}$ is estimated by fitting the data points to the Hill equation $\{I_{rel} = 1/[1 + ([ATP]/K_{1/2})^H]\}$, with I_{rel} being the current relative to the current in the absence of ATP. Each data point represents the average of 8-9 patches, with the error bar being the SEM. $H = 1.4$ and 1.2 for FLAG-SUR1_{AAA} and FLAG- F1388 SUR1_{AAA} channels, respectively. (B) Representative current traces recorded from inside-out membrane patches containing FLAG-wild type (WT) SUR1, FLAG-SUR1_{AAA}, or FLAG-F1388 SUR1_{AAA} channels. Currents were recorded at 50 mV. Inward currents are shown as upward deflections. Patches were exposed to differing concentrations of ATP and ADP, as indicated by the bars above the records. Free $[Mg^{2+}]$ was maintained at 1 mM in all ATP-containing solutions. (C) Representative current traces showing the lack of response to diazoxide of FLAG- F1388 SUR1_{AAA} channels, in contrast to FLAG-SUR1_{AAA} channels. Patches were exposed to differing concentrations of ATP and diazoxide, as indicated by the bars above the records. Free $[Mg^{2+}]$ was maintained at 1 mM in all ATP-containing solutions.

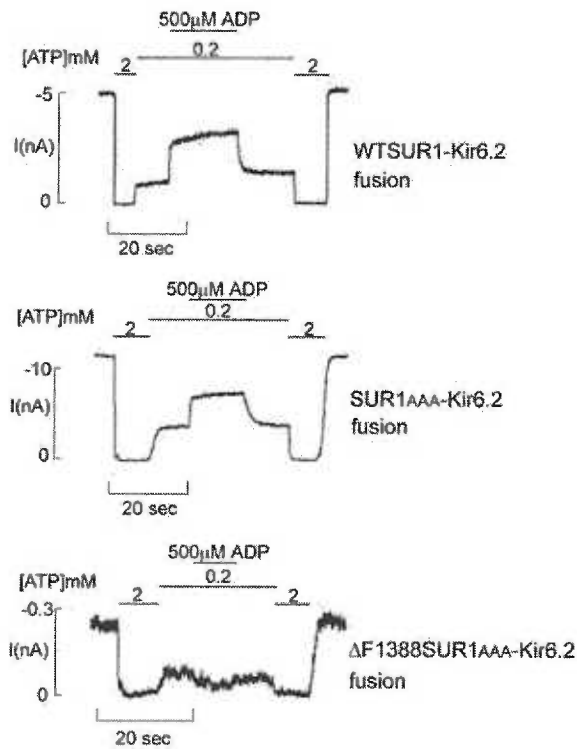


Fig. 12. F1388 SUR1_{AAA}-Kir6.2 fusion channels also lack response to MgADP. Patches containing fusion channels were exposed to differing concentrations of ATP and MgADP, as indicated by the bars above the records. Free $[Mg^{2+}]$ was maintained at 1 mM in all ATP-containing solutions. Currents were recorded at 50mV. Inward currents are shown as upward deflections. The higher ATP concentration used (200 μ M) was necessary to achieve sufficient inhibition of channel activity, because the fusion channels have lower ATP sensitivity ($K_{1/2} \sim 50 \mu$ M) compared with normal wild-type channels formed by SUR1 and Kir6.2 as individual subunits ($K_{1/2} \sim 10 \mu$ M) (5, 7).

Discussion

Mutations in K_{ATP} channels of pancreatic β cells are the major cause of the recessive form of PHHI [149, 150]. The molecular consequences of the known PHHI mutations include protein truncation because of premature stop codons and reduction or abolition of channel response to MgADP [52, 76, 152]. Our study of a single amino acid deletion mutation in SUR1, Δ F1388, provides direct evidence that, in addition, defective trafficking of K_{ATP} channels is also an underlying molecular mechanism of the disease. Future genetic and functional studies are expected to reveal more disease-associated mutant K_{ATP} channels that have trafficking defects.

Defective trafficking of a number of ion channels are known to cause human diseases. For example, the most prevalent cystic fibrosis-causing mutation of CFTR, Δ F508, results in mistrafficking of the channel protein [85]. Several mutations in the human *ether-a-go-go* potassium channels identified in congenital long QT syndrome (OMIM 152427) have processing and trafficking defects [159]. Studies of Δ F508 CFTR have shown that the defective trafficking is a consequence of its structural misfolding [129] [160] [161]. SUR1 shares structural similarity with CFTR. They both belong to the ATP-binding cassette (ABC) transporter family and contain two intracellular NBFs that are highly conserved [22]. Intriguingly, both F508 of CFTR and F1388 of SUR1 are located in the NBFs. It will be interesting to determine whether Δ F1388 SUR1 also adopts a misfolded conformation. One of the hallmarks of CFTR Δ F508 is that the mutant protein is rapidly degraded by the proteasome-dependent pathway [162], resulting in reduced cellular protein levels. We did not observe significant differences in the steady-state

protein levels between wild-type SUR1 and Δ F1388 mutant SUR1. However, our immunoblots provide only a rough assessment of total protein levels; more sensitive kinetic measurements may be required to see whether the degradation rates of wild-type SUR1 and Δ F1388 SUR1 differ. Comparative studies of Δ F508 CFTR and Δ F1388 SUR1 mentioned above will provide insight into the role of these phenylalanine residues in the folding and function of the NBFs and ABC transporters.

Various strategies have been developed to correct protein misfolding. These include temperature reduction, the use of generic chemical chaperones such as glycerol, and the use of specific ligands that bind to the protein [163, 164] [165] [166]. Recently, it was shown in CFTR that inactivation of arginine-framed ER-retention signals partially overcomes the trafficking defect caused by the Δ F508 mutation [157]. We demonstrate here that inactivation of RKR in SUR1 also partially overcomes the trafficking defect caused by the Δ F1388 mutation. Although the mechanism by which inactivation of RKR signal allows partial surface expression of Δ F1388 SUR1 is not yet clear, we speculate that inactivation of the retention signal may allow some misfolded mutant protein that is destined to degradation to escape the ER quality control mechanism. Interestingly, in the case of CFTR, multiple arginine-framed signals are present, and the extent of rescue of the Δ F508 mutant was greater when all four arginine-framed signals were inactivated simultaneously than when they were inactivated individually [157]. It would be important to search for additional arginine-framed signals in SUR1 and examine how they affect the trafficking of the wild-type and the Δ F1388 mutant SUR1/K_{ATP} channel complex.

would not be physiologically functional because they would not be able to sense changes in glucose levels.

In summary, two molecular consequences arise from the Δ F1388 mutation in SUR1: (i) defective trafficking of K_{ATP} channels, resulting in lack of channel expression on the cell surface, and (ii) changes in channel response to ATP and MgADP. These results suggest that F1388 provides structural elements critical for the correct trafficking and function of K_{ATP} channels. Although a potential interpretation of our findings is that the Δ F1388 mutation does not directly affect the trafficking of the channel and that intracellular retention of the mutant channel results from ER quality-control mechanisms that prevent the exit of dysfunctional channels, we do not favor this interpretation because a number of other PHHI mutant K_{ATP} channels that do not respond to MgADP and are physiologically nonfunctional have surface expression levels equivalent to that of wild-type channels [76, 152].

Abbreviations.

PHHI, persistent hyperinsulinemic hypoglycemia of infancy; CFTR, cystic fibrosis transmembrane conductance regulator; ER, endoplasmic reticulum; NBF2, second nucleotide-binding fold.

CHAPTER TWO

Modulation of the Trafficking Efficiency and Functional Properties of ATP-sensitive Potassium Channels through a Single Amino Acid in the Sulfonylurea Receptor

Etienne A. Cartier, Shu Shen, and Show-Ling Shyng

From the Center for Research on Occupational and Environmental Toxicology, Oregon Health and Science University, Portland, Oregon 97201

Abstract

Mutations in the sulfonylurea receptor 1 (SUR1), a subunit of ATP-sensitive potassium (K_{ATP}) channels, cause familial hyperinsulinism. One such mutation, deletion of phenylalanine 1388 (Δ Phe-1388), leads to defects in both trafficking and MgADP response of K_{ATP} channels. Here we investigated the biochemical features of Phe-1388 that control the proper trafficking and function of K_{ATP} channels by substituting the residue with all other 19 amino acids. Whereas surface expression is largely dependent on hydrophobicity, channel response to MgADP is governed by multiple factors and involves the detailed architecture of the amino acid side chain. Thus, structural features in SUR1 required for proper channel function are distinct from those required for correct protein trafficking. Remarkably, replacing Phe-1388 by leucine profoundly alters the physiological and pharmacological properties of the channel. The F1388L-SUR1 channel has increased sensitivity to MgADP and metabolic inhibition, decreased sensitivity to glibenclamide, and responds to both diazoxide and pinacidil. Because this conservative amino acid substitution occurs in the SUR2A and SUR2B isoforms, the mutation provides

a mechanism by which functional diversities in K_{ATP} channels are generated.

Introduction.

ATP-sensitive potassium (K_{ATP}) channels play a key role in linking metabolism to membrane excitability in muscle, neurons, and endocrine cells [6] [27]. Each K_{ATP} channel complex is composed of four subunits of a regulatory sulfonylurea receptor (SUR)¹ and four subunits of a pore-forming inward rectifier potassium channel Kir6.2 [24] [144] [145]. The activity of K_{ATP} channels is regulated by intracellular ATP and ADP; ATP inhibits channel activity via nonhydrolytic binding to the channel, whereas ADP stimulates channel activity in the presence of Mg^{2+} in a nucleotide hydrolysis-dependent way [6] [27]. Structure-function studies have led to the current view that the Kir6.2 subunit mediates channel inhibition by ATP [28] [32], and the SUR subunit mediates the stimulatory effects of MgADP as well as channel response to sulfonylureas and potassium channel openers (KCOs) [4] [49] [10] [51]. There are two known SUR genes, *SUR1* and *SUR2*. *SUR2* further gives rise to several splice variants, the major ones being SUR2A and -2B, which differ in the last 42 amino acids. SUR1, SUR2A, and SUR2B, when combined with Kir6.2, form the pancreatic, cardiac, and vascular smooth muscle subtypes of K_{ATP} channels, respectively [168] [11] [15]. These subtypes of K_{ATP} channels differ in their sensitivities to nucleotides, sulfonylureas, and KCOs [4] [169]. SURs belong to the ATP Binding Cassette family of membrane proteins (ABC transporters); each SUR molecule contains two of the nucleotide binding domains (NBD) that are highly conserved in all ABC transporters. Biochemical evidence suggests that

hydrolysis of MgATP at NBD2 stabilizes binding of ATP at NBD1 and thereby facilitates functional coupling between SUR1 and Kir6.2 and channel activation[56] [59] [170]. An increase in ADP concentrations stimulates channel activity likely by slowing the rate of ATP hydrolysis at NBD2, locking NBD2 in a post-hydrolytic MgADP-bound state [59] . Because the stimulatory effect of ADP requires Mg²⁺ and hydrolyzable nucleotides, we will refer to the effect as the MgADP response.

In the pancreas, K_{ATP} channels regulate insulin secretion in response to changes in blood glucose levels. Loss of functional K_{ATP} channels as a result of genetic mutations is a major cause of familial hyperinsulinism, a disease characterized by excessive insulin secretion and severe hypoglycemia [75] [150]. In many cases, mutations in SUR1 or Kir6.2 attenuate or abolish K_{ATP} channel function by causing protein truncations or by affecting the ability of the channel to respond to MgADP [76] [75] [150] [152]. Recently, defective trafficking of K_{ATP} channels has emerged as another important mechanism underlying the disease [123, 171] [172] [173]. Under normal conditions, trafficking of K_{ATP} channel complexes out of the endoplasmic reticulum (ER) is controlled by a tripeptide Arg-Lys-Arg (RKR) retention/retrieval signal present in each of the SUR and Kir6.2 subunits [12]. Upon successful assembly of SUR and Kir into an octameric complex, the -RKR- motifs are concealed to allow the channel to translocate from the ER to the Golgi, where the sugar moiety on SUR is modified before further translocation to the plasma membrane [24] [123] [12] [156, 174]. Thus, the -RKR- trafficking signal provides a quality control mechanism to prevent individual subunits as well as incompletely assembled channel complexes from trafficking to the cell surface.

One mutation that we have reported previously to cause defective channel trafficking is the deletion of phenylalanine at position 1388 of SUR1 (Δ Phe-1388). The Δ Phe-1388-SUR1 mutant channels were retained in the ER, unable to reach the cell surface [173]. However, a small percentage of them could escape to the cell surface when the RKR retention signal in SUR1 was inactivated by mutation [173]. The mutant channels thus expressed on the cell surface showed no response to MgADP and therefore would not be able to respond to metabolic changes. These observations indicate that Phe-1388 of SUR1 is critical for both correct trafficking and function of K_{ATP} channels. In the present study, we investigated the biochemical properties of the phenylalanine residue that are important in each aspect of channel regulation by substituting Phe-1388 in SUR1 with other amino acids (collectively referred to as F1388X-SUR1 mutants). We show that the substitutions have differential effects on channel trafficking and channel response to MgADP (hence channel function). Whereas hydrophobicity determines the efficiency of channel trafficking, the detailed architecture of the amino acid side chain appears to be important in ensuring proper channel response to MgADP. Importantly, replacing Phe-1388 by leucine dramatically potentiated channel response to MgADP. Such a "gain of MgADP response" phenotype may be exploited for therapeutic purposes in managing insulin secretion. Moreover, F1388L-SUR1 mutant channels exhibit reduced sensitivities to glibenclamide and are stimulated by both diazoxide and pinacidil, properties resembling the SUR2B/Kir6.2 channels found in vascular smooth muscle [4] [169] [69]. These results demonstrate the role that the 1388 residue of SUR1 plays in modulating the physiological and pharmacological properties of K_{ATP} channels. Because the SUR1-Phe-1388 equivalent position in SUR2A and SUR2B is occupied by a leucine, our results also

suggest that the conservative change between phenylalanine and leucine may serve as a mechanism for generating functional diversity in K_{ATP} channels.

Experimental Procedures

Construction of SUR1 Mutations-- Point mutations of SUR1 were introduced into hamster FLAG-SUR1 cDNA in the pECE plasmid using the QuickChange site-directed mutagenesis kit (Stratagene) as described previously [173]. Epitope tag and mutations were confirmed by DNA sequencing. All SUR1 constructs are in the pECE vector and mouse Kir6.2 cDNA in the pCMV6b vector (a gift from Dr. S. Seino). In immunoblotting experiments, a rat Kir6.2 in pCDNA3 (a gift from Dr. C. Vandenberg) was used for cotransfection. Mutant clones from multiple PCRs were analyzed in all experiments to avoid false results caused by undesired mutations introduced by PCR. In some cases, an additional subcloning step (a restriction fragment of *NotI* and *EcoRI* corresponding to nucleotide positions 4135-4858 of the plasmid) was used to minimize potential PCR-introduced artifacts.

Chemiluminescence Assay-- Surface expression of channels was quantified as described previously [172]. COSm6 cells plated in 35-mm dishes were fixed with 4% paraformaldehyde for 30 min at 4 °C, 48-72 h after transfection. Fixed cells were pre-blocked in PBS + 0.1% BSA for 30 min or overnight, incubated in M2 anti-FLAG antibody (10 µg/ml) for an hour, washed 4 times for 30 min in PBS + 0.1% BSA, incubated in horseradish peroxidase-conjugated anti-mouse (The Jackson Laboratories,

1:1000 dilution) for 20 min, washed again 4 times for 30 min in PBS + 0.1% BSA, and 2 times for 5 min in PBS. Chemiluminescence signal of each dish was quantified in a TD-20/20 luminometer (Turner Designs) following 15 s of incubation in Power Signal Elisa luminol solution (Pierce). All steps after fixation were carried out at room temperature. Results of each experiment are the average of duplicate or triplicate dishes. For each mutant, 3-10 independent experiments were performed (see Fig. 1).

Immunoblotting-- Immunoblotting analyses were performed using COS-1 instead of COSm6 cells to avoid high background [172]. Although both gave qualitatively similar results, the rat Kir6.2 in pCDNA3 consistently yielded better expression of Kir6.2 than mouse Kir6.2 in pCMV6b when transfected in COS-1 cells; we therefore used rat Kir6.2 for immunoblotting experiments shown in Fig.2. Cells in 35-mm dishes were transfected with 0.6 μ g of SUR1 and 0.4 μ g of rat Kir6.2 per dish using FuGENE. Cells were lysed 48-72 h later in 20 mM HEPES, pH 7.0, 5 mM EDTA, 150 mM NaCl, 1% Nonidet P-40 with CompleteTM protease inhibitors (Roche Molecular Biochemicals). Proteins in cell lysates were separated by SDS-PAGE (8%), transferred to nitrocellulose, analyzed by incubation with the M2 anti-FLAG antibody followed by horseradish peroxidase-conjugated anti-mouse secondary antibodies (Amersham Biosciences), and visualized by chemiluminescence (Super Signal West Femto; Pierce).

Patch Clamp Recordings-- COSm6 cells were transfected using FuGENE and plated onto coverslips. The cDNA for the green fluorescent protein was cotransfected with SUR1 and Kir6.2 to facilitate identification of positively transfected cells. Patch clamp recordings were made 36-72 h post-transfection. All experiments were performed at room

temperature as described previously [173]. Micropipettes were pulled from non-heparinized Kimble glass (Fisher) on a horizontal puller (Sutter Instrument, Co., Novato, CA). Electrode resistance was typically 0.5-1 megohms when filled with K-INT solution (below). Inside-out patches were voltage-clamped with an Axopatch 1D amplifier (Axon Inc., Foster City, CA). The standard bath (intracellular) and pipette (extracellular) solution (K-INT) had the following composition: 140 mM KCl, 10 mM K-Hepes, 1 mM K-EGTA, pH 7.3. In experiments shown in Fig. 5A and the *inset* of Fig. 5B (dose-response curve to ATP and ADP), 1 mM EDTA was added to K-INT to chelate residual Mg^{2+} ; inclusion of EDTA in the K-INT solution significantly reduced channel rundown, making quantification of channel activities more reliable. All currents were measured at a membrane potential of -50 mV (pipette voltage = $+50$ mV). Data were analyzed using pCLAMP software (Axon Instrument). Off-line analysis was performed using Microsoft Excel programs. Data were presented as means \pm S.E. in most cases where $n \geq 3$ patches; in one case where $n = 2$ patches (F1388D-SUR1 mutant in Fig. 4), the value represents the mean \pm the difference between the individual value and the mean.

⁸⁶Rb⁺ Efflux Assay-- Cells were incubated for 24 h in culture medium containing ⁸⁶RbCl (1 μ Ci/ml) 2-3 days after transfection. Before measurement of Rb^{+} efflux, cells were incubated for 30 min at 25 °C in Krebs-Ringer solution, with different metabolic inhibitors (0.5-1 mM 2-deoxy-D-glucose, 2.5 μ g/ml oligomycin, or a combination of both). At selected time points, the solution was aspirated from the cells and replaced with fresh solution. At the end of a 40-min period, cells were lysed in Ringer's solution containing 2% SDS. The ⁸⁶Rb⁺ in the aspirated solution and the cell lysates was counted. The percentage efflux at each time point was calculated as the cumulative counts in the

aspirated solution divided by the total counts from the solutions and the cell lysates.

Results

Cell Surface Expression of the F1388X-SUR1 Mutant Channels-- Deletion of Phe-1388 of SUR1 causes failure of K_{ATP} channels to express on the cell surface. To examine which chemical features of the phenylalanine residue are critical for proper trafficking of the channel, we substituted Phe-1388 in SUR1 with all other 19 amino acids and determined how the substitutions affected surface expression of K_{ATP} channels. For all F1388X-SUR1 mutant constructs, a FLAG epitope tag was added to the N terminus to allow surface labeling of the protein. Each mutant SUR1 construct was cotransfected with wild-type (WT) Kir6.2 into COS cells, and surface expression of K_{ATP} channels was quantified by a chemiluminescence assay [172]. Results from chemiluminescence assays were further confirmed by immunofluorescent microscopy of surface-labeled FLAG-SUR1 (not shown). Based on surface expression levels, the mutants can be classified into two groups: those that give rise to expression levels above 50% that of the WT, and those that give rise to levels below 50% that of the WT (Fig. 13). Amino acids in the first group include Phe, Cys, Ala, Val, Leu, Ile, Met, and Trp; these amino acids are in general considered hydrophobic. By contrast, amino acids with polar and charged side chains dramatically reduced surface expression of the channel.

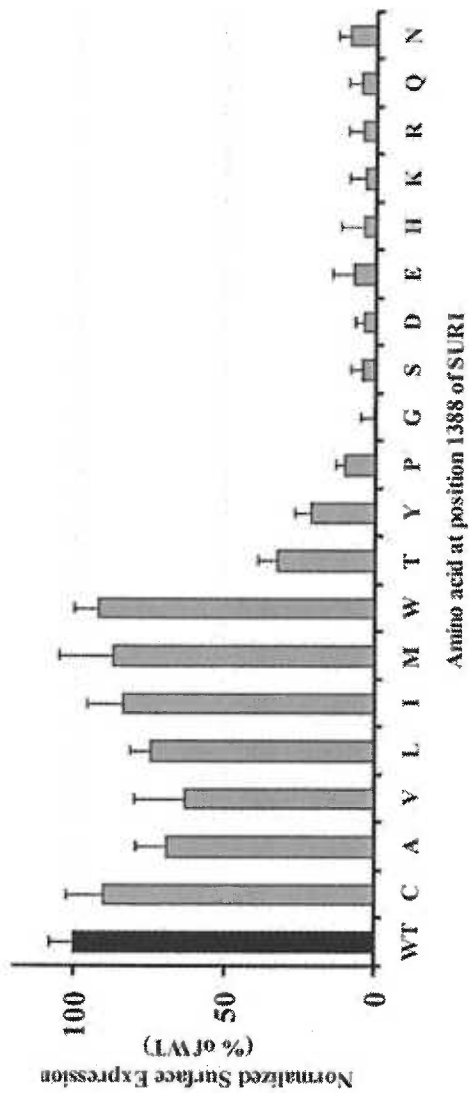


Fig. 13. Surface expression of the SUR1-F1388X mutant channels. COSM6 cells transiently expressing Kir6.2 and either the FLAG-tagged wild-type SUR1 (fWT) or the various FLAG-tagged F1388X-SUR1 mutants (fF1388X) were subjected to the chemiluminescence assay to monitor surface expression of the channel. Surface expression of all fF1388X-SUR1 mutant channels was normalized to that of the fWT channel (*error bars* represent standard error of the means of 3-10 independent experiments for each mutant). Channels with hydrophobic amino acids substituting Phe-1388 are grouped together and shown on the *left side* of the graph

Western Blot Analysis-- SUR1 protein that is expressed on the cell surface has traversed the Golgi apparatus where it becomes complex-glycosylated; this complex-glycosylated SUR1 has lower mobility than the core-glycosylated form on the SDS-PAGE and is referred to as the "upper band"[172] [173] [99] [174]. We examined the glycosylation pattern of F1388X-SUR1 mutants in cells coexpressing Kir6.2 by Western blots. All of the mutants in the first group of Fig.13 (Cys, Ile, Leu, Met, Val, Ala, and Trp) have an upper band that corresponds to the complex-glycosylated form, similar to the WT protein. On the other hand, all of the mutants in the second group of Fig. 13 have none or have a barely detectable (when overexposed, not shown) upper band. These results are consistent with surface expression results obtained by the chemiluminescence assay. Previous work [173] has found that the Δ Phe-1388 mutation abolished surface expression of K_{ATP} channels without significantly altering the steady-state SUR1 protein levels. We found that the steady-state total protein levels of F1388X-SUR1 mutants (the sum of the upper and the lower bands) in the first group are largely unaltered compared with the WT SUR1 (*upper two panels* of Fig. 14). However, mutants in the second group in general exhibited lower protein levels (*lower two panels* of Fig. 14), in particular, when Phe-1388 was substituted by Pro or Ser (marked with *asterisks* in Fig. 14). Similar results were obtained in cells expressing SUR1 mutant protein alone (not shown).

MgADP Response-- Earlier studies have demonstrated that a small percentage of the Δ Phe-1388-SUR1 mutant channels retained in the ER could escape to the cell surface when the -RKR- ER retention/retrieval motif in SUR1 was inactivated by mutation to AAA [173]. However, unlike the WT channels, the Δ Phe-1388_{RKR→AAA}-SUR1 channels

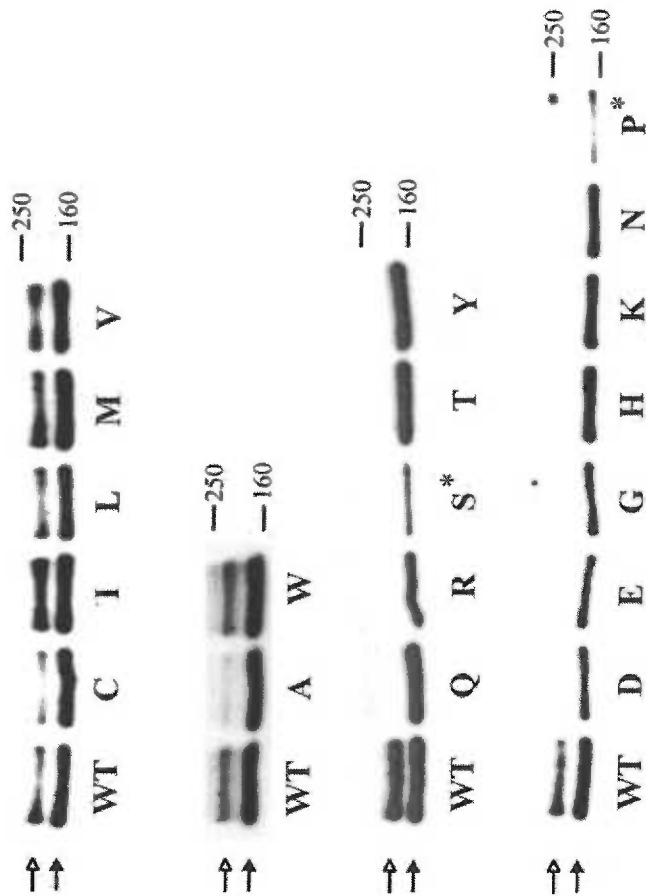


Fig. 14. Western blot analysis of the F1388X-SUR1 mutants. Steady-state SUR1 protein levels in COS-1 cells coexpressing Kir6.2 and one of the FLAG-tagged F1388X-SUR1 mutant proteins were estimated by Western blots using the M2 anti-FLAG antibody. *Solid arrow* indicates core-glycosylated SUR1; *open arrow* indicates complex-glycosylated SUR1. Molecular mass markers (kDa) are indicated on the *right*. Mutants are divided into two groups based on their surface expression levels (Fig. 1). Both core- and complex-glycosylated bands are present for mutants in group I; the ratio of complex- to core-glycosylated band roughly corresponds to the surface expression level of the protein. For mutant proteins in group II, however, only the core-glycosylated band is seen without overexposure of the film. In some cases (marked with *asterisk*), a clear reduction in the total protein level is observed.

expressed on the cell surface failed to respond to MgADP. The data presented above demonstrate that hydrophobicity of the amino acid at SUR1 position 1388 is a critical parameter in determining the ability of the channel to exit ER and express on the cell surface. To test if the same parameter governs channel response to MgADP, we performed inside-out patch clamp recordings of the F1388X-SUR1 mutant channels. Of the mutants that had poor surface expression, we managed to obtain a few patches from the F1388T, F1388Y, F1388P, F1388S ($n = 3-5$), and F1388D ($n = 2$) mutants. No patches containing detectable currents were obtained for the F1388G, F1388E, F1388H, F1388K, F1388N, F1388Q, and F1388R mutants. Typical current traces from the WT and the mutant channels are shown in Fig. 15. The MgADP response was quantified as the current in a solution containing 0.1 mM ATP, 0.5 mM ADP, and 1 mM free Mg^{2+} , relative to the current in the absence of any nucleotides. This response in mutant channels was further normalized to the response obtained in WT channels and is shown in Fig. 4.

Comparing Fig. 16 (MgADP response) to Fig. 13 (cell surface expression), it becomes immediately clear that the chemical properties of the amino acid at the SUR1 1388 site governing channel expression are distinct from those governing channel response to MgADP. Many of the amino acid substitutions that are tolerated for surface expression have very poor response to MgADP (for example, F1388C, F1388V, and F1388I), and vice versa, some of the amino acid substitutions that render poor surface expression of the channel still retain the ability to respond to MgADP (for example, F1388T and F1388S). Remarkably, the leucine and isoleucine substitutions, although both resulted in efficient channel expression, differed dramatically in their response to MgADP. Whereas leucine potentiated channel response to MgADP by nearly 1.7-fold (Fig. 4), isoleucine almost

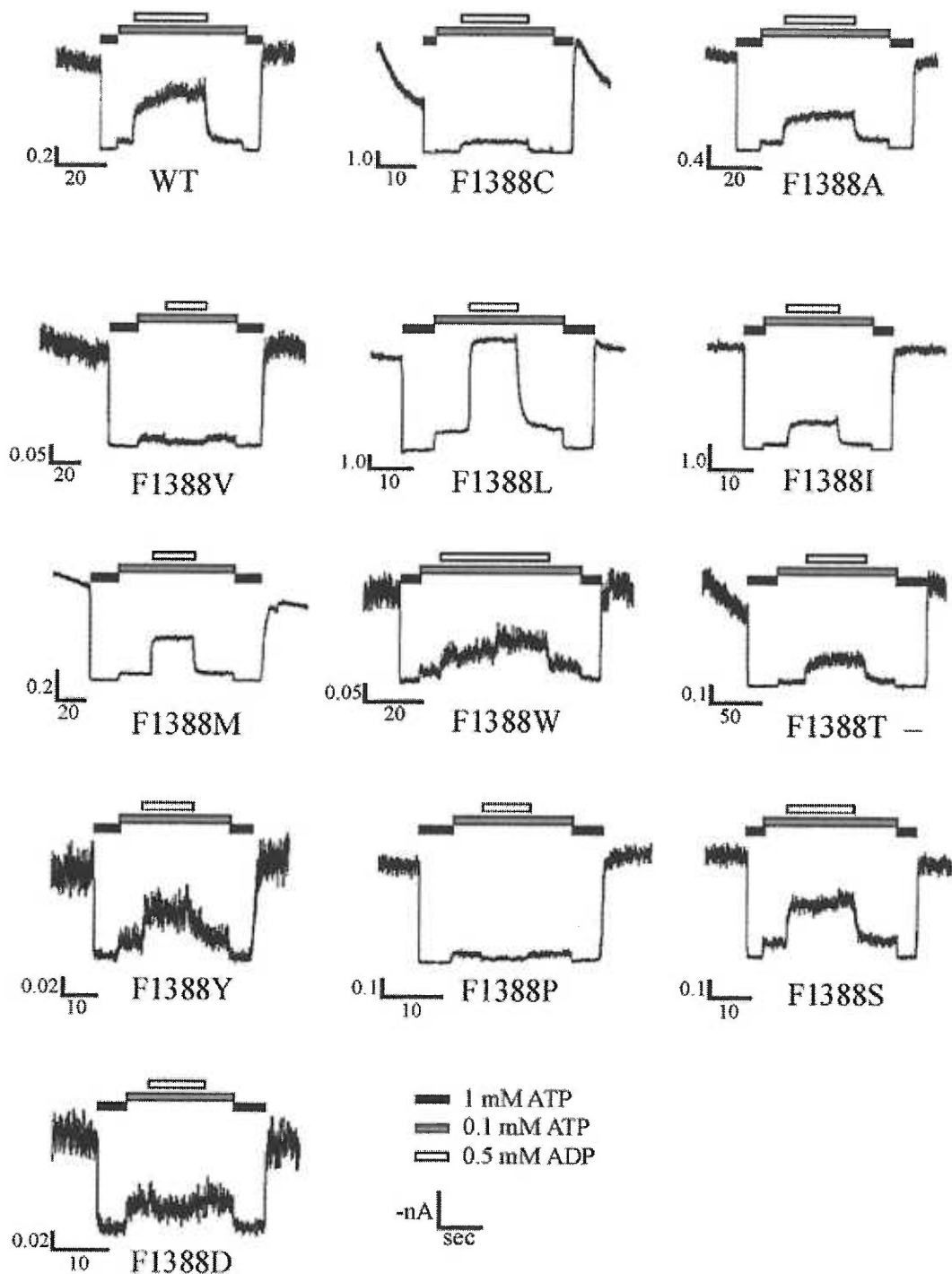


Fig. 15. MgADP response of F1388X-SUR1 mutant channels. Representative recordings from inside-out membrane patches containing WT or F1388X-SUR1 channels. Patches were excised into K-INT solution (140 mM KCl, 10 mM K-Hepes, 1 mM K-EGTA, pH 7.3) and exposed to differing concentrations of ATP and ADP, as indicated by the *bars above* the records. In all solutions containing nucleotides, free Mg^{2+} concentration was kept ~ 1 mM. Currents in this and subsequent figures were recorded at 50 mV, and inward currents are shown as upward deflections. Similar results were obtained from SUR1 mutant constructs with the N-terminal FLAG tag (not shown).

abolished channel response to MgADP (Figs. 15 and 16). The two amino acids have the exact same chemical compositions and similar physical chemical properties; the only difference between them is the architecture of the side chain. Therefore, the parameters required for conferring MgADP response appear to involve detailed side chain structures and not just hydrophobicity.

Characterization of the Physiological and Pharmacological Properties of the F1388L-SUR1 Mutant Channel-- The observation that the F1388L-SUR1 mutant channels are better stimulated by MgADP prompted us to characterize these channels in greater detail. Sequence comparison between SUR1 and SUR2A and -2B reveals that the SUR1-Phe-1388 equivalent residue in SUR2A and -2B is a leucine [10]. SUR1, SUR2A, and SUR2B, when combined with Kir6.2, form the pancreatic, cardiac, and vascular smooth muscle subtypes of K_{ATP} channels, respectively. These K_{ATP} channel subtypes display different sensitivities to ATP, MgADP, sulfonylureas, and potassium channel openers [4] [169] [69] [175]. The SUR1/Kir6.2 recombinant channels have high sensitivities to inhibition by ATP ($K_i \sim 10 \mu\text{M}$) and glibenclamide ($K_i < 10 \text{ nM}$) and are stimulated only by the KCO diazoxide. Channels containing the SUR2 isoforms, on the other hand, have lower sensitivities to ATP and glibenclamide but are stimulated by potassium channel openers other than diazoxide, such as pinacidil and cromakalim [4] [10, 11, 73, 74, 169, 176]. We wondered whether the conservative exchange between phenylalanine and leucine accounts for some of these physiological and pharmacological differences.

ATP dose-response measurements in the absence of Mg^{2+} yielded a K_i of $13.8 \pm 4.3 \mu M$ for the WT channels and $16.4 \pm 3.5 \mu M$ for the F1388L-SUR1 channels (Fig. 17A). These values are not significantly different from one another (at $p = 0.1$), indicating that Phe-1388 is not a determinant of channel sensitivity to ATP^{4-} . As shown in Figs. 15 and 16, F1388L-SUR1 channels are better stimulated than WT channels by 0.5 mM MgADP in the presence of 0.1 mM inhibitory ATP. We next examined the dose-response relationship of these two channels for MgADP activation in detail in the absence of ATP. Although MgADP stimulates channel activity via the SUR subunit, it also inhibits channel activity by interacting with Kir6.2, with less potency than ATP. To remove the inhibitory effect of ADP from our analysis, we first constructed ADP inhibition dose-response curves for both WT and Phe-1388-SUR1 mutant channels. These curves were obtained in the absence of Mg^{2+} (K-INT plus 1 mM EDTA) because the inhibitory effect of ADP on Kir6.2 does not require Mg^{2+} . Similar to ATP inhibition, no significant difference in ADP inhibition was observed between WT and mutant channels (not shown). Therefore, data from the two channels were pooled to generate one ADP inhibition dose-response curve (*inset* of Fig. 17B). The inhibitory effects of ADP were then compensated for in constructing the dose-response curves for the stimulatory effects of MgADP (Fig. 17B). The data for both WT and the F1388L-SUR1 mutant channels thus generated are well fitted by a modified Hill equation (see legends for Fig. 17B), giving rise to an EC_{50} (half-maximal stimulation concentration) of 131 μM and 1.8-fold maximal stimulation for WT channels, and an EC_{50} of 36 μM and 2.3-fold maximal stimulation for the F1388L-SUR1 mutant channels. These results clearly demonstrate that the F1388L-SUR1 channels are much more sensitive to a small increase in ADP concentrations than WT channels, and

predict that the F1388L-SUR1 channels would open more readily when cells are challenged by metabolic inhibition. To confirm this, we subjected cells transfected with either WT or F1388L-SUR1 channels to different metabolic conditions and used the Rb^+ efflux assay to monitor channel activities in intact cells. In the absence of metabolic inhibitors, F1388L-SUR1 channels displayed higher basal activities than WT channels (Fig.18). In cells treated with 0.1 to 1 mM 2-deoxy-D-glucose, the F1388L-SUR1 channel continued to show higher activities. These results are consistent with our prediction. When cell metabolism was maximally inhibited by 1 mM 2-deoxy-D-glucose plus 2.5 μ g/ml oligomycin, the difference between F1388L-SUR1 and WT channels diminished, likely because both channels were now maximally activated, and the Rb^+ efflux rates were saturated.

Next, we examined glibenclamide sensitivities. WT channels were inhibited by ~60% at 10 nM glibenclamide (Fig. 19A), consistent with a $K_i < 10$ nM from previous reports [4]. The F1388L-SUR1 channels, however, were less sensitive to glibenclamide, showing only ~30% inhibition at 10 nM. Finally, we looked at how channel sensitivities to the potassium channel openers diazoxide, pinacidil, and cromakalim might be altered. Both WT and F1388L-SUR1 channels were stimulated by diazoxide. However, like MgADP, diazoxide is much more potent in stimulating F1388L-SUR1 than WT channels (Fig. 19B). Both cromakalim and pinacidil are effective KCOs for the SUR2A/Kir6.2 and SUR2B/Kir6.2 channels but not for the SUR1/Kir6.2 channels [4] [169] [69]. By using the same protocol as shown in Fig. 7B (except that diazoxide was now substituted by cromakalim), neither WT nor F1388L-SUR1 channels were activated by cromakalim, even at 500 μ M (data not shown). Interestingly, however, pinacidil stimulated the

F1388L-SUR1 mutant channels at concentrations of 300 μM and above (Fig. 19C), although it remained ineffective on WT channels even above 500 μM . The overall physiological and pharmacological profile of the F1388L-SUR1 mutant channels led us to conclude that the F1388L mutation significantly shifts the functional properties of the channel toward those resembling subtypes containing the SUR2B isoform.

Discussion

Many mutant proteins with trafficking defects are retained in the ER because they are unable to fold properly or efficiently. The same mutations that cause protein misfolding may also alter protein function. In these cases, the altered function may be due to direct involvement of the mutated residues in protein function or may be an indirect consequence of protein misfolding. Our previous work on a disease-causing SUR1 mutation, $\Delta\text{Phe-1388}$, has found that the mutation not only causes ER retention, and thereby defective trafficking, of the protein and its associated channel subunit Kir6.2, but also abolishes channel response to MgADP. By substituting Phe-1388 with different amino acids and analyzing the effect of each substitution on the trafficking and function of K_{ATP} channels, we demonstrate here that the biochemical criteria for correct channel trafficking are separable from those for proper channel function, specifically channel response to MgADP. These results support the notion that Phe-1388 in SUR1 plays a direct role in channel function. This notion is further strengthened by the observations that conservative substitution of Phe-1388 by leucine, although with little effect on channel trafficking, markedly changed the sensitivities of the channel to MgADP, metabolic inhibition, glibenclamide, and potassium channel openers.

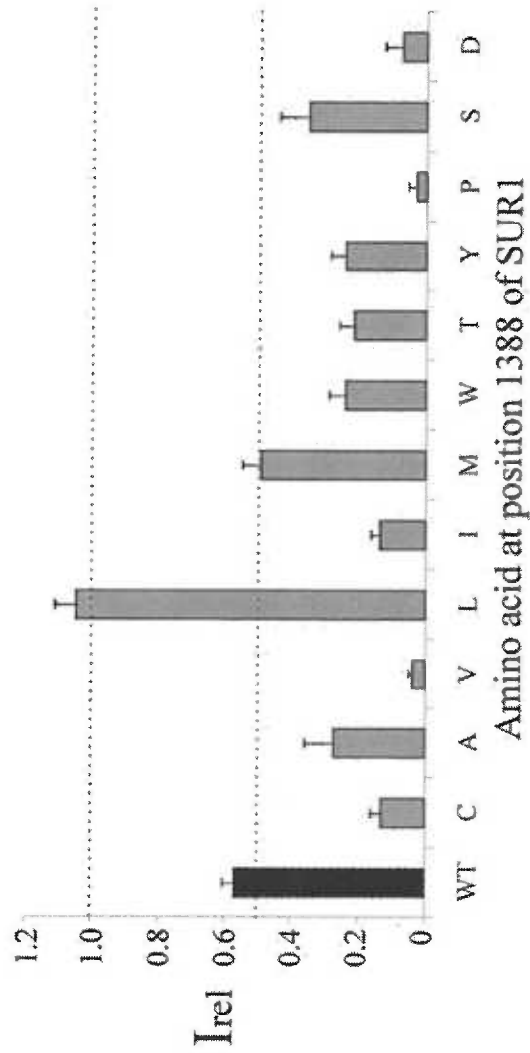
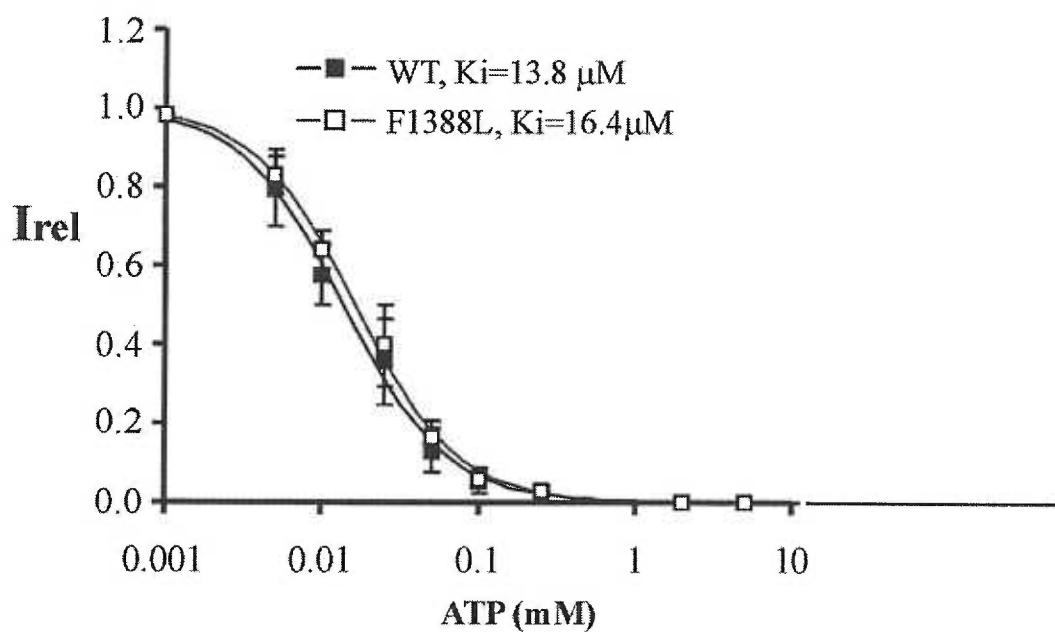
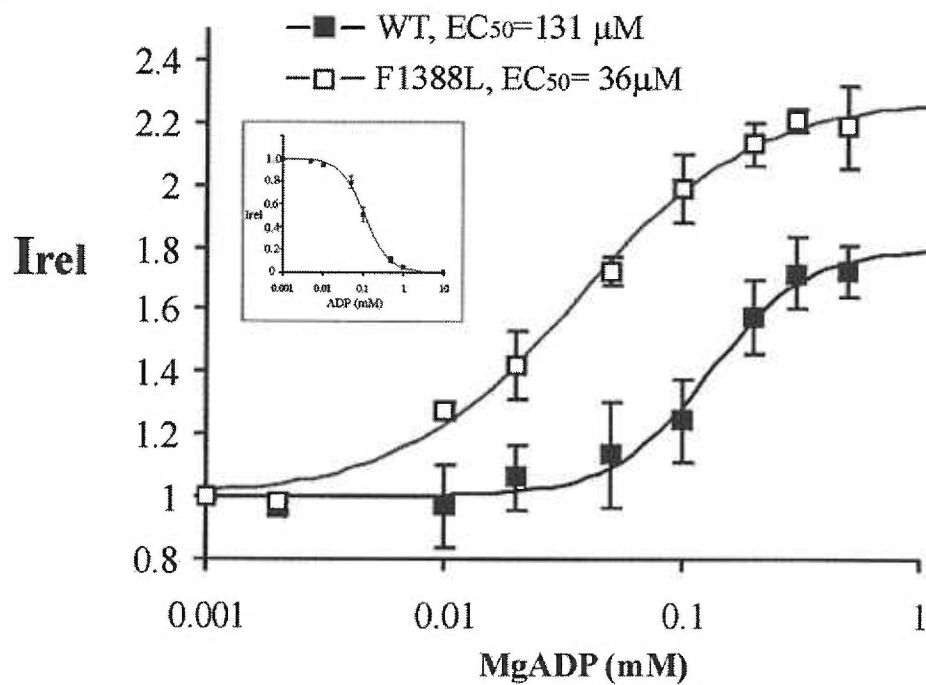


Fig. 16. Quantitation of the MgADP response. The MgADP response of a mutant channel was first calculated as the maximal currents obtained in K-INT solution containing 0.1 mM ATP, 0.5 mM ADP, and 1 mM free Mg^{2+} , relative to that in K-INT. This value was then expressed as a fraction of that obtained from WT channels. With the exception of F1388D, the values in the *bar graph* represent the average of 3-12 patches, with *error bars* representing the S.E. of the mean. For the F1388D mutant channel, the mean value is the average of 2 patches, with the *error bar* showing the difference between the individual values and the average. Note the differential effects of amino acid substitutions on surface expression (Fig. 1) and MgADP response.

Fig. 17. Nucleotide sensitivities of F1388L-SUR1 mutant channels. *A*, dose response of F1388L-SUR1 mutant channels to ATP, compared with that of WT channels. Currents in various concentrations of ATP are expressed as a fraction of the mean of currents obtained in the absence of ATP (I_{rel}). Both pipette and bath solutions contained K-INT plus 1 mM EDTA to minimize channel rundown. The curves are fitted to the Hill equation: $I_{rel} = 1/\{1 + ([ATP]/K_i)^H\}$, where K_i is the ATP concentration that gives half-maximal inhibition. For WT channels (*black squares*; $n = 4-7$ patches for each data point), $K_i = 13.8 \mu\text{M}$, and $H = 1.3$; for F1388L-SUR1 mutant channels (*open squares*; $n = 4-7$), $K_i = 16.4 \mu\text{M}$, and $H = 1.4$. *B*, dose response of WT and F1388L-SUR1 mutant channels to the stimulatory effect of MgADP. To correct for the inhibitory effect of ADP mediated by the Kir6.2 subunit, an ADP dose-response curve was first constructed in the absence of Mg^{2+} (see *inset*; because no significant difference was seen between WT and Phe-1388-SUR1 channels, the data were pooled to generate one curve fitted to the Hill equation described above, with $K_i = 110 \mu\text{M}$, and $H = 1.5$). To obtain the net stimulatory effects of MgADP, patches were excised into K-INT solutions and then exposed to various concentrations of MgADP (free Mg^{2+} concentration was kept at 1 mM). The relative current in each concentration of MgADP, calculated as a fraction of the mean of currents obtained before and after exposure to MgADP, was then added to the relative current inhibited by the same concentration of ADP (obtained from the ADP inhibition dose-response curve shown in the *inset*) to compensate for the inhibitory effect of ADP. The final I_{rel} thus obtained was then plotted against MgADP concentrations. The curves are fitted to the modified Hill equation: $I_{rel} = I_{max} + (1 - I_{max})/\{1 + ([\text{MgADP}]/\text{EC}_{50})^H\}$, where EC_{50} is the MgADP concentration that gives half-maximal stimulation and I_{max} is the maximal stimulation. For WT channels (*black squares*; $n = 3-5$ patches), $I_{max} = 1.8$, $H = 2.1$, and $\text{EC}_{50} = 131 \mu\text{M}$; for F1388L-SUR1 mutant channels (*open squares*; $n = 3-5$ patches), $I_{max} = 2.3$, $H = 1.2$, and $\text{EC}_{50} = 36 \mu\text{M}$.



A**B**

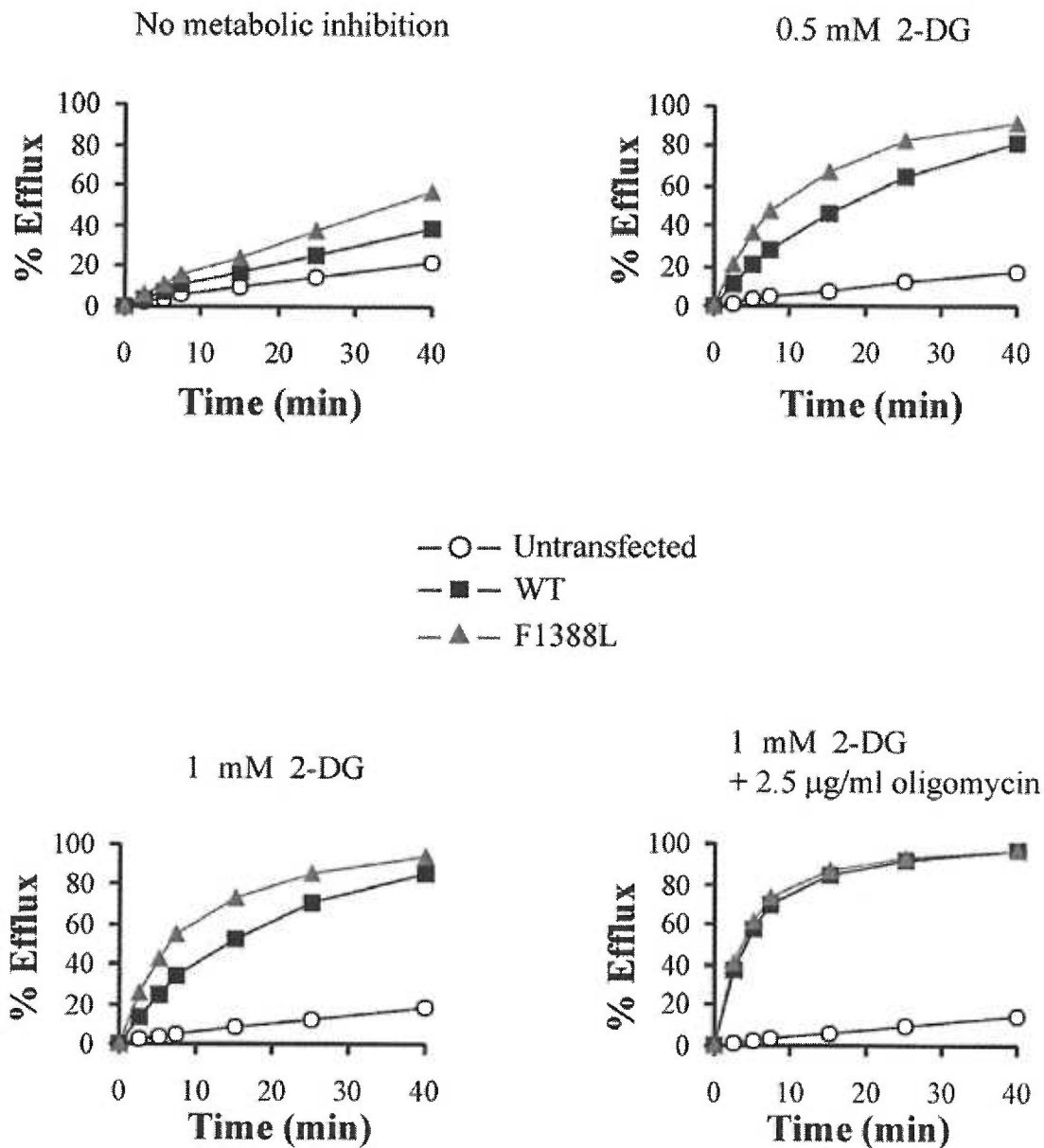
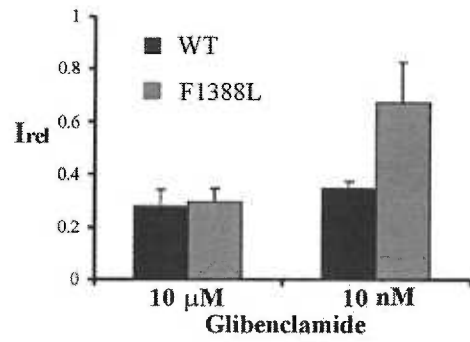
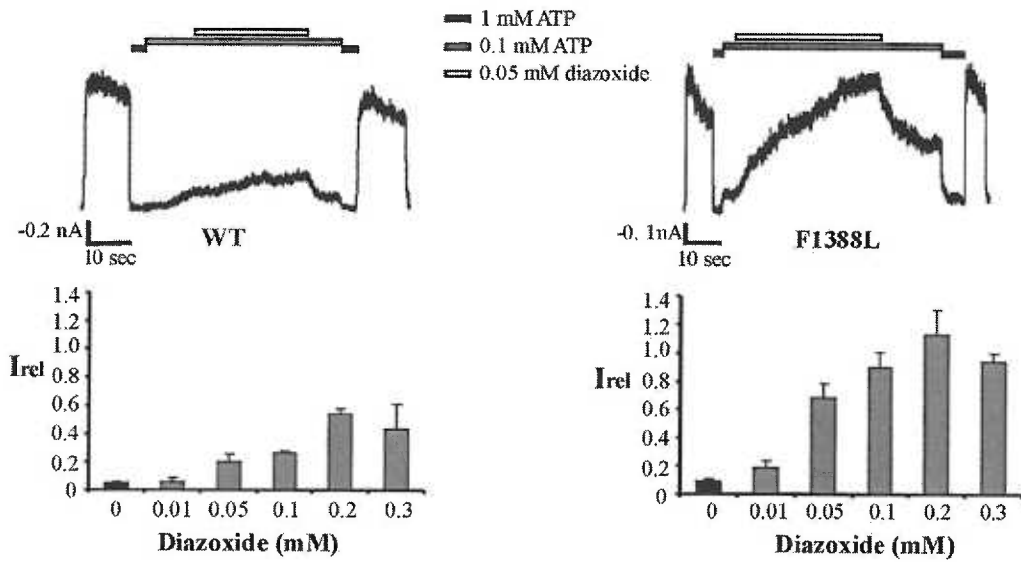
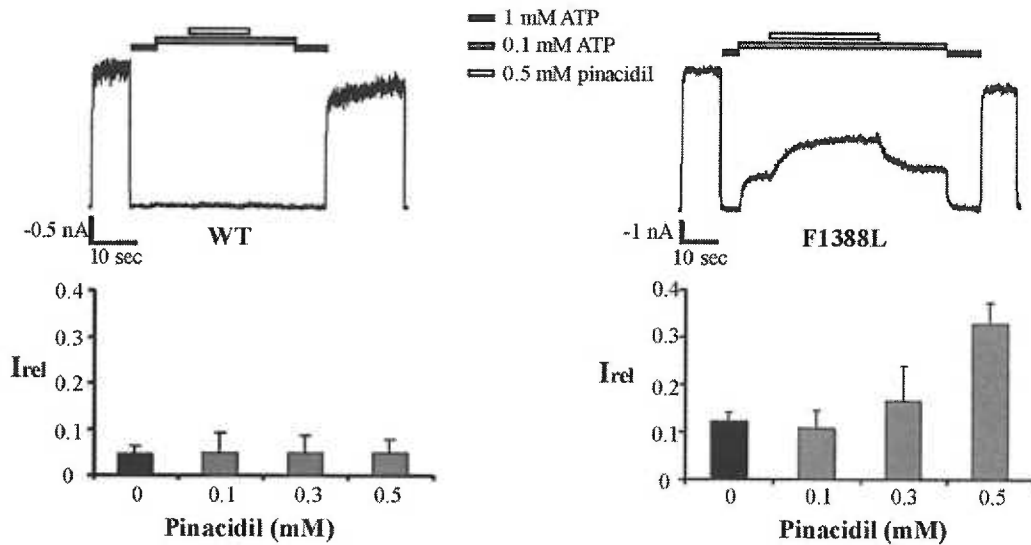


Fig. 18. Response of F1388L-SUR1 mutant channels to metabolic signals. Response of WT and F1388L-SUR1 mutant channels to metabolic inhibition in intact cells. Cells were preincubated for 30 min in Ringer's solution containing no drugs, 0.5 or 1 mM 2-deoxy-D-glucose (DG), or 1 mM 2-deoxy-D-glucose plus 2.5 $\mu\text{g/ml}$ oligomycin, before Rb^+ flux measurements. Similar results were obtained from 4 independent experiments. For clarity, efflux profile from only one representative experiment is shown for each metabolic condition

Fig. 19. Pharmacological properties of the F1388L-SUR1 mutant channels. *A*, channel response to glibenclamide. The current in 10 nM or 10 μ M glibenclamide was expressed as a fraction of that obtained in K-INT (I_{rel}); $n = 4-8$ patches for each bar. *B*, channel response to diazoxide. *Upper*, representative current recordings from inside-out membrane patches containing WT or F1388L-SUR1 channels. Patches were excised into K-INT solutions and exposed to 1 mM ATP, 0.1 mM ATP, or 0.1 mM ATP plus 50 μ M diazoxide. Free Mg^{2+} concentration was kept at 1 mM in all solutions. *Lower*, quantification of diazoxide response. Diazoxide response is expressed as currents obtained in K-INT solution containing diazoxide plus 0.1 mM ATP and 1 mM free Mg^{2+} , relative to currents obtained in K-INT. Data points are mean \pm S.E., $n = 4-5$ patches. *C*, same as *B* except the channels were now tested for pinacidil response. Data points are mean \pm S.E., $n = 3-6$ patches. Note that the WT channel activity in 0.1 mM ATP is lower than that of the F1388L-SUR1 mutant channels in both *B* and *C*. This is because in the presence of Mg^{2+} , ATP undergoes hydrolysis at SUR1 to generate MgADP, which stimulates channel activity. Because the mutant channel is more sensitive to MgADP stimulation, as demonstrated in Fig. 5, it exhibits higher activity than the WT channels.



A**B****C**

Correlation between Structure and Function-- SUR is a member of the ABC transporter protein superfamily. The crystal structures of a number of bacterial ABC transporters or their nucleotide binding domains have been published [177]. These studies show that the nucleotide binding domains from different ABC transporters share the same basic fold. Amino acid sequence alignment places Phe-1388 of SUR1 in the α -helix immediately following the Walker A motif. In terms of channel trafficking, most hydrophobic amino acid substitutions at the 1388 position are tolerated. It is not surprising that deletion of Phe-1388 or substitution of Phe-1388 by charged amino acids may disrupt the folding of the α -helix, thereby impeding subsequent trafficking of the protein. Interestingly, however, in the nucleotide binding domain of some ABC transporters, including MalK and the NBD1 of human glycoprotein and multidrug-resistant protein, the homologous position is occupied by a threonine [178-180]. This suggests that threonine should allow proper folding of the protein. However, in the case of SUR1, substitution of Phe-1388 by threonine significantly compromised the trafficking efficiency of K_{ATP} channels. It is possible that this substitution affects events that are downstream of protein folding and that are relevant to channel trafficking. For example, it might affect the efficiency of assembly between SUR1 subunits and/or between SUR1 and Kir6.2 subunits or it might affect the shielding of the -RKR- ER retention/retrieval signals in the channel complex.

In some mutants, especially F1388P and F1388S, a lower steady-state protein level was seen (Fig. 14). One possible explanation is that these mutant proteins are rapidly degraded. Many proteins retained in the ER undergo ER-associated degradation via the

ubiquitin-proteasome pathway [137]. We found that treating cells with proteasome inhibitors led to a marked increase in the levels of the aforementioned SUR1 mutant proteins, as assessed by immunostaining. In Western blots, the same treatment led to the appearance of higher molecular weight complexes suggestive of polyubiquitinated forms of mutant SUR1.² These findings provide preliminary evidence that like the Δ F508 mutant of CFTR, some F1388X-SUR1 mutants are rapidly degraded by the proteasomes. They also raise an interesting future question of why some F1388X-SUR1 mutants are more prone to degradation than others.

How is Phe-1388 of SUR1 involved in channel response to MgADP? The side chain architecture of the amino acid appears important in conferring proper channel response to MgADP. This is most clearly demonstrated by comparing the leucine and isoleucine substitutions. Leucine and isoleucine have the same chemical composition, similar physical-chemical properties, and both are found in the Phe-1388 homologous position in other ABC transporters. Neither substitution leads to substantial reduction in surface expression of the channel. However, leucine greatly potentiates channel response to MgADP, whereas isoleucine nearly abolishes channel response to MgADP (assayed as currents stimulated by 0.5 mM MgADP in the presence of 0.1 mM ATP; Figs. 15 and 16). Given the proximity of this amino acid to the nucleotide binding Walker A motif, it is conceivable that the architecture of the side chain might directly influence nucleotide binding and its subsequent hydrolysis. Alternatively, it might play a role in the transduction step linking ATPase activity to channel opening. Recent work by Matsuo *et al.* [50] suggests that the linker motifs of both NBDs of SUR (at least SUR1 and 2B) participate in transducing ATP binding and hydrolysis at the NBDs to channel activity;

mutations in the linker motifs reduced (NBD1) or abolished (NBD2) channel response to MgADP without altering nucleotide binding or hydrolysis. It is also evident that although in SUR, ATP hydrolysis occurs primarily at NBD2, both NBDs are required for transducing the enzymatic activity of SUR to channel activity [49] [51] [58]. Thus, it is possible that the Phe-1388 residue may contact the linker or NBD1 during the transduction process. To distinguish these possibilities, future biochemical studies that compare nucleotide binding and hydrolysis between NBD2 of WT SUR1 and NBD2 containing the F1388L mutation will be required. Insight into the structural role of Phe-1388 in SUR1 might also be gained by comparing crystal structures of bacterial ABC transporters bearing Phe or Leu at the homologous site.

Physiological, Pharmacological, and Therapeutic Implications-- The key to the function of K_{ATP} channels in sensing the energetic state of a cell is their ability to respond to changes in the concentrations of intracellular ATP and MgADP. In pancreatic β -cells, an increase in ADP/ATP ratio following glucose starvation activates the channel to stop insulin secretion. Many SUR1 mutations identified in patients with familial hyperinsulinism specifically abolish channel response to MgADP stimulation, causing persistent insulin secretion despite low blood glucose levels [76] [152]. These findings underscore the importance of MgADP in determining K_{ATP} channel activity in physiological conditions. Significantly, substituting Phe-1388 with Leu substantially increases channel sensitivity to MgADP. Because in intact cells, the activity of K_{ATP} channels is dependent on the MgADP/ATP ratio, such a "gain of function" phenotype in MgADP response is expected to result in higher channel activity at a given metabolic condition. Indeed, our Rb^+ efflux experiments using several metabolic conditions clearly

demonstrate that the F1388L channels are more sensitive to metabolic stress than WT channels. These results and the observation that channel response to diazoxide is also enhanced by the F1388L mutation point to the potential of this site as a drug target in the management of familial hyperinsulinism. In this regard, it would be important to determine whether the F1388L mutation is able to compensate for the MgADP defects caused by other mutations in SUR1.

The realization that the leucine mutation occurs naturally in SUR2 suggests that this conservative amino acid substitution may be a mechanism for generating functional diversities in K_{ATP} channels. The SUR1/Kir6.2, SUR2A/Kir6.2, and SUR2B/Kir6.2 channels exhibit differential sensitivities to nucleotides and pharmacological agents. Several studies have examined the structural basis that underlies these differences. At the primary sequence level, SUR1 and SUR2A are 68% identical. SUR2B, a splice variant of the *SUR2* gene, differs from SUR2A only in the last 42 amino acids. Interestingly, the C-terminal 42 amino acids of SUR2B share only ~30% homology to those of SUR2A but ~70% homology to SUR1 [69]. The F1388L-SUR1 is therefore structurally closer to SUR2B than to SUR2A. This fits our observations that the functional properties of the F1388L-SUR1 mutant channel are more similar to the SUR2B/Kir6.2 than to the SUR2A/Kir6.2 channel.

By using the chimeric protein approach, Bebenko *et al.* [181] found that the distal C terminus of SUR2A (~50 amino acids) is sufficient to confer the lower ATP sensitivity seen in the cardiac SUR2A/Kir6.2 channels. Consistent with this, we did not observe a significant difference between WT and F1388L-SUR1 channels in ATP sensitivity. The

regions involved in MgADP response are more complex. Obviously, NBD2 is required for nucleotide binding, but NBD1 is also essential [49]-51] [56] [58] [76]. In addition, the C-terminal tail plays a role. First, a disease-associated point mutation located in the C terminus of SUR1, L1544P, diminishes channel response to MgADP [172]. Second, analysis of chimeric SURs has led to the proposal that the C-terminal 42 amino acids of SUR2A imparts an inhibitory effect on MgADP-induced channel activation, explaining the lower sensitivity of the SUR2A/Kir6.2 channel to MgADP [182]. Although SUR2A also has a leucine at the 1388-equivalent site, the potentiation effect of leucine is likely masked by the inhibitory effect imposed by the SUR2A C-terminal tail.

Pharmacologically, the F1388L-SUR1 channels show decreased glibenclamide sensitivity and altered KCO specificity. Sulfonylureas inhibit K_{ATP} channel activity by antagonizing the stimulatory effect of MgADP [183]. The high affinity sulfonylurea-binding site has been localized to the C-terminal group of transmembrane helices [66] [67] [184]. The decreased glibenclamide sensitivity of the F1388L-SUR1 channel therefore is probably not due to a change in the binding site peptide sequence but rather a consequence of increased channel sensitivity to MgADP. With regard to KCO response, the F1388L mutation caused increased sensitivity to diazoxide and rendered the channel sensitive to stimulation by pinacidil but not by cromakalim. Binding studies using a pinacidil analogue, P1075, showed that the KCO binds with high affinity to SUR2A and SUR2B but does not bind to SUR1 [68, 184] [71]. The critical regions in SUR2 that confer high sensitivity to pinacidil and cromakalim have been mapped to TMs 16-17 and part of the cytosolic loop between TMs 13-14 [69] [73] [185] [72]. Moreau *et al.* [74] further narrowed down the structural basis for the differential KCO sensitivities to two amino

acids in the last transmembrane segment (TM 17) of SUR. The fact that the F1388L-SUR1 channels are stimulated by pinacidil at high concentrations suggests that pinacidil does bind F1388L-SUR1 channels with low affinity. Again, although it is possible that Phe-1388 in SUR1 is part of the pinacidil-binding site, a more likely explanation for the increased sensitivity to pinacidil is a result of the increased MgADP sensitivity. This would be in agreement with the idea that KCO responsiveness and even binding affinity is modulated by nucleotides [49] [51, 71, 186, 187] [53, 181, 188].

In conclusion, our results show that the Phe-1388 residue in SUR1 plays an important role in the trafficking and function of K_{ATP} channels. The biochemical features of this residue that govern trafficking efficiency are distinct from those that govern functional properties. The F1388L mutation in SUR1 makes the overall physiological and pharmacological profile of the channel shift toward that of the SUR2B/Kir6.2 channel. Thus, genetic variation at this amino acid accounts for some of the functional differences seen in different subtypes of K_{ATP} channels, providing a mechanism for diversity.

The abbreviations used are: SUR, sulfonylurea receptor; NBD, nucleotide binding domain; TM, transmembrane; ER, endoplasmic reticulum; PBS, phosphate-buffered saline; BSA, bovine serum albumin; WT, wild type; KCOs, potassium channel openers.

CHAPTER THREE

K_{ATP} channel degradation through the ubiquitin-proteasome pathway.

Etienne A. Cartier, Fei-Fei Yan, and Show-Ling Shyng

From the Center for Research on Occupational and Environmental Toxicology, Oregon Health and Science University, Portland, Oregon 97239

Abstract

The pancreatic ATP-sensitive potassium (K_{ATP}) channel regulates insulin secretion by linking metabolic changes to the β-cell membrane potential. K_{ATP} channels are oligomeric complexes composed by the sulfonylurea receptor 1 (SUR1) and the inward rectifier Kir6.2. The channel biogenesis is under the surveillance of a number of ER quality control mechanisms. Among those, a tripeptide RKR retention signal present in both subunits prevents ER exit of unassembled subunits; a SUR1 C-terminus export signal controls K_{ATP} channel exit out of the ER; and the SUR1 glycosylation confers export competence to the SUR1 subunit. A number of mutations in K_{ATP} channel subunits seem to affect their folding, causing the mutant proteins to be retained in the ER. We report here that K_{ATP} channel subunits are degraded in the ER by a process that appears to be dependent on the subunit folding state and subunit heteromeric assembly. K_{ATP} channel biogenesis appears to be inefficient: ~70% of the channel subunits are rapidly degraded by this ER mechanism, and only ~30 % acquires metabolic stability and can be incorporated into channel complexes which eventually reach the plasma membrane. By contrast, the K_{ATP} channel trafficking mutant, SUR-ΔF1388, is rapidly degraded showing monophasic kinetics. Inhibition of proteasome function slows down the turnover of all

wild-type and mutant subunits and leads to their accumulation as deglycosylated and/or polyubiquitinated species. Under this condition, the undegraded K_{ATP} channel subunits are found in perinuclear inclusions that can be co-immunostained with aggresome markers such as ubiquitin and vimentin. These results suggest that the ubiquitin-proteasome pathway is involved in the degradation of K_{ATP} channels under both normal and pathological conditions.

Introduction

The endoplasmic reticulum (ER) plays an essential role in the folding and degradation of newly synthesized proteins [88, 89]. In the ER lumen, proteins undergo covalent modifications and acquire their secondary and tertiary structures. While still in this compartment, many also assemble into homo- or hetero-oligomers (e.g. octameric K_{ATP} channels). It is well established that the three-dimensional structure and oligomeric state of a protein controls not only its functional properties, but also its intracellular targeting and life span. In the ER, misfolded, misassembled, and unassembled polypeptides are generally retained and eventually degraded. These properties of the ER provide *quality control* (QC) in the secretory pathway [88, 89]. Thus, proteins in export-competent form usually correspond to the compactly folded native conformation that has undergone correct co- and posttranslational processing, and for most oligomeric proteins, a correct quaternary structure is also required [91].

The QC of the K_{ATP} channels involves several levels of regulation. First, correct trafficking and cell-surface expression of K_{ATP} channels are controlled by a tripeptide ER-retention/retrieval signal, RKR, present in both the SUR1 and Kir 6.2 subunits [12].

This retention signal is shielded only after the complete assembly of octameric K_{ATP} channels. In this manner, the ER quality control prevents the export of unassembled subunits[12]. Similar RXR motifs regulate the proper folding [157], assembly [106] [104, 105], and export[106] [104, 105] of other channels and receptors. A second level of QC in K_{ATP} channel expression involves an ER-export signal identified within the C-terminus of SUR1 [123]. Deleting as few as 7 amino acids from the C-terminus of SUR1 markedly reduces surface expression of the channels[123]. Finally, K_{ATP} channel trafficking and cell-surface expression appears to be critically dependent on SUR1 glycosylation [23, 174].

Mutations can impair K_{ATP} channel physiology, or trafficking, or both [5]. Normally, the relative concentrations of intracellular ATP and ADP determine the membrane potential of pancreatic β -cells by regulating the activity of K_{ATP} channels in the plasma membrane. When the blood glucose concentration rises, the increased intracellular [ATP/ADP] ratio favors K_{ATP} channels closure, resulting in membrane depolarization, Ca^{2+} influx and insulin secretion. When the blood glucose concentration falls (hypoglycemia), these molecular events reverse, preventing insulin release [5, 189]. If mutations disrupt K_{ATP} channel trafficking or assembly within pancreatic β -cells, K_{ATP} channels fail to activate during glucose starvation [5, 173, 189]. In this event, β -cells remain depolarized, and insulin secretion persists, leading to severe hypoglycemia resulting in a clinical disorder known as persistent hyperinsulinemia of the infancy (HI).

A number of K_{ATP} channel trafficking defects associated with HI have been characterized. The SUR1 $\Delta F1388$ mutation (referred as $\Delta F1388$) causes K_{ATP} channels to be retained in the ER, thus preventing expression at the plasma membrane of β -cells

[173, 190]. A recent report characterized the degradation rate of overexpressed K_{ATP} channels in COS cells and native K_{ATP} channels from the INS (insulin secreting) cell line [191]. They showed that HI-causing mutations that prevents channel trafficking, such as SUR1- Δ F1388 or others, were engineered into the SUR1 or Kir6.2 subunits, degradation rates of the mutated subunits were apparently faster than wild-type subunits. A likely explanation is that K_{ATP} channel subunit degradation is determined by its folding state and that the mutant channel subunits are degraded more rapidly because they fail to fold correctly. Supporting this view, it has been demonstrated that tolbutamide, acting as a chemical chaperone, is capable of decreasing the degradation rate of the SUR1 A116P HI-linked trafficking mutant [192].

Current evidence indicates that ER- retained membrane proteins are recognized by chaperones, retrotranslocated to the cytoplasm, polyubiquitinated and degraded by the 26S proteasome[91]. Pharmacological inhibition of proteasomes causes cytoplasmic accumulation of large perinuclear inclusions of protein aggregates known as ‘aggresomes’ [138]. Ubiquitination and proteasome-mediated degradation can be regulated in response to cellular signals and there is strong evidence that cell-surface expression of certain membrane proteins for example connexin 43 (Cx43) and aquaporin-1 (AQP-1) [139, 140] can be regulated by the rate of degradation through the ubiquitin-proteasome pathway. Given the potential role that ERAD may play on regulating the number of surface K_{ATP} channel under normal and pathological conditions, it is important to first establish the involvement of this pathway in the degradation of K_{ATP} channel subunits.

Here we report that the majority of the wild-type K_{ATP} channel subunits synthesized de novo is degraded via ERAD. The K_{ATP} channel subunit degradation rates seem to be determined by their folding state and by their putative assembly as K_{ATP} channels; disease-associated mutant channel subunits retained in the ER are degraded faster than the wild-type subunits. The ER degradation of K_{ATP} channel subunits, involves their ubiquitination and retrotranslocation to the cytoplasm where they can accumulate in aggresome-like inclusions bodies after proteasome inhibition. Ubiquitinated K_{ATP} channel subunits are targeted for degradation through the cytoplasmic 26S proteasome.

Experimental Procedures

Molecular Biology. SUR1 hamster was tagged at the C terminus with the V5 epitope by subcloning into the vector pcDNA3.1/V5HisA (Invitrogen), a gift from Carol Vandenberg. SUR1 Δ F1388 was introduced into SUR1 with the V5 epitope in pcDNA3.1/V5HisA with ligation. FLAG epitope (DYKDDDDK) was inserted at the N terminus of the hamster SUR1 cDNA in the pECE plasmid by sequential overlap extension PCR. Epitope tag and mutations were confirmed by DNA sequencing. Rat Kir6.2 in pCDNA3 (a gift from Dr. C. Vandenberg) was used for co-transfection. Recombinant adenovirus expressing rat Kir6.2-wt produced by cDNA subcloned into pShuttleCMV vector using AdEasy Adenoviral Vector System (Stratagene). Inserts were recombined into pAdeasy-1 vector. Recombinant viruses were generated by transfecting the viral construct into HEK293 cells. It was kindly provided by Chia-Wei Lin.

Immunofluorescence Staining. COS-1 cells were plated in 6-well tissue culture plates, transfected with Fugene (Roche) according to the manufacturer's directions, and analyzed 48 h posttransfection. Cellular staining of FLAG-tagged SUR1 was performed with cells fixed with cold (-20°C) methanol for 5 min. Fixed cells were incubated with one or two of the following primary antibodies. The anti-FLAG M2 mAb ($10\ \mu\text{g}/\text{ml}$ in PBS, 1% BSA), anti-Kir6.2 (1:500 in PBS, 1% BSA), anti-ubiquitin (1:500 in PBS, 1% BSA), anti-vimentin (1:300 in PBS, 1% BSA) at room temperature for 1 h, washed in PBS, incubated with Cy3-conjugated donkey anti-mouse or Alexa-conjugated rabbit anti-rat secondary antibodies for 30 min at room temperature, and washed again in PBS before viewing. Cells were viewed using a Leica fluorescent microscope.

Immunoblotting. COS1 cells were plated onto 35-mm culture dishes and transiently transfected with FLAG-tagged SUR1 constructs in the presence or absence of Kir6.2 by using Fugene. Cells coexpressing SUR1 and Kir6.2 were transfected with $0.6\ \mu\text{g}$ SUR1 and $0.4\ \mu\text{g}$ Kir6.2 per 35-mm dish; cells expressing SUR1 alone were transfected with $1\ \mu\text{g}$ SUR1 per 35-mm dish. Cells were lysed 48 h posttransfection or infection in 20 mM HEPES, pH 7.0/5 mM EDTA/150 mM NaCl/1% Nonidet P-40 with Complete protease inhibitors (Roche). SUR insoluble fraction was obtained by centrifugation at 14,000 rpm of 1% NP40 lysates. Pellet was recovered, suspended in 1% SDS for 10 min and diluted with NP40 buffer (final concentration, 0.2% SDS). Proteins in the cell lysates were separated by SDS/PAGE (10%), transferred to nitrocellulose, analyzed by M2 anti-FLAG antibody (Sigma) followed by horseradish peroxidase-conjugated anti-mouse secondary antibodies (Amersham Pharmacia), and visualized by chemiluminescence (Super Signal West Femto; Pierce).

Immunoprecipitation. COS cells were plated onto 35-mm culture dishes and transiently transfected with v5-SUR1, v5ΔF1388 and/or Kir6.2 by using Fugene. Cells coexpressing SUR and Kir6.2 were transfected with 0.6 μg SUR1 and 0.4 μg Kir6.2 per 35-mm dish; cells expressing SUR or Kir6.2 alone were transfected with 1 μg SUR1 or 1 μg Kir6.2 per 35-mm dish. 48 h after transfection, cells were treated or not during 8 hours with lactacystin 6 μM or MG132 10 μM. Cells were lysed in 20 mM Hepes, pH 7.0/5 mM EDTA/150 mM NaCl/1% Nonidet P-40 with Complete protease inhibitors (Roche) and separated in two sister samples. Each sample was separated by SDS/PAGE (10%), transferred to nitrocellulose, and immunoblotted with either anti-V5/anti-Kir6.2 or anti-ubiquitin followed by horseradish peroxidase-conjugated anti-mouse secondary antibodies (Amersham Pharmacia), and visualized by chemiluminescence (Super Signal West Femto; Pierce).

Metabolic Labeling. COS1 cells grown in 35-mm dishes were transfected with v5-SUR1, v5ΔF1388 and/or Kir6.2 for 36 h. The cells were starved in methionine/cysteine-free Dulbecco's modified Eagle's medium supplemented with 5% dialyzed fetal bovine serum for 30 min prior to labeling with L-[³⁵S]methionine (ICN Tran³⁵S-Label, 150–250 μCi/ml) for 30 min. Labeled cultures were chased for various times in regular medium supplemented with 10 mM methionine at 37 °C. At the end of the chase, the cells were lysed in 500 μl of the lysis buffer (see above). For immunoprecipitation, 500 μl of cell lysate was incubated with 1 μg of anti-V5 or rabbit anti-Kir 6.2 antibodies for 1 h at 4 °C and then with protein A-Sepharose 4B (Bio-Rad) for 2 h at 4 °C. The precipitate was washed three times in the lysis buffer, and the proteins were eluted using the Laemmli sample buffer. The eluted proteins were separated by 8% SDS-PAGE, and the gel was

subjected to fluorography. The dried gels were analyzed using a Bio-Rad PhosphorImager.

Results

Individually expressed K_{ATP} channel subunits are degraded with biphasic kinetics—

K_{ATP} channels are multimeric proteins composed of two kinds of subunits, SUR1 and Kir6.2. Studies on the nicotinic acetylcholine receptor (AChR) pentameric channel have established that ~70% of synthesized subunits remain unassembled inside the ER and are rapidly degraded ($t_{1/2} < 1h$). Another report documented that a majority (~60-80%) of synthesized CFTR [86, 87], a channel that shares structural similarities with SUR1, is also rapidly degraded by ER-associated degradation (ERAD) ($t_{1/2} \sim 30min$). In contrast, other studies have found that ABC proteins like MDR1 [193] and SUR1 [191] have long (>24h) half-lives. Few studies have aimed to determine turnover of inward rectifier potassium channels.

We characterized the degradation rate of individual K_{ATP} channel subunits expressed on COS-1 or COSm6 cells. Either v5SUR1wt (referred as SUR1), v5SUR1 $\Delta F1388$ (referred as $\Delta F1388$) or Kir6.2 were pulse-labeled with ^{35}S [Met/Cys] for 30 min, and then chased with unlabeled methionine. Degradation of SUR1 is biphasic: around 70% of SUR1 is rapidly degraded with a half-life of 1.35 ± 0.03 h (fast rate; $n=5$); the remaining 30% degrades very slowly with a half-life of 21.5 ± 1.33 h (slow rate; $n=5$) (Fig 20A). It has been established that fully folded proteins or assembled oligomers are less prone to degradation [94, 194, 195]. We propose that the SUR1 with the slower degradation rate represents a population of SUR1 that has acquired a fully folded

conformation and is resistant to rapid degradation. The rapidly degraded SUR1 may represent SUR1 in a number of conformations that are readily prone to ER degradation.

Channel trafficking defects seen in some mutants are results of protein misfolding. A well-documented example is the CFTR $\Delta F508$ mutant that is retained in the ER and degraded by ERAD [85]. We have previously reported that the SUR1 $\Delta F1388$ mutation causes ER retention, resulting in defective trafficking of K_{ATP} channels. We engineered the SUR1 $\Delta F1388$ mutation and performed pulse-chase analysis. In contrast to SUR1, $\Delta F1388$ degrades with a single half-life of 1.41 ± 0.1 h ($n=5$; Fig 20A). This half-life is similar to the half-life of the rapidly degraded SUR1 (1.35 ± 0.03 h). We suggest that $\Delta F1388$ might correspond to an unfolded variant of SUR1.

The turnover of Kir6.2 expressed alone is also biphasic (Fig 20B). Around 60% of the labeled Kir6.2 degrades rapidly with a half-life of 50 ± 3.34 min (fast rate; $n=3$). The remaining 40% degrades more slowly, with a half-life of 10.4 ± 0.30 h (slow rate; $n=3$). There are two possible interpretations of these results. First, as it has been proposed [191], the biphasic decay of Kir6.2 may represent the assembly of Kir6.2 subunits in tetramers, that are less prone to fast degradation. However, a second alternative is also possible: Kir6.2 subunits may become resistant to rapid degradation once they reach a fully folded conformation. This rapid degradation-resistant state would be independent of the Kir6.2 oligomeric state.

Figure 20

A.

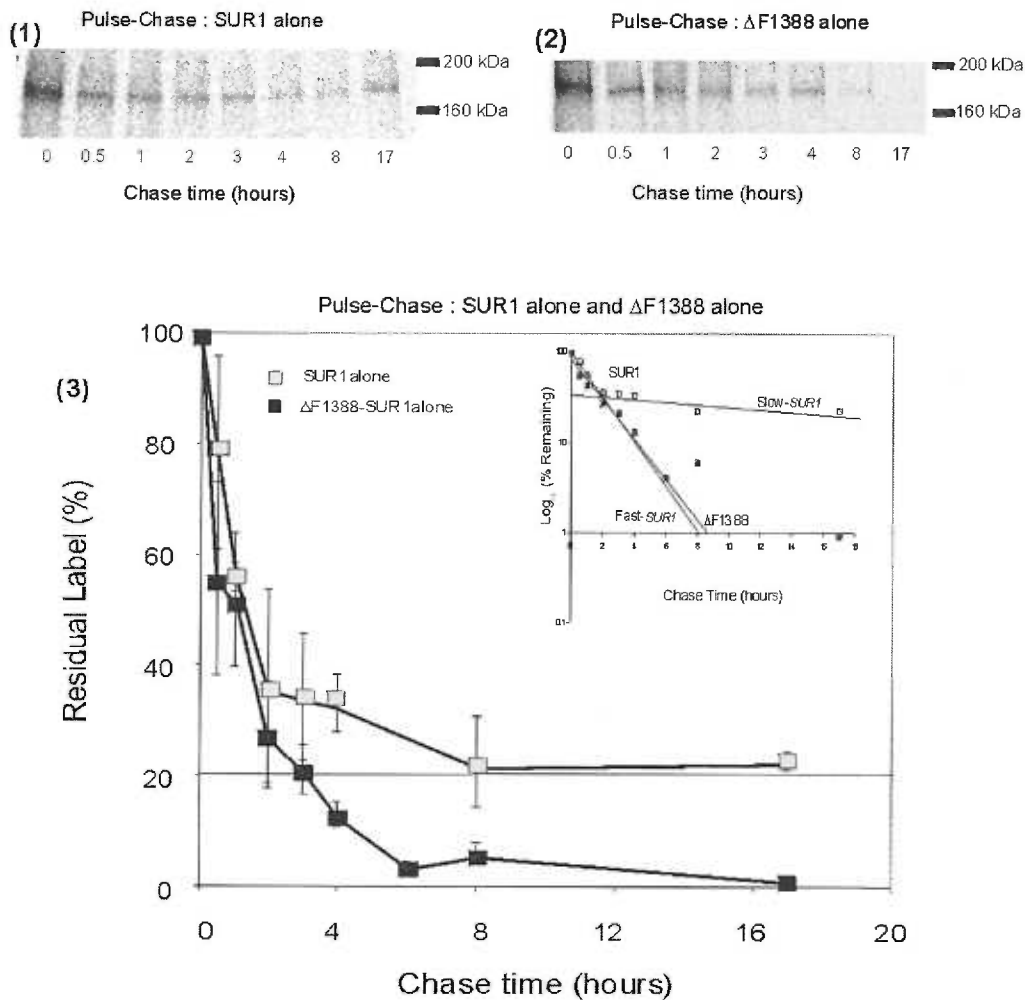


Figure 20A. Degradation of SUR1 and ΔF1388 subunits. Metabolic labeling (pulse) and chase of SUR1 (1) and ΔF1388 (2) expressed alone. Cells were pulse-labeled for 30 min. and chased for various times as indicated. SUR and ΔF1388 were immunoprecipitated with anti-V5 antibody. Single immature bands appear through the chase in both cases. After four hours of chase, SUR1 achieves a degradation-resistant conformation whereas ΔF1388 is degraded completely. (3) Degradation of SUR1 and ΔF1388 alone. SUR1 degradation rate (*open squares*) is biphasic with ~70% SUR1 being rapidly lost. Data can be fit with two different exponential functions in a semilog plot (fast and slow rates respectively). The SUR1 $t_{1/2}$ are 1.35 ± 0.03 h (fast rate) and 21.5 ± 1.33 h (slow rate). ΔF1388 is totally degraded. ΔF1388 degradation rate ($t_{1/2} = 1.41 \pm 0.1$ h; *filled squares*) can be fit with one single exponential function (insert) and it is comparable to the fast rate of SUR1. Each point represents the averaged value from five independent experiments, with the *error bar* representing the S.E. *Insert*: Semilog plot showing the fast (FAST-SUR1), slow (SLOW-SUR1), and ΔF1388 degradation rates, respectively.

Figure 20

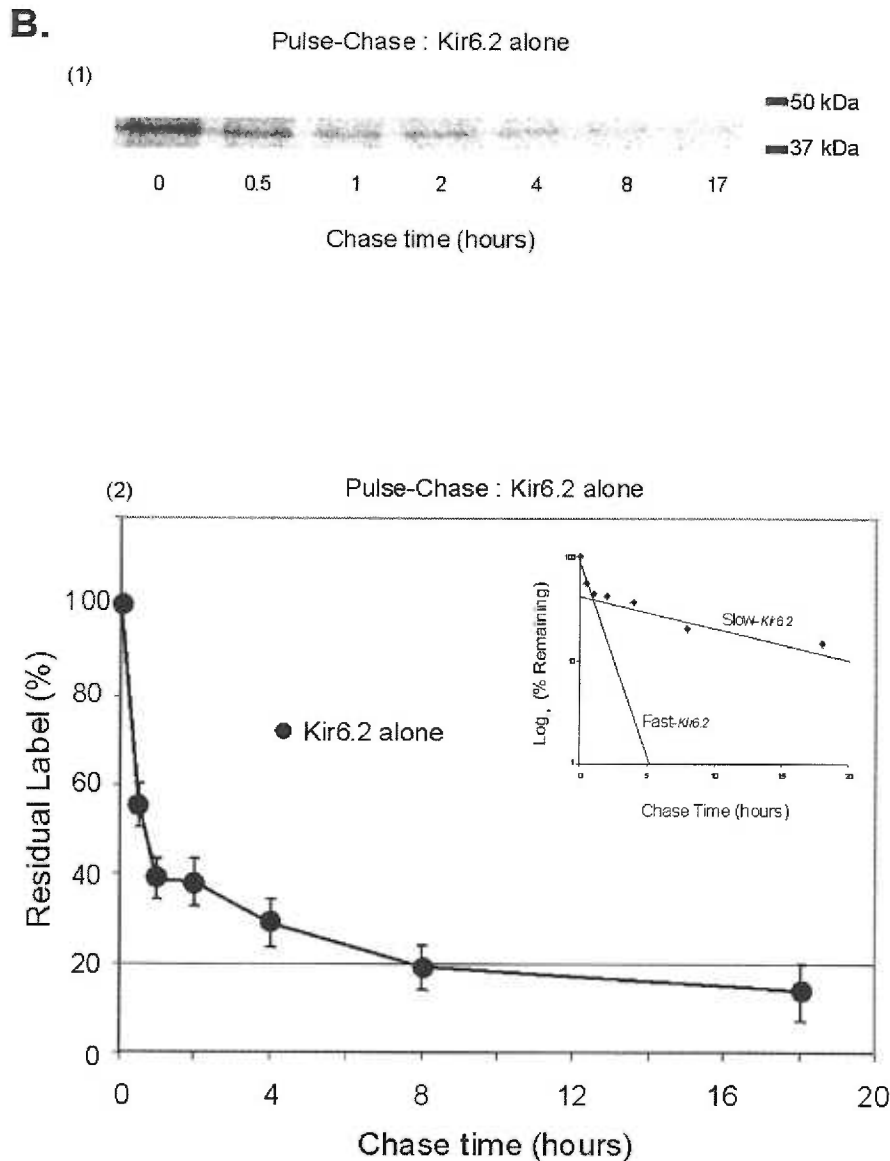


Figure 20B. Kir6.2 subunit degradation is biphasic. (1) Metabolic labeling (pulse) and chase of Kir6.2 expressed alone. Cells were pulse-labeled for 30 min and chased for various times as indicated. Kir6.2 was immunoprecipitated with polyclonal anti-Kir6.2 antibody. Single non-glycosylated bands appear during the chase. (2) Turnover of Kir6.2 alone. The degradation rate is biphasic with ~60% Kir6.2 being rapidly lost. Data can be fit with two different exponential functions (fast and slow rates respectively). The Kir6.2 $t_{1/2}$ are 50 ± 3.34 min (fast rate) and 10.4 ± 0.30 h (slow rate). Each point represents the averaged value from three independent experiments, with the *error bar* representing the S.E. *Insert*: Semilog plot showing the Kir6.2 fast (FAST-Kir6.2) and slow (SLOW-Kir6.2) degradation rates, respectively.

Degradation of co-expressed SUR1 and Kir6.2—

A number of studies have established that oligomer association in multimeric complexes (i.e, AChR [94] and T receptor[195]) affects oligomer turnover. Thus, if SUR1 and Kir6.2 are co-expressed, their association and assembly might have an effect on their turnover stability. On the other hand, degradation of SUR1 and Kir6.2 subunits may be independent of their interaction. To test whether heteromeric subunit-subunit interaction affects K_{ATP} channel subunit stability, pulse-chase experiments were performed as described in ‘*Experimental procedures*’. Under normal circumstances, when SUR1 is co-expressed with Kir6.2, two forms of SUR1 can be detected: an immature core-glycosylated form and a mature complex-glycosylated form that has traversed the medial Golgi. The latter represents properly assembled K_{ATP} channels (Fig 21A).

Quantification of the residual labeling of both immature and mature bands shows that the two forms degrade at different rates (Fig 21A). The SUR1 immature form is almost completely degraded in the 24 h time course of the chase. Its turnover is also biphasic: ~80% is rapidly degraded during the first four hours of chase with a half-life of 1.4 ± 0.01 h (fast rate; n=4). Interestingly, this rapid turnover is similar to that shown for SUR1 ($t_{1/2}=1.35$ h) and $\Delta F1388$ alone ($t_{1/2}=1.41$ h). This suggests that the ER resident SUR1 immature fraction may correspond to a form of SUR1 that is not assembled with Kir6.2. The remaining ~20% is slowly degraded with a half-life of 11.6 ± 0.86 h (slow rate; n=4). This slow turnover of the SUR1 immature band, is faster than the slow degradation rate observed in SUR1 alone ($t_{1/2}=21.5$ h; Fig. 21B). Consequently, the apparently slow turnover behavior of the SUR1 immature band seems to be affected not

only by direct ER degradation but also by its conversion to the SUR1 mature form. The SUR1 mature form corresponds to assembled K_{ATP} channels that have left the ER. They are degraded in a post-ER compartment with a half-life of 11.61 ± 0.86 h ($n=4$). Interestingly, this SUR1 mature fraction, which leaves the ER as K_{ATP} channel complexes and is fully glycosylated, makes up $\sim 15\%$ of the initially labeled SUR1. The SUR1 mature fraction may represent part of the same $\sim 30\%$ fraction that reaches a rapid degradation-resistant conformation when SUR1 is expressed alone. Overall, these findings suggest that only $\sim 30\%$ of SUR1 alone reaches a conformation that is stable and this conformation may be the only one able to assemble with Kir6.2 and form K_{ATP} channels.

The above data show that a fraction of SUR1 can assemble with Kir6.2, forming K_{ATP} channels that are readily exported out of the ER. However, our experiments cannot determine whether the SUR1-Kir6.2 assembly results in K_{ATP} channel subunit turnover stabilization inside the ER. In order to keep the assembled K_{ATP} channels inside the ER and examine whether their association affects their degradation, we tested the effect of brefeldin A on the SUR1 turnover co-expressed with Kir6.2. This fungal metabolite induces a rapid and reversible disassembly of the Golgi apparatus and mixing of the Golgi contents with the ER. Hence, BFA inhibits the export of proteins out of the ER. In the presence of brefeldin A, SUR1 turns over in two phases: $\sim 60\%$ of SUR1 is rapidly degraded with a half-life of 2.3 ± 0.06 h (fast rate; $n=4$), which is significantly slower ($p < 0.005$) than the fast degradation rate obtained for SUR1 expressed alone ($t_{1/2} = 1.35$ h). The remaining $\sim 40\%$ of SUR1 degrades slowly with a half-life of 12.5 ± 0.30 h (slow rate; $n=4$; Fig 21B).

Figure 21

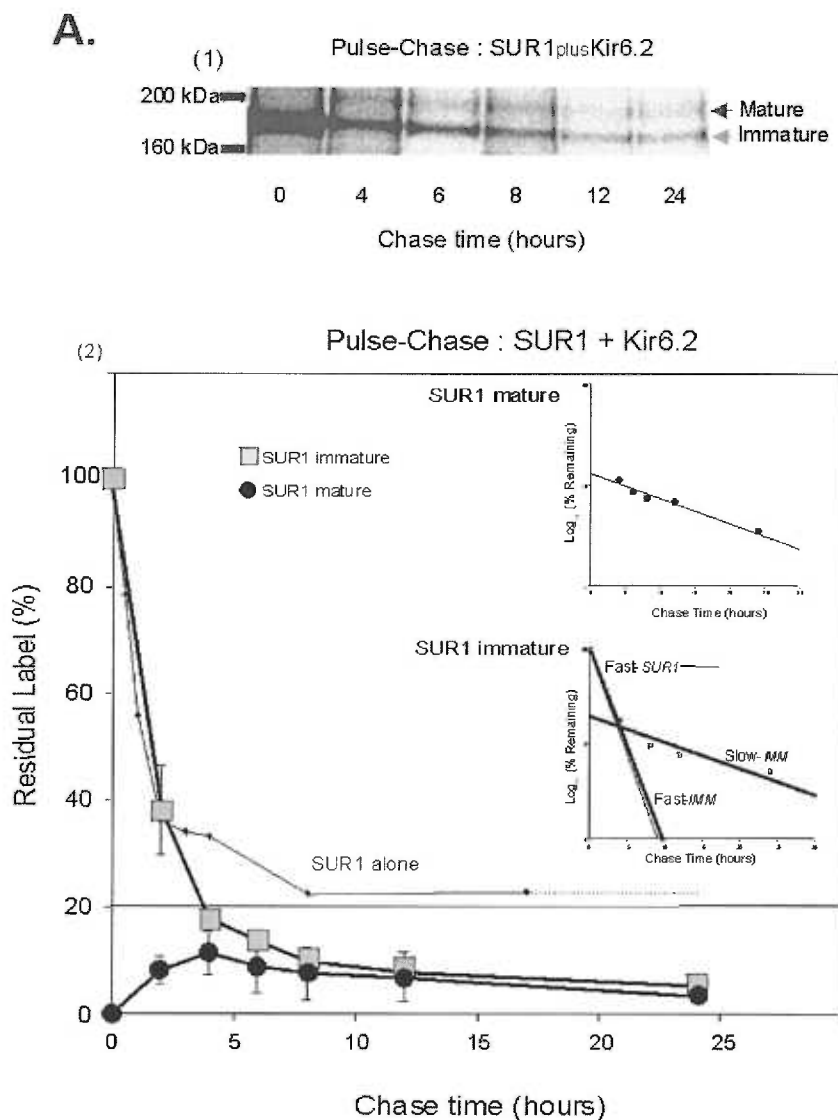


Figure 21A. SUR1 co-expressed with Kir6.2 matures to K_{ATP} channels. Metabolic labeling (pulse) and chase of SUR1 co-expressed with Kir6.2. Cells were labeled for 30 min and chased for various times as indicated. SUR1 was immunoprecipitated with anti-V5 antibody. (1) SUR1 co-expressed with Kir6.2 appear as a single immature band that is converted to a mature band. (2) Degradation of the immature SUR1 band compared with the appearance of the mature SUR1 band that corresponds to assembled K_{ATP} channels. SUR1 immature degradation rate (*open squares*) is biphasic with ~80% SUR1 being rapidly lost. Data can be fit with two different exponential functions (fast and slow rates respectively). The SUR1 immature $t_{1/2}$ are 1.4 ± 0.01 h (fast rate) and 11.6 ± 0.86 h (slow rate) respectively. The fast rate is similar to values obtained for SUR1 and $\Delta F1388$ alone. The SUR1 mature (*filled circles*) corresponds to ~15% of the initial label and it is degraded in a post-ER compartment with a $t_{1/2} = 11.61 \pm 0.86$ h. Each point represents the averaged value from three independent experiments, with the *error bar* representing the S.E. *Insert: Lower*, Semilog plot showing the fast (FAST-IMM), slow (SLOW-IMM), and fast (FAST-SUR1) degradation rates of the SUR1 immature band (IMM) and SUR1 alone, respectively. *Upper*, turnover of the SUR1 mature band.

Figure 21

B.

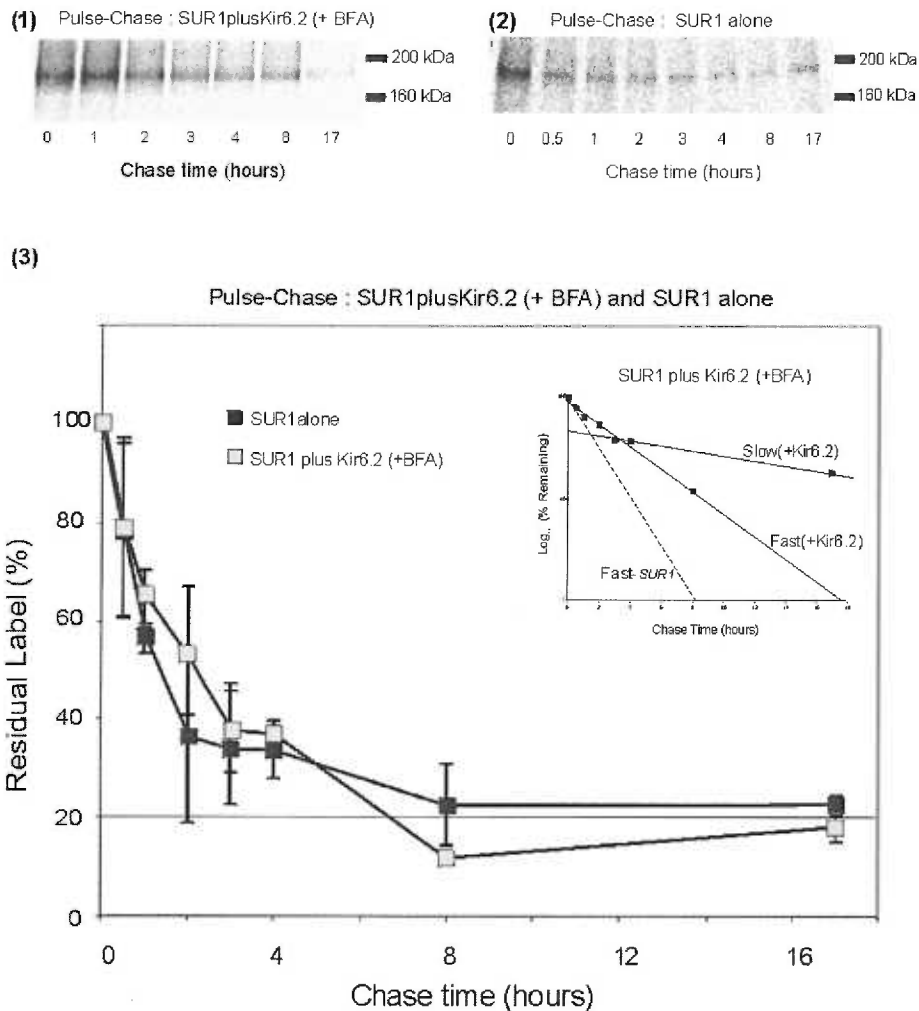


Figure 21B. Degradation of SUR1 co-expressed with Kir6.2. Metabolic labeling (pulse) and chase of SUR1 plus Kir6.2 under the presence of brefeldin A that keeps assembled K_{ATP} channels inside the ER compared with SUR1 alone. Cells were pulse-labeled for 30 min and chased for various times as indicated. SUR1 was immunoprecipitated with anti-V5 antibody. (1) SUR1 plus Kir6.2 under the presence of brefeldin A appears as a single immature band that reaches a long-life state after two hours of chasing. SUR1 alone (2) has been included for comparison purposes. (3) Degradation of SUR1 plus Kir6.2 inside the ER (+ brefeldin A) compared with SUR1 alone. SUR1+Kir6.2 degradation rate (*open squares*) is biphasic with ~60% SUR1 being rapidly lost. Data can be fit with two different exponential functions (fast and slow rates respectively). The SUR1+Kir6.2 $t_{1/2}$ are 2.3 ± 0.06 h (fast rate) and 12.5 ± 0.3 h (slow rate) respectively. The fast rate is significantly higher than values obtained for SUR1 alone ($p < 0.005$, at 0.05 level). The SUR1 alone curve (*filled squares*) has been included for comparison purposes. Each point represents the averaged value from five (SUR1 alone) or three (SUR1 + Kir6.2) independent experiments, with the *error bar* representing the S.E. *Insert:* Semilog plot showing the fast SUR1+Kir6.2 (FAST+ Kir6.2), slow SUR1+ Kir6.2 (SLOW+Kir6.2), and fast SUR1 alone (FAST-SUR1) degradation rates, respectively.

This suggests that SUR1-Kir6.2 oligomerization may slow down SUR1 rapid degradation.

Under certain circumstances, $\Delta F1388$ and Kir6.2 can interact and assemble because they can co-immunoprecipitate and form active K_{ATP} channels. Therefore, $\Delta F1388$ co-expression with Kir6.2 might affect its turnover. When we co-expressed $\Delta F1388$ with Kir6.2 (molar ratio 1:1), $\Delta F1388$ is degraded with a single half-life of 1.96 ± 0.26 h a rate, which is not significantly different ($p > 0.1$) from that obtained for $\Delta F1388$ alone ($t_{1/2} = 1.41$ h; Fig. 21C) and immature SUR1 (Fig 21A). These results suggest that the turnover behavior of $\Delta F1388$ co-expressed with Kir6.2, almost identical to that of $\Delta F1388$ alone, may be the result of a weak interaction between the two subunits.

Pulse-chase of the Kir6.2 subunit in the presence of SUR1 also shows a biphasic turnover. 60% of Kir6.2 co-expressed with SUR1 degrades rapidly with a half-life of 1.5 ± 0.12 h (fast rate; $n=3$) (Fig 22) similar to Kir6.2 alone. The remaining 40% degrades slowly, with a half-life of 17.6 ± 1.5 h (slow rate; $n=3$), which is higher than the time obtained for Kir6.2 alone ($t_{1/2} = 10.4$ h). Under the present circumstances, it is not possible to determine which fraction of the synthesized Kir6.2 assembles with SUR1 and leaves the ER, since Kir6.2 is a non-glycosylated protein. These results suggest that degradation of Kir6.2 may be dependent on expression of its partner SUR1.

Overall, these results might indicate that co-expression of SUR1 and Kir6.2 slows down the fast degradation rate, indicating that SUR1 and Kir6.2 assembly makes each subunit less prone to degradation.

Figure 21

C.

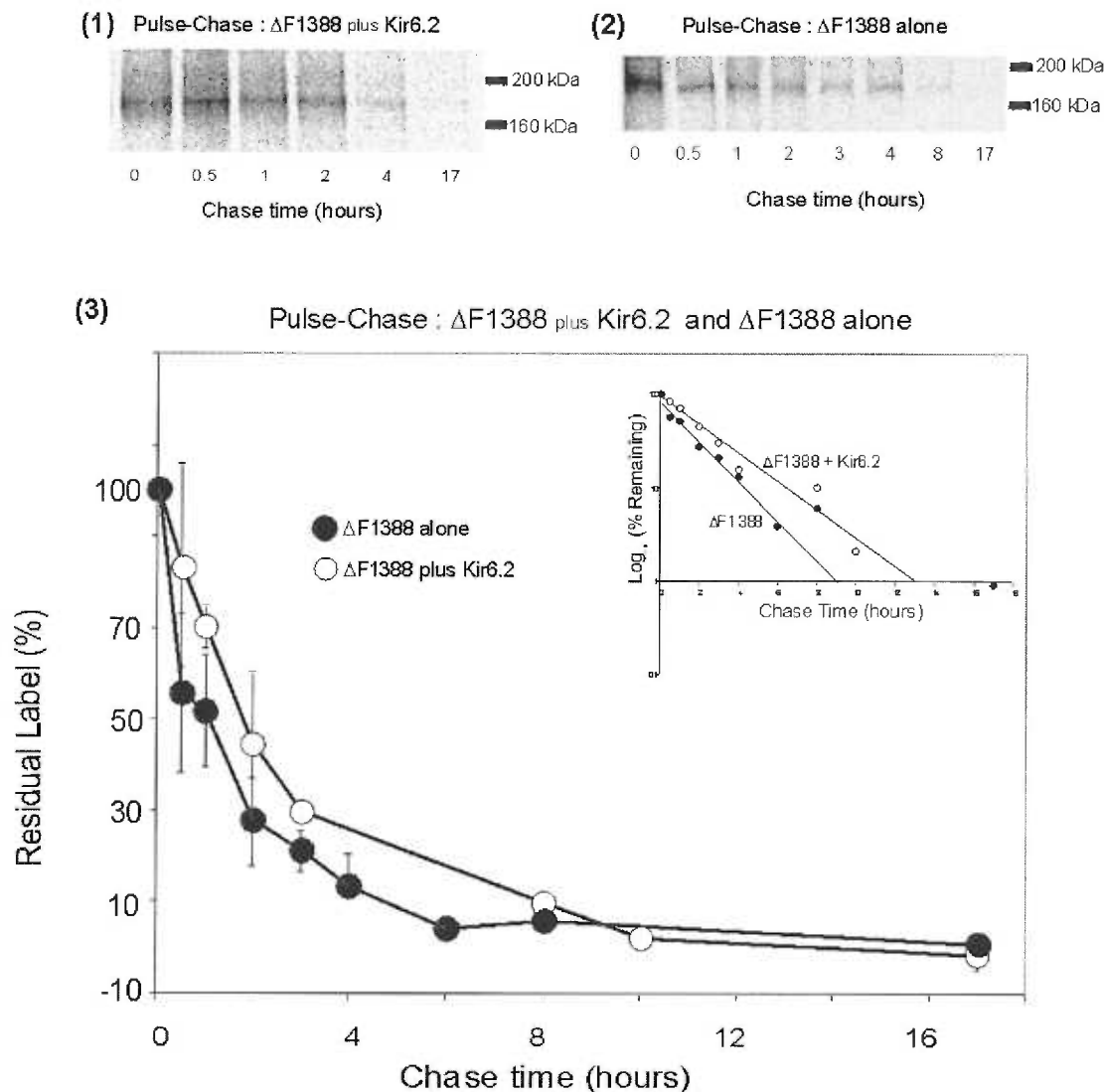


Figure 21C. Degradation of $\Delta F1388$ co-expressed with Kir6.2. Metabolic labeling (pulse) and chase of $\Delta F1388$ +Kir6.2 compared with $\Delta F1388$ alone. Cells were pulse-labeled for 30 min and chased for various times as indicated. $\Delta F1388$ was immunoprecipitated with anti-V5 antibody. (1) $\Delta F1388$ +Kir6.2 appears as a single immature band through out the chase. $\Delta F1388$ alone (2) has been included for comparison purposes. (3) Degradation of $\Delta F1388$ co-expressed with Kir6.2 compared with $\Delta F1388$ alone. $\Delta F1388$ co-expressed with Kir6.2 degradation rate (*open circles*) can be fit with one single exponential function (fast rate). The $\Delta F1388$ co-expressed with Kir6.2 $t_{1/2} = 1.96 \pm 0.26$ h. The $\Delta F1388$ alone curve (*filled circles*) has been included for comparison ($t_{1/2} = 1.41 \pm 0.1$ h). Each point represents the averaged value from five ($\Delta F1388$) and three ($\Delta F1388$ +Kir6.2) independent experiments, with the *error bar* representing the S.E. *Insert:* Semilog plot showing the $\Delta F1388$ and the $\Delta F1388$ +Kir6.2 degradation rates, respectively.

Figure 22

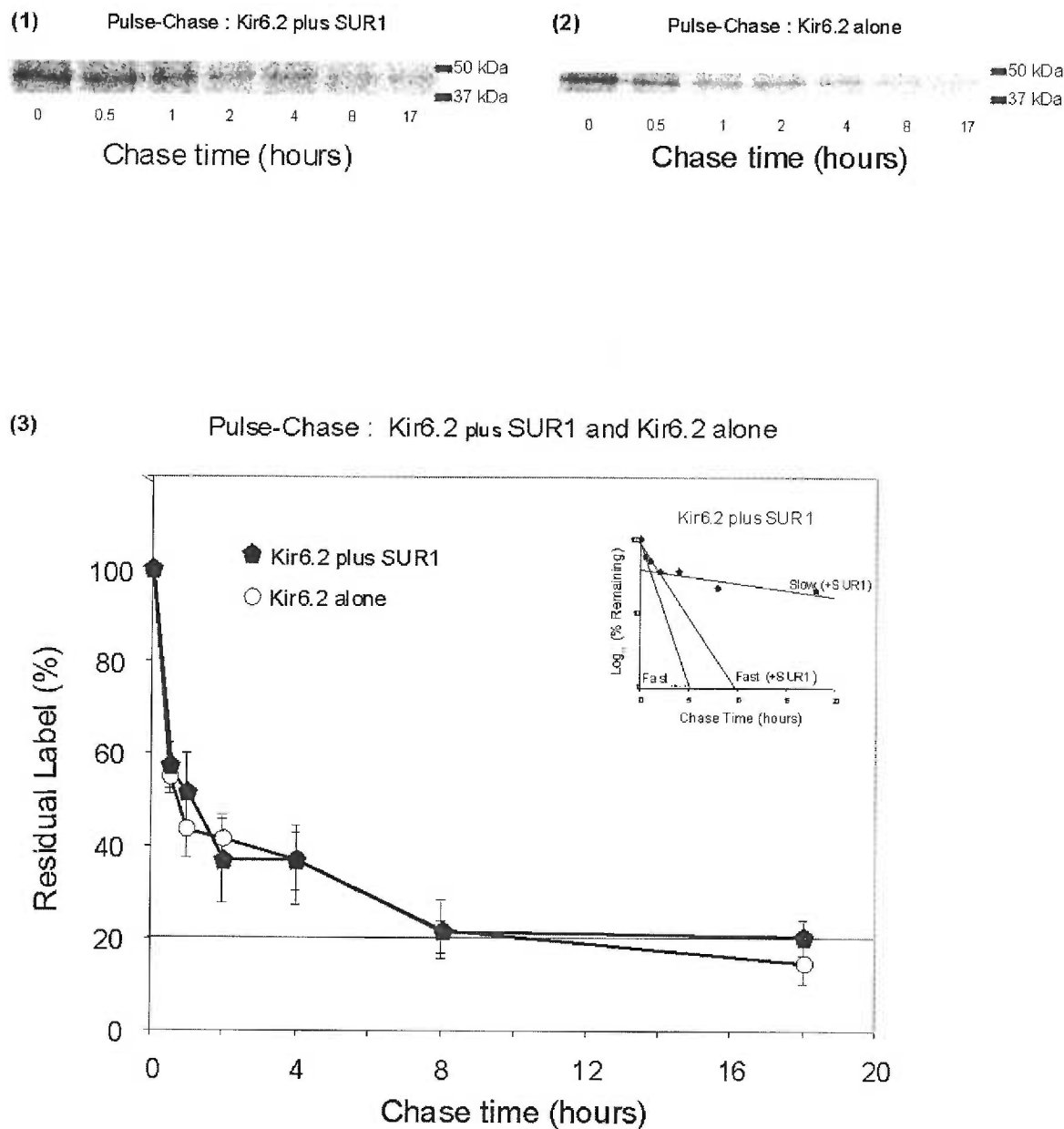


Figure 22. Degradation rate of Kir6.2 co-expressed with SUR1. Metabolic labeling (pulse) and chase of Kir6.2 (+ SUR1) compared with Kir6.2 alone. Cells were pulse-labeled for 30 min and chased for various times as indicated. Kir6.2 was immunoprecipitated with anti-Kir6.2 antibody. (1) Kir6.2 (+ SUR1) appears as a single band that reaches a long-life state after two hours of chasing. (2) Kir6.2 alone has been included for comparison purposes. (3) Degradation of Kir6.2 (+ SUR1) compared with Kir6.2 alone. Kir6.2 (+ SUR1) degradation rate (*closed pentagons*) is biphasic with ~60% Kir6.2 being rapidly lost. Data can be fit with two different exponential functions (fast and slow rates respectively). The Kir6.2(+ SUR1) $t_{1/2}$ are 1.5 ± 0.12 h (fast rate) and 17.6 ± 1.5 h (slow rate) respectively. The Kir6.2 alone curve (*open circles*) has been included for comparison purposes. Each point represents the averaged value from three independent experiments, with the error bar representing the S.E. *Insert:* Semilog plot showing the Kir6.2+SUR1 degradation rates fast (FAST+SUR1) and slow (SLOW+SUR1) compared with the fast degradation rate of Kir6.2 alone (FAST-alone).

Proteasome inhibition slows down ER-degradation of K_{ATP} channel subunits—

Several lines of evidence suggest that misfolded proteins are substrates for the ubiquitin-proteasome degradation pathway. Treatment of cells expressing CFTR or $\Delta F508$ with proteasome inhibitors, such as lactacystin or MG132, causes the accumulation of multi-ubiquitinated forms of CFTR and generates protein cytoplasmic inclusions known as aggresomes [86, 87, 138, 191]. Similar observations have been made with other membrane proteins. Importantly, when transfected cells are treated with proteasome inhibitors a protein fraction insoluble to mild detergents is generated (Fig. 25A). This makes it necessary to use stronger detergents (1% SDS) in order to observe the complete effect of proteasome inhibitors on protein turnover (Fig 24).

We hypothesized that the ubiquitin-proteasome pathway mediates the ER-degradation of K_{ATP} channels. In order to establish the extent to which proteasome inhibition affects degradation of K_{ATP} channel subunits, pulse-chase experiments were performed on single subunits with $6\mu\text{M}$ lactacystin during the total pulse-chase time period as explained in *Experimental procedures*. SUR1 expressed alone under the presence of lactacystin exhibits biphasic turnover. Around $\sim 60\%$ is degraded with a half-life of $2.82\pm 0.07\text{h}$ (fast rate; $n=3$). The remaining $\sim 40\%$ is stable and degrades with a half-life of $12.2\pm 0.1\text{h}$ (slow rate; $n=3$). In this case, the fast rate ($t_{1/2}=2.82\text{h}$) of SUR1 (+Lact) is higher than that obtained for SUR1 chased in the absence of lactacystin ($t_{1/2}=1.35\text{h}$). Moreover, the fraction of slowly-degraded SUR1 protein increases from $\sim 20\%$ to $\sim 40\%$ after lactacystin treatment (Figure 25A). Thus, proteasome inhibition appears to double the amount of the slowly-degraded fraction of SUR1 protein. We have already shown that in pulse-chase experiments $\sim 20\%$ of SUR1 is degraded slowly and

may correspond to SUR1 that has acquired a fully folded conformation (Fig 20A). Proteasome inhibition with lactacystin clearly increases the amount of slowly degrading SUR1 protein (~40%). However, the increase seen in the slowly-degrading component is unlikely due to an increase in folding efficiency. Rather, it likely represents unfolded, insoluble SUR1 that has been accumulated in the cytoplasm (Fig 25C), unable to be degraded by the inhibited proteasome, since it is only recovered by solubilization with 1% SDS.

Δ F1388 expressed alone in the presence of lactacystin has a biphasic turnover similar to SUR1. Around ~60% is degraded with a half-life of 1.73 ± 0.07 h (fast rate; n=4) during the first two hours of chase. The remaining ~40% is stable and degrades with a half-life of 16.7 ± 0.1 h (slow rate; n=4). Interestingly, Δ F1388 expressed alone without lactacystin is totally degraded by a monophasic turnover whereas Δ F1388 (+lactacystin) generates a biphasic turnover and a significantly non-degraded fraction (~40%). As previously suggested, this non-degraded fraction may not represent a Δ F1388 folded conformation but rather an unfolded one that is not digested by the inhibited proteasome. These results suggest that SUR1 and its mutant Δ F1388 are degraded via the ubiquitin-proteasome pathway.

Figure 23

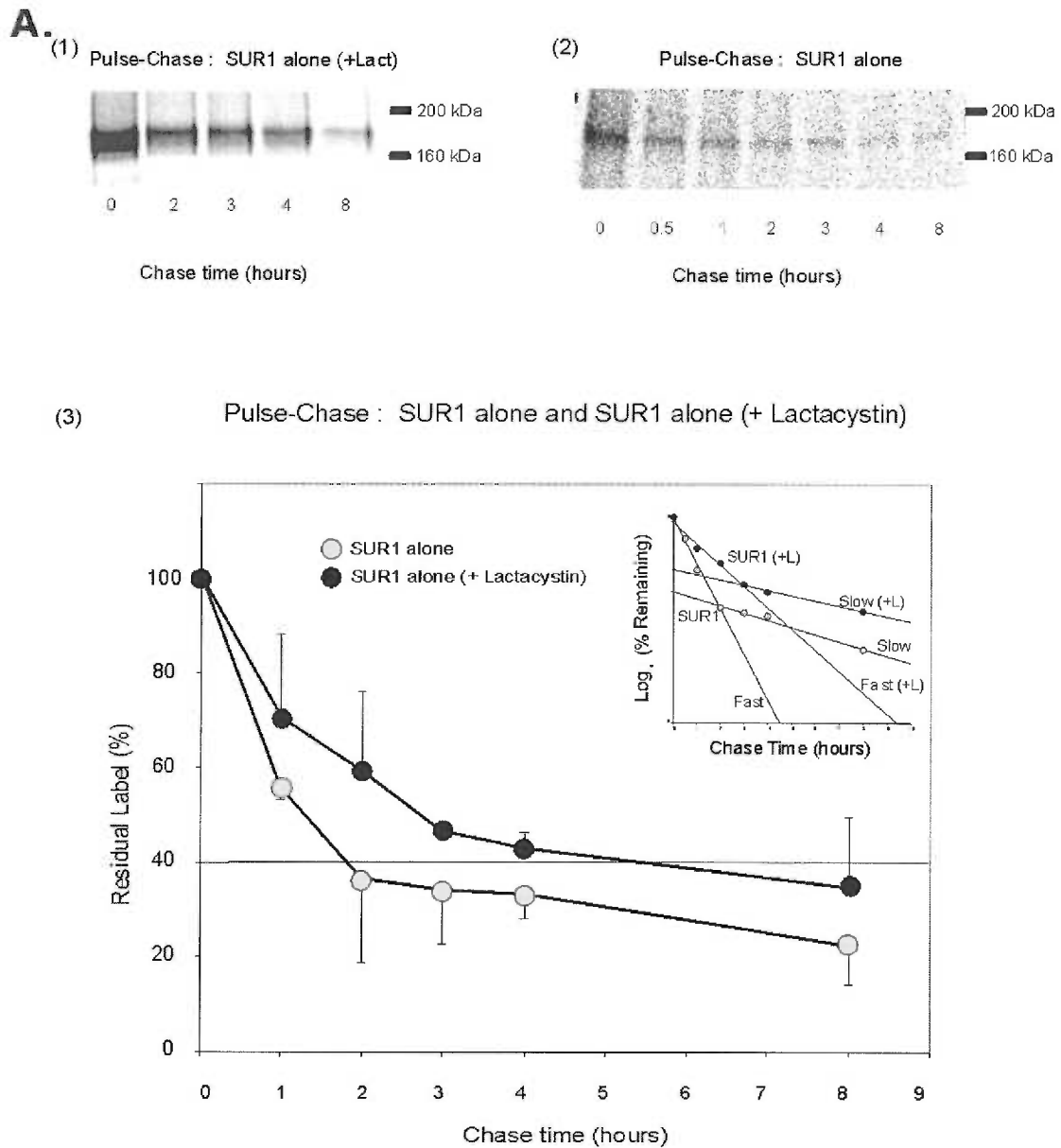


Figure 23A. Proteasome inhibition slows down degradation of SUR1. Metabolic labeling (pulse) and chase of SUR1 alone in the presence of lactacystin (SUR1+L) compared with SUR1. Cells were pulse-labeled for 30 min and chased for various times as indicated. SUR1 was immunoprecipitated with anti-v5 antibody. (1) SUR1 (+L) appears as a single immature band. (2) SUR1 alone has been included for comparison. (3) Degradation of SUR1(+ L) compared with SUR. SUR1(+ L) degradation rate (*closed circles*) is biphasic with ~60% of SUR1 being lost during the first three hours of chase. Data can be fit with two different exponential functions (fast and slow rates respectively). The SUR1 (+L) $t_{1/2}$ are 2.82 ± 0.07 h (fast rate) and 12.2 ± 0.1 h (slow rate). The fast rate is higher than values obtained for SUR1 ($t_{1/2} = 1.35$ h). The SUR1 alone curve (*open circles*) has been included. Each point represents the averaged value from three independent experiments, with the *error bar* representing the S.E. *Insert:* Semilog plot showing the degradation rates of SUR1 in the presence [SUR1 (+L)] or absence (SUR1) of lactacystin. Degradation rates were labeled as follows. SUR1 fast [Fast (+L)] and slow [Slow (+L)] rates in the presence of lactacystin; SUR1 fast (FAST) and slow (SLOW) in the absence of lastacystin.

Figure 23

B.

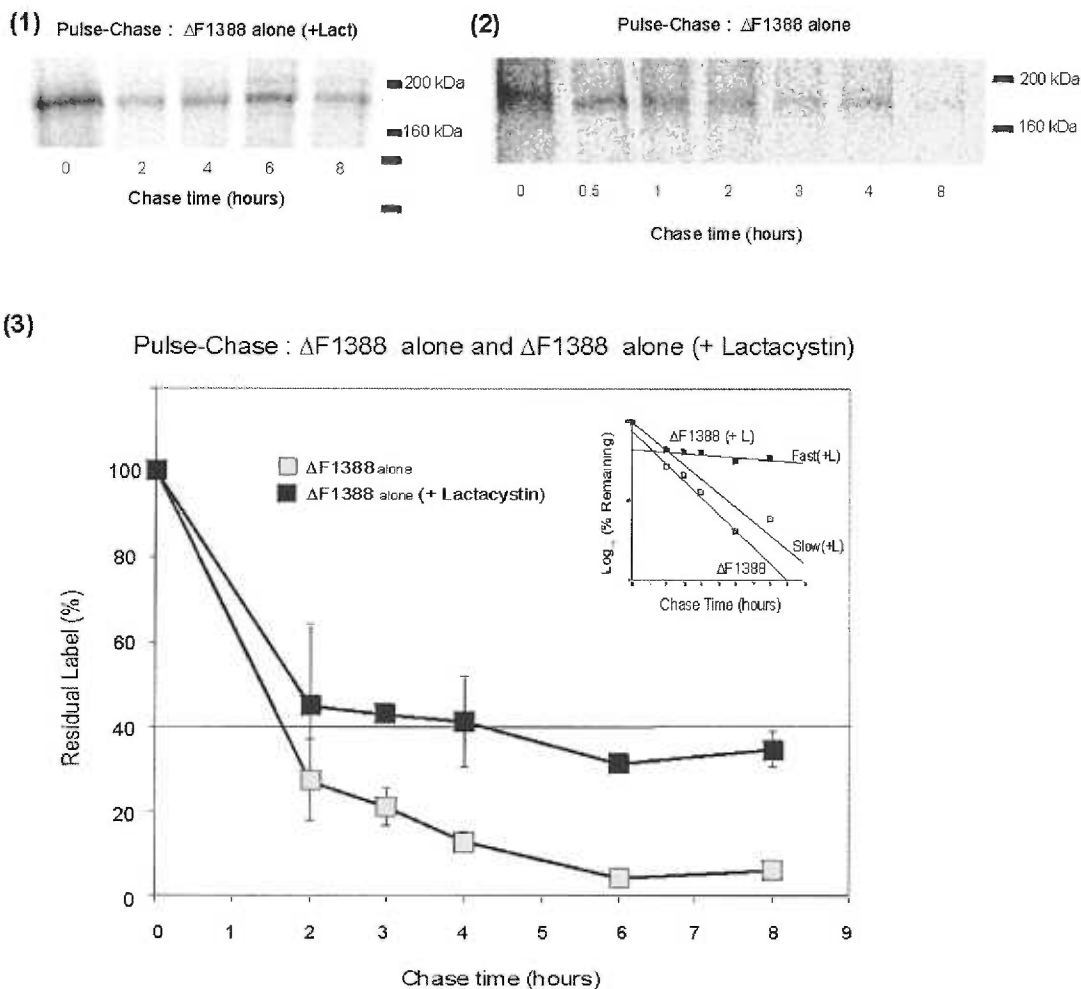


Figure 23B. Proteasome inhibition slows down degradation of $\Delta F1388$. Metabolic labeling (pulse) and chase of $\Delta F1388$ alone in the presence of lactacystin ($\Delta F1388+L$) compared with $\Delta F1388$ alone. Cells were pulse-labeled for 30 min and chased for various times as indicated. $\Delta F1388$ was immunoprecipitated with anti-v5 antibody. (1) $\Delta F1388$ (+L) appears as a single stable immature band. (2) $\Delta F1388$ alone has been included for comparison purposes. (3) Degradation of $\Delta F1388$ (+ L) compared with $\Delta F1388$ alone. $\Delta F1388$ (+ L) degradation rate (*closed squares*) is biphasic with ~40% of $\Delta F1388$ being lost during the first two hours of chase. Data can be fit with two different exponential functions (fast and slow rates respectively). The $\Delta F1388$ (+ L) $t_{1/2}$ are 1.73 ± 0.07 h (fast rate) and 16.7 ± 0.1 h (slow rate) respectively. The fast rate is higher than values obtained for $\Delta F1388$ alone. The $\Delta F1388$ alone curve (*open squares*) has been included for comparison purposes. Each point represents the averaged value from five independent experiments, with the *error bar* representing the S.E. *Insert:* Semilog plot showing the degradation rates of $\Delta F1388$ in the presence [$\Delta F1388$ (+L)] or absence ($\Delta F1388$) of lactacystin. Degradation rates were labeled as follows. $\Delta F1388$ fast [Fast (+L)] and slow [Slow (+L)] rates in the presence of lactacystin; $\Delta F1388$ in the absence of lastacystin.

Proteasome inhibition leads to accumulation of polyubiquitinated K_{ATP} channel subunits—

Proteins targeted for proteasome degradation are recognized by polyubiquitination. Thus, we examined whether channel proteins are ubiquitinated to further test the hypothesis that K_{ATP} channel subunits are degraded via the ubiquitin-proteasome pathway. To maximize the signal of ubiquitinated proteins, COS-1 cells were transfected with individual subunits SUR1, $\Delta F1388$, or Kir6.2 and treated with the proteasome inhibitor MG132 10 μ M for eight hours. Cells were lysed with 1% SDS buffer, immunoprecipitated and divided into two equal (sister) samples. Sister samples were immunoblotted using either an antibody employed in immunoprecipitation or with an anti-ubiquitin antibody. MG132 treatment resulted in a significant increase in the amount of immunoprecipitated protein in all cases. No protein was detected in untransfected COS-1 cells (data not shown). These results further support the hypothesis that K_{ATP} channel subunits are degraded through the proteasome. Moreover, inhibition of proteasome function leads to accumulation of high molecular weight species (HMWs) [87, 196] that are recognized by the anti-ubiquitin antibodies.

Interestingly, HMWs are not detectable in untreated cells, suggesting that overexpression does not saturate the proteasome. It is evident that proteasome inhibition seems to have a more pronounced effect on the mutant $\Delta F1388$. We have also performed experiments in which both SUR1 and $\Delta F1388$ were exposed in the same gel with similar results (data not shown). This is probably due to the fact that $\Delta F1388$ is completely degraded (Fig 1A), whereas a fraction (~30%) of SUR1 reaches a conformation that is resistant to degradation. The Kir6.2 subunit was also overexpressed in the insulin

secreting cell line, INS-1. Although, INS-1 cells normally express endogenous K_{ATP} channels subunits, these were undetectable under our experimental conditions. Similar to that observed in COSm6 cells, treatment with proteasome inhibitors in INS-1 cells overexpressing Kir6.2 also led to accumulation of polyubiquitinated Kir6.2. Taken together, these results suggest that proteasome inhibition leads to the appearance of HMW complexes that are ubiquitinated.

To further determine if ubiquitination is involved in targeting K_{ATP} channel subunits for degradation, we co-expressed SUR1-Kir6.2 or $\Delta F1388$ -Kir6.2 with the ubiquitin mutant K48R (Ub-K48R). Ub-K48R impairs polyubiquitination, thus preventing proteasome degradation. We predicted that overexpression of Ub-K48R would result in accumulation of ubiquitinated species that are unable to acquire a long chain of polyubiquitin. Indeed, co-expression of K_{ATP} channel subunits with Ub-K48R generates an accumulation of multiubiquitinated HMW complexes (Fig 5C).

These results demonstrate that K_{ATP} channel subunits are polyubiquitinated before they are targeted for proteasome degradation.

Figure 24

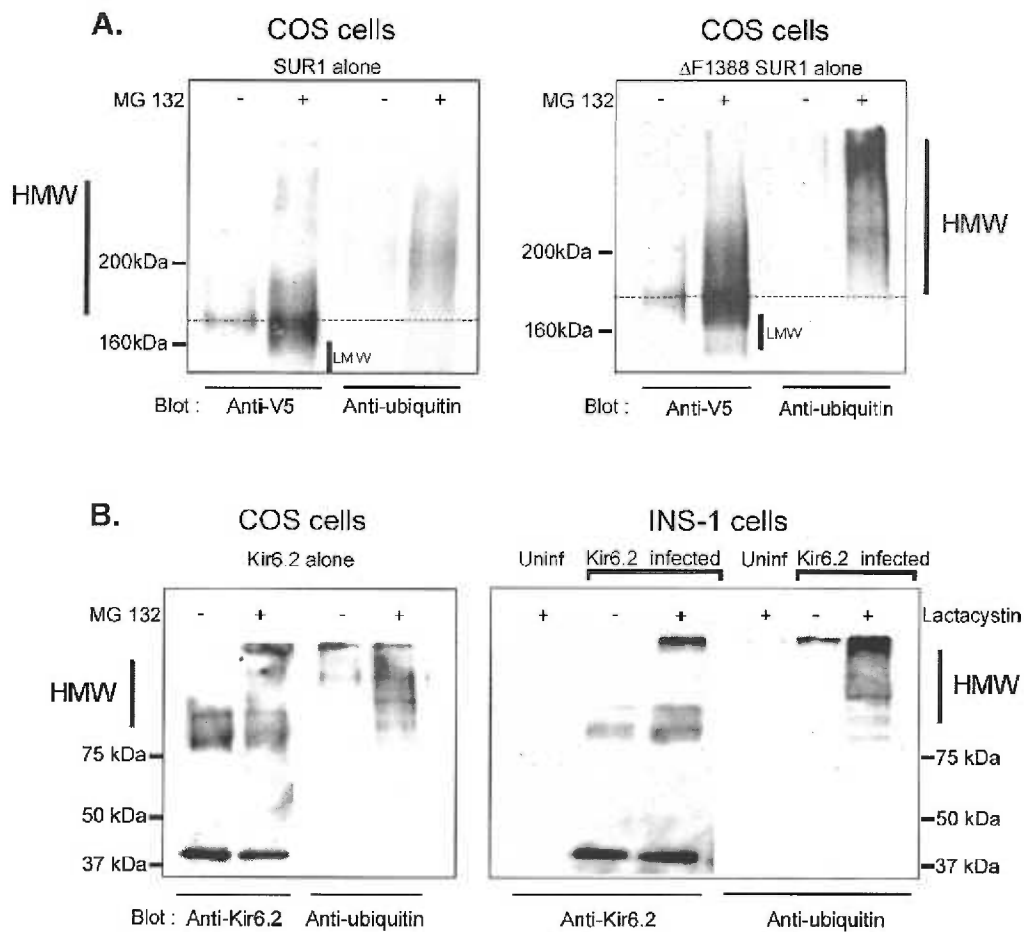


Figure 24. Proteasome inhibition leads to accumulation of K_{ATP} channel subunits. Immunoprecipitation and blotting of K_{ATP} channel subunits after 8h treatment with MG132 or lactacystin. COS or INS-1 cells were transfected or infected respectively. After treatment, cells were lysed with 1%SDS buffer, immunoprecipitated and divided in two sister samples. Sister samples were immunoblotted using either a antibody employed in immunoprecipitation or with anti-ubiquitin antibody. **A.** SUR1 and $\Delta F1388$ show a significant increase after MG132 treatment. Most of this increase is due to the appearance of HMW and LMW range. HMW complexes are mostly ubiquitinated. Notice the difference between the ubiquitination level between SUR1 and $\Delta F1388$, after MG132 treatment. **B.** Kir6.2 expressed in COS or INS-1 cells. Most of its increase is determined by the appearance of HMW complexes that can be blotted with anti-ubiquitin antibody.

Figure 24

C.

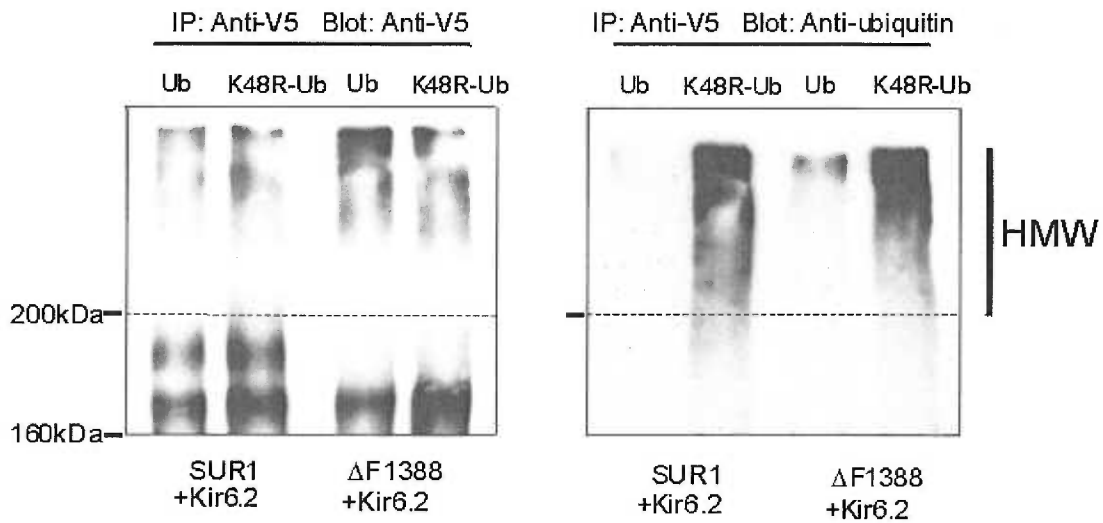


Figure 24C. Inhibition of polyubiquitination leads to accumulation of ubiquitinated species. COS cells were trans- fected with K_{ATP} channels subunits and either wild-type ubiquitin or the ubiquitin mutant, K48R. K_{ATP} channel subunits were immunoprecipitated and divided in two sister samples. Sister samples were immunoblotted using either an antibody employed in immunoprecipitation or with anti-ubiquitin antibody. HMW of non-degraded and ubiquitinated species are revealed in those cells co-transfected with the K48R mutant.

Proteasome inhibition yields insoluble and unglycosylated species—

In addition to the HMW species, proteasome inhibition also leads to the appearance of some lower molecular weight (LMW) SUR species (Fig 24A). Studies have demonstrated that proteasome inhibition often results in accumulation of insoluble, unglycosylated protein species [133, 135]. These species correspond to protein that has been ubiquitinated and processed by cytosolic deglycosylases and accumulate in perinuclear inclusions known as aggresomes[138].

We tested whether the LMW SUR1 species seen in cells treated with proteasome inhibitors corresponded to the unglycosylated forms. COS-1 cells were transfected with SUR1 or Δ F1388 alone. Untreated cells or those treated with MG132 for 8 hours were lysed with mild detergents (1% NP-40) (soluble fraction), centrifuged at 14,000 rpm, pellet- recovered and solubilized with 1% SDS (insoluble fraction), and then blotted. Untreated cells expressing SUR1 or Δ F1388 showed the existence of only a ‘soluble’ immature band that may correspond to the ER membrane-inserted subunit. After MG132 treatment an ‘insoluble’ fraction appeared (Fig 25A). The SUR1 and the Δ F1388 insoluble fractions appear to be composed of several species of different molecular weights all showing equal or lower molecular weight than the ‘soluble’ immature band. Interestingly, proteasome inhibition seems to have differential effects on SUR1 and Δ F1388. MG132 treatment renders a SUR1 insoluble fraction that is minor and SUR1 remains mostly ‘soluble’. In contrast, MG132 treatment shifts most of the Δ F1388 from being soluble to being insoluble. These results suggest that SUR1 is able to reach a folded conformation that makes it less prone to being targeted for proteasome degradation, whereas Δ F1388

may be improperly folded, making it a target for retrotranslocation and degradation (Fig 25A).

In order to establish the glycosylation level of the soluble and insoluble SUR species, we treated cell lysates with the glycosidase EndoH, which deglycosylates core-glycosylated (immature) SUR species. Soluble SUR1 and $\Delta F1388$ treatment with EndoH revealed them as immature core glycosylated subunits (Fig 25B). Comparing soluble SUR species treated with EndoH or left untreated with the insoluble fraction of $\Delta F1388$, we found that the $\Delta F1388$ insoluble fraction appears like a smear of multiple bands with different molecular weights. EndoH treatment reduces this $\Delta F1388$ insoluble smear to two prominent bands: one migrates at the same level as the SUR1 and $\Delta F1388$ soluble fractions treated with EndoH (deglycosylated species) and the second band migrates at a lower molecular weight that may correspond to partially degraded $\Delta F1388$ (Fig 25B). These results suggest that proteasome inhibition generates a fraction that is physicochemically different from the membrane-associated one and that represents a mix of glycosylated, deglycosylated, and partially degraded SUR species.

Figure 25

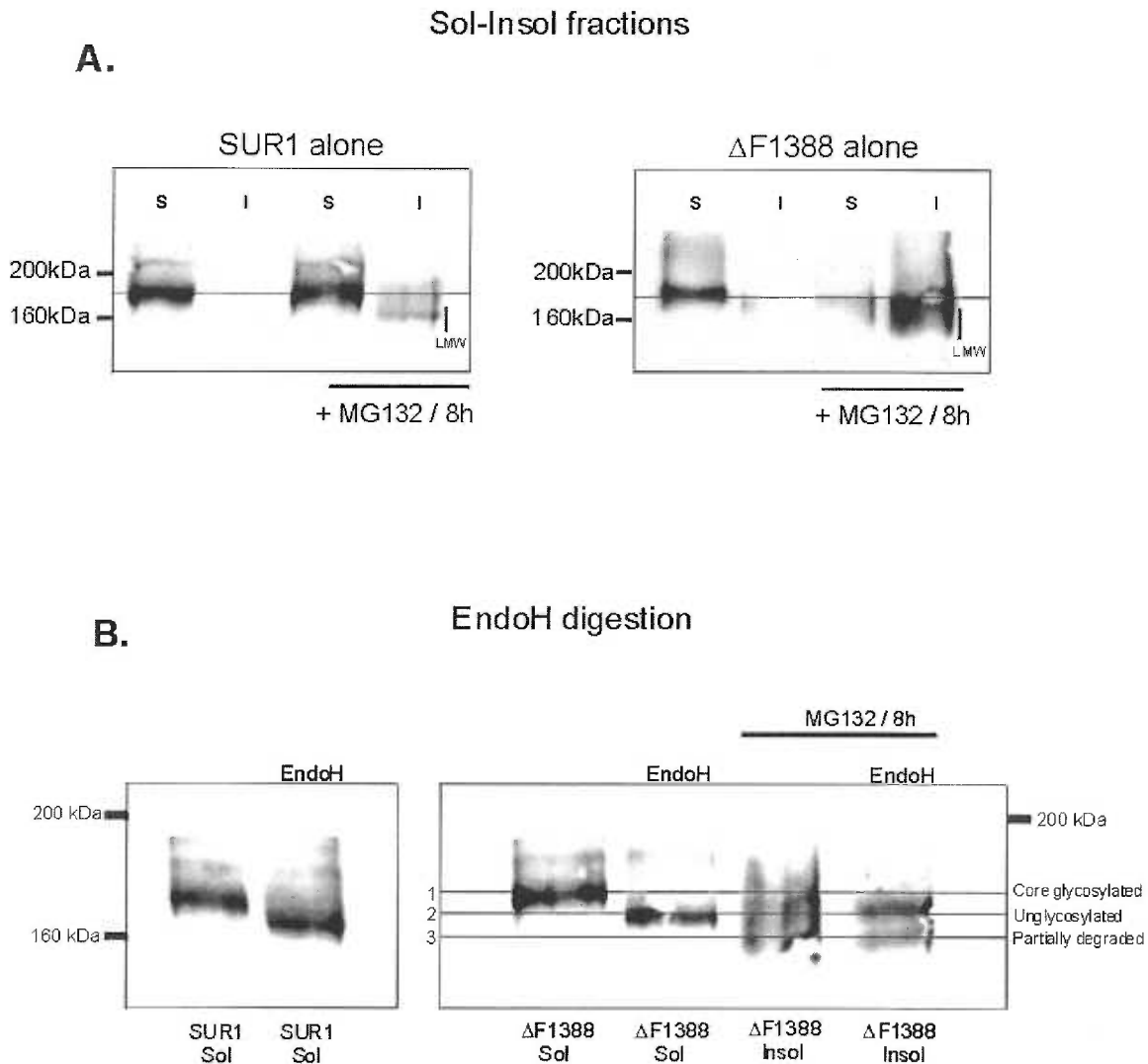


Figure 25. Proteasome inhibition yields insoluble and unglycosylated species. A. Immunoblotting of SUR species after 8h treatment with MG132. COS cells were transfected with either SUR1 or Δ F1388 alone. After treatment, cells were lysed with mild detergents (1% NP40) generating a 'soluble' fraction (S). Alternatively, samples were centrifuged, and pellet-recovered and solubilized with 1% SDS to obtain a 'insoluble' fraction (I). The I fraction appear to be composed of several species of different molecular weights that can be grouped as LMW (low molecular weight) complexes. **B.** Endo H treatment reveals SUR1 and Δ F1388 as core glycosylated proteins. Δ F1388 insoluble (I) fraction generated after MG132 treatment, appears as a smear of multiple bands with different molecular weights. EndoH reduces this insoluble smear to two bands: one migrates at the level of unglycosilated species and the second band migrates at a lower molecular weight that may correspond to partially degraded Δ F1388.

Proteasome inhibition results in cytoplasmic accumulation of K_{ATP} subunits in aggresomes—

It has been demonstrated that proteasome inhibition generates cytoplasmic inclusions that localize in a well-defined perinuclear location—that is, aggresomes [138]. We examined whether proteasome inhibition in COS-1 cells expressing K_{ATP} channel subunits would lead to the formation of aggresomes. Cells were co-expressed with SUR1 or ΔF1388 and Kir6.2 subunits and treated with MG132 for 8 hours. MG132 treatment led to the appearance of prominent perinuclear inclusions (Fig 25C) that correspond well with the appearance of an insoluble fraction after eight hours of MG132 treatment. We suggest that these perinuclear inclusions correspond to aggresomes and may be composed of a mix of undegraded, deglycosylated, polyubiquitinated, and partially digested K_{ATP} channel subunits.

To further characterize these inclusions, we performed double immunofluorescence staining experiments using two known markers for aggresome, ubiquitin and vimentin, after 8 hours of lactacystin treatment. As shown in Figure 7, the inclusions co-localized with both K_{ATP} channel subunits, SUR1 or ΔF1388 and Kir6.2. The inclusions also co-localized Kir6.2 with ubiquitin and vimentin when expressed with ΔF1388. Similar results were obtained with SUR1.

These results indicate that proteasome inhibition leads to the accumulation of K_{ATP} subunits in a cytosolic perinuclear location that corresponds to aggresomes.

Figure 25

C.

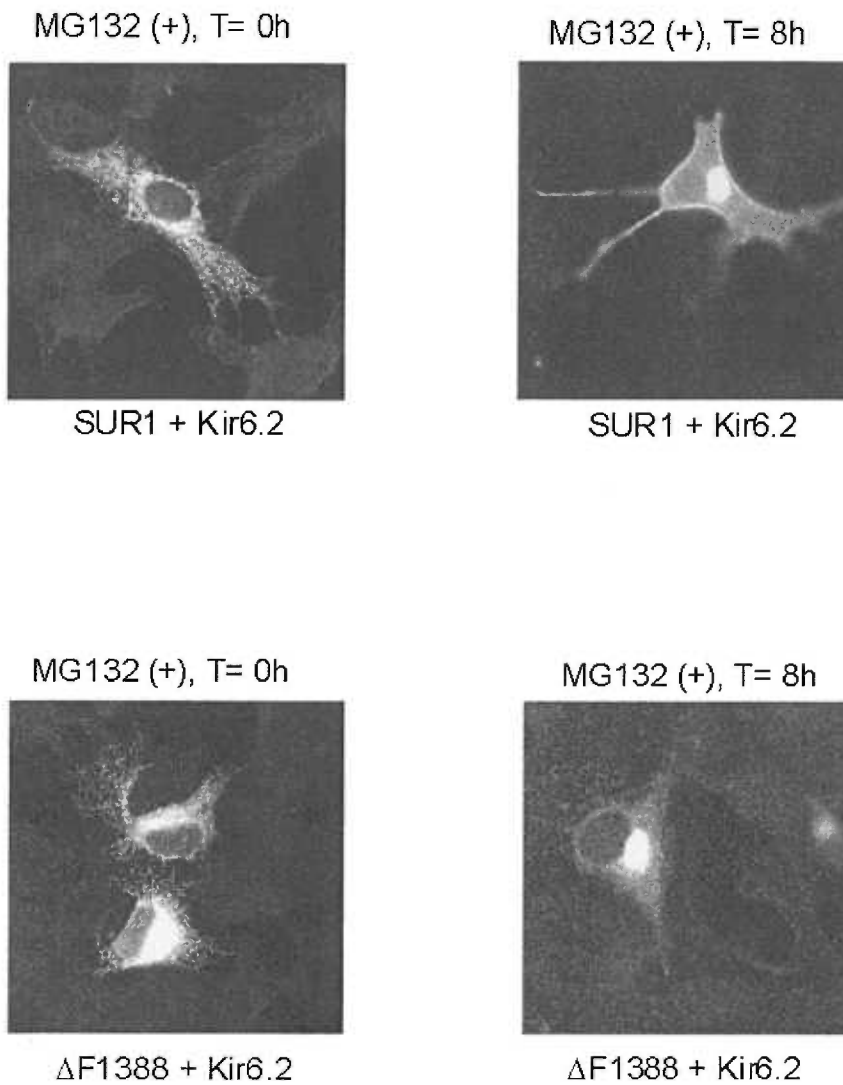


Figure 25C. Proteasome inhibition results in cytoplasmic accumulation of K_{ATP} channel subunits in perinuclear inclusions. COS cells were transfected with K_{ATP} channel subunits and treated or not with MG132 for 8h. Cells were fixed with methanol and immunostained with anti-FLAG (primary antibody) and Cy3 conjugated anti-mouse (secondary antibody) revealing FLAG tagged SUR species. MG132 treatment leads to the appearance of prominent perinuclear inclusions that are correlated with the appearance of the insoluble (I) SUR fraction after 8 hours of proteasome inhibition.

Co-localization of K_{ATP} channel subunits with aggresome markers (+ Lact, 8 h)

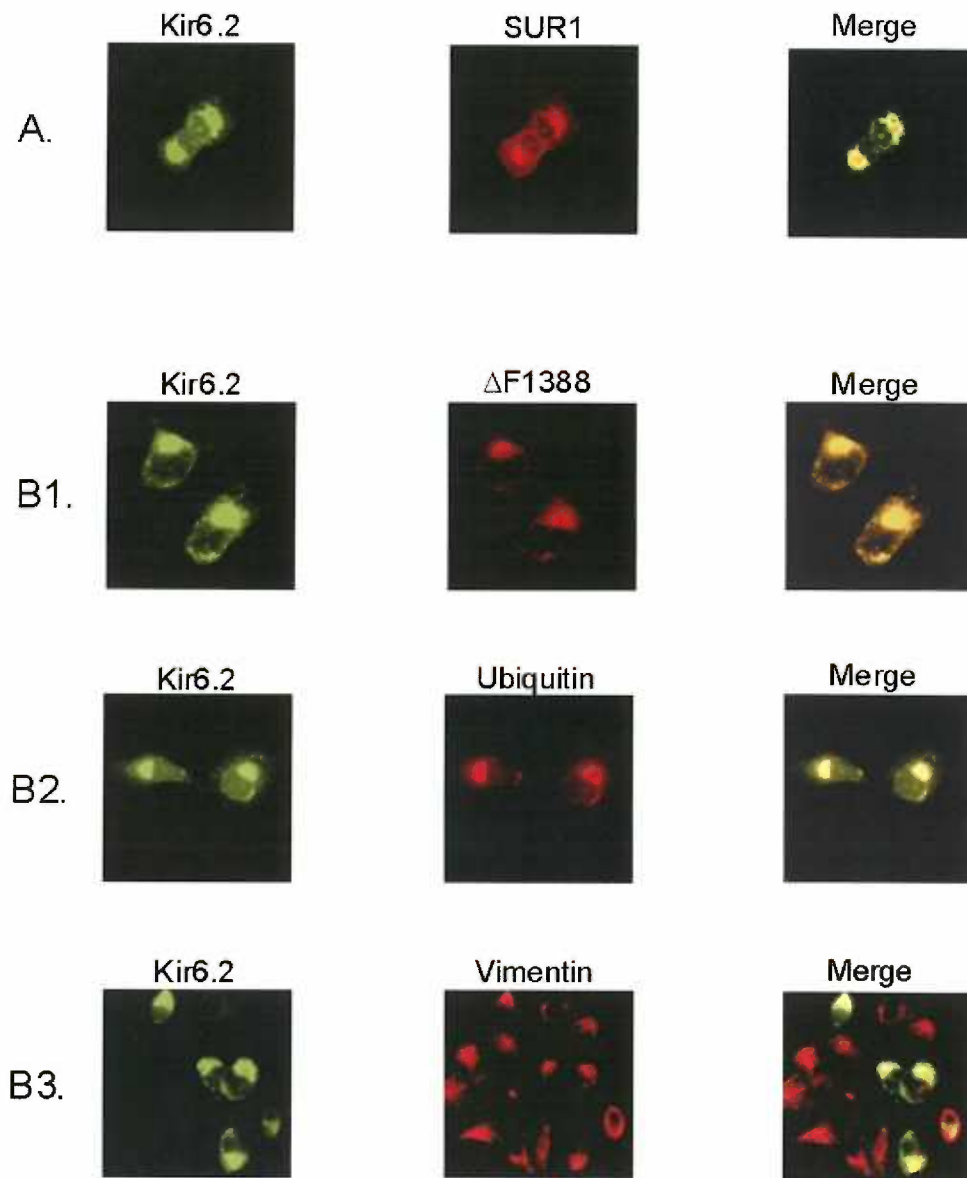


Figure 26

Figure 26. Perinuclear Inclusions co-localize with K_{ATP} channel subunits and aggresome markers. COS cells were transfected with K_{ATP} channels subunits and treated or not with lactacystin for 8h. Cells were fixed with methanol and immunostained with anti-FLAG (SUR species), anti-Kir6.2, anti-vimentin, and anti-ubiquitin as primary antibodies. Cy3-conjugated (red) and Alexa-conjugated (green) anti-mouse or rat, were used as secondary antibodies respectively. Lactacystin treatment leads to the appearance of prominent perinuclear inclusions after 8 hours of proteasome inhibition. The perinuclear inclusions co-localize with Kir6.2 and SUR1 (A), Kir6.2 and $\Delta F1388$ (B1), Kir6.2 (+ $\Delta F1388$) and ubiquitin (B2), and Kir6.2 (+ $\Delta F1388$) and vimentin (B3). Ubiquitin and vimentin are known aggresome markers.

DISCUSSION

In this study, we have examined several aspects of the biogenesis and ER degradation of K_{ATP} channels expressed in COS and in the insulin secreting INS-1 cell lines.

Pancreatic β -cell function relies on proper metabolic regulation of K_{ATP} channel activity, which in turn depends on proper plasma membrane localization of the channel. The number of K_{ATP} channels present at the cell surface appears to be regulated by processes such as endocytosis, retention/retrieval and export signals, and interaction with proteins such as 14-3-3 [103] [102]. However, it is probable that other mechanisms, such as K_{ATP} channel folding and degradation, play a role in the delivery of K_{ATP} channels to forward compartments. A recent study found that neuronal activity seems to regulate synaptic accumulation and ER export of NMDA receptors [124]. These findings describe new pathway linking trafficking regulation at the ER/Golgi level with neuronal activity. This and many other studies have established that the exit from the ER is the limiting step in the overall processing of membrane proteins [133-135].

Degradation of individual K_{ATP} channel subunits. Folding and ER degradation are two intrinsically associated processes. Unfolded proteins in the ER are recognized by chaperones, retrotranslocated to the cytoplasm and finally degraded. Our results indicate that SUR1 turnover is biphasic (fast and slow degradation rates). We propose that the fast

SUR1 degradation rate correspond to the presence of unfolded SUR1, which would be prone to rapid degradation. Moreover, the SUR1 fast degradation rate is similar to the degradation rate established for $\Delta F1388$. This similarity raises the possibility that $\Delta F1388$ may correspond to one or more unfolded variants of SUR1. $\Delta F1388$ is totally degraded by a single rate that is similar to the fast rate of the SUR1 turnover. The only difference between the SUR1 turnover and the $\Delta F1388$ turnover is that the latter lacks the slow component. We propose that the $\Delta F1388$ mutation may cause a folding kinetic impairment that does not allow $\Delta F1388$ to reach its fully folded conformation and became degradation-resistant [86]. Nevertheless, although our data supports our explanation, we are aware that the subunit turnover rate cannot be equated to a putative folding or assembly state.

The SUR1 biphasic turnover also determines a slow degradation rate. There are two alternative explanations for the slow component. First, SUR1 may oligomerize with itself, which will make SUR1 less prone to degradation. However, currently there is no evidence for self-oligomerization of SUR1. A second explanation is that SUR1 acquires a fully folded conformation, which may become degradation resistant by itself or once it is sorted within the ER. The sorted SUR1 would be the one available for assembly into multimeric K_{ATP} channels. This implies that the SUR1 primary structure is sufficient to provide all requirements needed by SUR1 in order to reach a rapid degradation-resistant conformation, without help from the Kir6.2 subunit.

These findings are somewhat different from those reported by Crane et al. [191] who demonstrated a significant difference between degradation rates of SUR1 and $\Delta F1388$. They established a half-life of 25.5h for SUR1 and 3h for $\Delta F1388$. The main

point of controversy resides in the SUR1 turnover rate. This may be explained by the fact that Crane et al. used a significantly higher amount of SUR1 cDNA than our experiments (8 μ g v/s 1 μ g, respectively). Moreover, in their case SUR1 cDNA transfection was made by electroporation that significantly improves transfection efficiency. This SUR1 overexpression may have rendered saturation of the QC system, slowing down the SUR1 turnover rates values.

The Kir6.2 subunit turnover is also biphasic, exhibiting fast and slow components. There are two possible interpretations for these results. First, as it has been proposed, the biphasic decay of Kir6.2 may represent the assembly of Kir6.2 in tetramers, which will make Kir6.2 less prone to rapid degradation (slow component). However, a second alternative is also possible: Kir6.2 subunits may become resistant to rapid degradation because they reach a fully folded conformation that may be sorted within the ER. This implies that the Kir6.2 rapid degradation-resistant conformation would be independent of Kir6.2 oligomeric state.

The proper folding and putative homo-oligomerization of K_{ATP} channel subunits appear to be inefficient processes, since degradation seems to be the fate for most synthesized K_{ATP} channel subunits. This situation is similar to the inefficient biogenesis reported for CFTR [86], AChR [94], δ -opioid receptor [103, 133, 135], and other membrane proteins. It is possible that this is the case for our heterologous and overexpressed system, which may overload the QC system. Nevertheless, strong evidence suggests that protein inefficient folding is also a common feature in non-overexpressed systems [130]. In any case, more studies are needed in order to establish

the molecular causes and the putative biological advantage of such inefficient K_{ATP} channel biogenesis [102].

Degradation of co-expressed K_{ATP} channel subunits. ER assembly of multimeric membrane proteins has been best characterized in the acetylcholine receptor (AChR) and the T receptor. A model describes AChR assembly. In the model ('sequential model') subunits rapidly assemble and the assembly process in turn facilitates folding of the individual subunits, which retards the turnover rate of the channels [94]. Nevertheless, it is also possible that channel assembly may facilitate their sorting into a different ER compartment, away from the degradation machinery. Our results may indicate that co-expression of SUR1 with Kir6.2 does significantly change K_{ATP} channel subunit fast degradation rates on both SUR1 and Kir6.2. This suggests that either SUR1-Kir6.2 association may affect their folding rates or they may be sorted to a degradation-resistant ER compartment. Nevertheless, we are aware that stronger experimental data is needed in order to validate this conclusion.

Assembled K_{ATP} channels are exported outside the ER and they can reach a 'mature' state in the middle Golgi. Our results show that around ~15% of the synthesized SUR1 co-expressed with Kir6.2 is able to reach a mature state. On the other hand, ~30% of SUR1 expressed alone is able to reach a conformation that is more resistant to degradation. Moreover, ~30% fraction of Kir 6.2 also reaches a rapid degradation-resistant state. We do not have a way to measure which fraction of Kir6.2 is able to mature along with SUR1, but we may assume that under our equimolar (1:1) conditions of SUR1: Kir6.2 co-expression, this Kir6.2 fraction should be around 20-30% as well.

Overall, these findings suggest the following. First, biogenesis of both SUR1 and Kir6.2 are inefficient processes in which ~70% is degraded rapidly, leaving only ~30% of SUR1 or Kir6.2 to reach a fully folded conformation that is resistant to rapid degradation. Second, the degradation-resistant conformation appears to be the only conformation capable of assembling into octameric K_{ATP} channels.

K_{ATP} channel subunit degradation is mediated by the ubiquitin- proteasome pathway.

Inside the ER, proteasomal degradation appears to be the main fate of a number of membrane proteins. CFTR is the best-studied case. CFTR and its mutant $\Delta F508$ appear to be degraded at a similar rate, although ~30% of CFTR is able to reach a degradation-resistant conformation and it is exported out of the ER. Within the ER, CFTR and $\Delta F508$ become ubiquitinated and retrotranslocated to the cytoplasm where they are degraded by the proteasome. Interestingly, new studies have demonstrated that CFTR degradation can be achieved by some specific mechanisms.

Proteasome inhibition also has several effects on K_{ATP} channel proteins. First, after proteasome inhibition, SUR1, $\Delta F1388$, and Kir6.2 (data not shown) fast degradation rates become slower. Second, ~40% or more of the synthesized K_{ATP} channel subunits become non-degraded. Third, a significant amount of this non-degraded fraction is insoluble in mild detergents and probably corresponds to cytosolic inclusions. Fourth, subunits become ubiquitinated, deglycosylated, and accumulate in perinuclear inclusions where they co-localize with aggresome markers. We assume that a general ER marker would not co-localize with those perinuclear aggresome-like inclusions that are

supposedly out of the ER. Experiments are currently underway to validate this assumption.

In our present study, once the proteasome was inhibited, the $\Delta F1388$ ubiquitination level was always higher than the SUR1 level. At the same time, after proteasome inhibition, $\Delta F1388$ rendered a significantly larger insoluble fraction than SUR1. These results may be explained by the fact that, although both subunits are degraded at the same rate, $\Delta F1388$ is degraded completely whereas SUR1 reaches a conformation that is resistant to rapid degradation.

Together, these results lead to the main conclusion that K_{ATP} channel subunits are individually degraded through the ubiquitin-proteasome pathway.

Future directions: Specificity.

Quality control is based on set of general mechanisms that recognize unfolded and misfolded proteins normally targeted for degradation. Recent studies have begun to delineate selective mechanisms that regulate export of individual protein species or protein families. Herrmann et al. [197] have distinguished among the mixture of specific QC proteins those that are needed to fold and assemble specific proteins as ‘outfitters’. The group of outfitters includes specialized chaperones and enzymes such as Nina A —a peptidyl-propyl *cis/trans* isomerase that ensures transport competence of specific rhodopsins in *Drosophila melanogaster*. Another specific factor is the co-chaperone CHIP protein that, together with Hsc70 [198], senses the folded state of CFTR and targets aberrant forms for proteasomal degradation by promoting their ubiquitination. Still

another is the Parking protein, which is an ubiquitin-protein isopeptidase ligase (E3) that seems to be specifically involved in Parkinson's Disease [196].

Moreover, QC specificity may be rendered by target sequences that are present in membrane proteins. In the pentameric nicotinic receptor channels [199], a transmembrane retention signal has been found in of all subunits. The signal seems to be critical, just like the RKR motif in K_{ATP} channels, in assuring assembly and proper subunit stoichiometry to the nicotinic receptor. The signal also targets the nicotinic receptor subunits to degradation.

The results and conclusions presented here about biogenesis and degradation of K_{ATP} channel subunits raise the possibility that K_{ATP} channel QC may be specifically based on a particular set of factors. The chaperone 14-3-3 has been implicated in the recognition of the RKR signal. It is possible that 14-3-3 may recognize RKR inside the ER, and it may have a major role in the folding and assembly of K_{ATP} channels [102]. Structural differences between SUR1 and Kir6.2 may render specific target sequences for retrotranslocation and degradation that would determine a different set of specific QC factors, depending on which subunit is being degraded.

The abbreviations used are: SUR, sulfonylurea receptor; ER, endoplasmic reticulum; PBS, phosphate-buffered saline; BSA, bovine serum albumin; WT, wild type; ERAD, Endoplasmic Reticulum Associated Degradation; CFTR, Cystic Fibrosis Transmembrane

Regulator; HMW, High Molecular Weight; LMW, Low Molecular Weight; QC, Quality Control.

SUMMARY and CONCLUSIONS

The questions addressed in this dissertation have been mainly devoted to characterize the cell-biology and physiology of the SUR1 mutation, $\Delta F1388$. Studies have shown that its co-expression with Kir6.2 resulted in no channel activity. I investigated the molecular mechanism by which this single phenylalanine deletion in SUR1 ($\Delta F1388$) causes HI.

A first set of formulated questions tried to address the cell biological aspects of the $\Delta F1388$ mutation. *Are the $\Delta F1388$ mutant channels able to reach the plasma membrane?* I demonstrated that the lack of functional expression is due to failure of the $\Delta F1388$ mutant channel to traffic to the cell surface. $\Delta F1388$ mutant channels seemed to be retained inside the ER. The study provided direct evidence that, in addition, defective trafficking of K_{ATP} channels was also an underlying molecular mechanism of HI. Trafficking of K_{ATP} channels required that the endoplasmic reticulum-retention signal, RKR, present in both SUR1 and Kir6.2, be shielded during channel assembly. The SUR1- $\Delta F1388$ trafficking defect was partially overcome inactivating the RKR retention signal in the SUR1- $\Delta F1388$ subunit by mutation to AAA. $\Delta F1388_{AAA}$ + Kir6.2 channels were able to reach the cell surface and render active channels. Compared with wild-type channels, the mutant channels had a reduced sensitivity for ATP and were insensitive to the stimulation by MgADP and diazoxide.

These results suggested that F1388 provides structural elements critical for the correct trafficking and function of K_{ATP} channels and provided the basis for the next set

of questions: *What is structurally important in the SUR1 F1388 site? And, which is the physicochemical basis of F1388 that makes K_{ATP} channels being functionally expressed?*

I investigated the biochemical features of the Phe-1388 that control the proper trafficking and function of K_{ATP} channels by substituting the residue with all other 19 amino acids. Whereas surface expression was largely dependent on hydrophobicity, channel response to MgADP was governed by multiple factors and involves the detailed architecture of the amino acid side chain. Thus, structural features in SUR1 required for proper channel function were distinct from those required for correct protein trafficking. Remarkably, replacing Phe-1388 by leucine profoundly altered the physiological and pharmacological properties of the channel. The F1388L-SUR1 channel had increased sensitivity to MgADP and metabolic inhibition, decreased sensitivity to glibenclamide, and responded to both diazoxide and pinacidil. The F1388L mutation in SUR1 made the overall physiological and pharmacological profile of the channel shift toward that of the SUR2B/Kir6.2 channel, which is normally found in smooth-muscle. Thus, genetic variation at this amino acid accounted for some of the functional differences seen in different subtypes of K_{ATP} channels, providing a mechanism for diversity.

I also sought to answer if ER retained channels due to $\Delta F1388$ were prone to rapid degradation by ERAD. I found that not only $\Delta F1388$ mutant channels but also wild type K_{ATP} channel subunits were degraded by the ERAD. Wild-type K_{ATP} channel biogenesis appeared to be inefficient: ~70% of the channel subunits were rapidly degraded by this ER mechanism, and only ~30 % acquired metabolic stability and had the capacity to be incorporated into channel complexes which eventually reached the plasma membrane. By contrast, the K_{ATP} channel trafficking mutant, SUR- $\Delta F1388$, was

rapidly degraded showing monophasic kinetics. Inhibition of proteasome function slowed down the turnover of all wild-type and mutant subunits and led to their accumulation as deglycosylated and/or polyubiquitinated species. Under this condition, the undegraded K_{ATP} channel subunits were found in perinuclear inclusions that could be co-immunostained with aggresome markers such as ubiquitin and vimentin. These results suggested that the ubiquitin-proteasome pathway is involved in the degradation of K_{ATP} channels under both normal and pathological conditions.

In conclusion, my results show that the SUR1- Δ F1388 mutation that causes Hyperinsulinism render channels that are unable to reach the cell surface because they become retained in the ER. The trafficking defect can be partially overcome inactivating the RKR retention signal present in the SUR- Δ F1388 subunit. Mutated channels are insensitive to stimulation by MgADP. Thus, although Δ F1388 mutated channels may reach the cell surface they are unable to be activated. The F1388 is involved controlling two different aspects of the K_{ATP} channel biology: trafficking and functionality. Amino acid substitutions on the F1388 site reveal that different physicochemical aspects of the residue control either the physiology or the trafficking of K_{ATP} channels. Finally, SUR1- Δ F1388 is rapidly degraded by the ubiquitin-proteasome pathway. Moreover, the ubiquitin-proteasome pathway is also involved in the degradation of most of the wild type unassembled K_{ATP} channel subunits.

Final discussion and future directions.

The ER export of K_{ATP} channels.

The K_{ATP} channels are expressed at the cell surface as glycosylated octameric arrangements. The proper assembly of the SUR1 and the Kir6.2 subunits achieves this octameric stoichiometry in the ER and shield the subunits RKR retention signals. Once assembled, K_{ATP} channels must overcome an additional checkpoint in order to be exported out of the ER: residues at the SUR1 C-terminus must be recognized by the ER-QC system as an export signal. In summary, in order to assure ER export of properly assembled K_{ATP} channels, their subunit retention signals must be hidden and the SUR1 export signal must be exposed. This picture of two precise signals leading K_{ATP} channel trafficking arises a number of specific questions and future directions.

What recognizes the RKR signal at the ER?

Recent studies have shown that the 14-3-3 protein can interact with RKR in vitro. The 14-3-3 is a cytosolic protein that appears to be involved in biological activities as diverse as apoptotic cell death, cell cycle control, mitogen signaling, and neuronal plasticity. It is possible to hypothesize that 14-3-3 isoforms may recognize the RKR signal of individual K_{ATP} channel subunits at the ER. In this way, each K_{ATP} channel subunit might form a complex with 14-3-3 before channel subunits become associated together. Therefore, the 14-3-3 protein may regulate K_{ATP} channel assembly. Moreover, since the 14-3-3 has been characterized as a scaffolding protein involved in signaling, it might be expected that signaling proteins (i.e. kinases) may be also part of an *assembly complex* formed by 14-3-3 and K_{ATP} channel subunits. The formation of an assembly

complex between K_{ATP} channel subunits and the 14-3-3 protein may direct K_{ATP} channels subunits into a specific ER compartment. This compartment might be located far away from the degradation ER machinery and closer to the ER exit sites. In addition, it would be important to determine whether the interaction between 14-3-3 and RKR can be regulated (i.e. by phosphorylation) and how these interactions regulate K_{ATP} channel delivery to forward compartments.

What recognizes the K_{ATP} channel export signal?

The C-terminus of SUR1 contains a signal that is essential for the ER export of K_{ATP} channels. Deletion of as few as 7 amino acids from the C-terminus of SUR1 markedly reduces surface expression of the K_{ATP} channels. The recognition of this export signal by putatively specific receptors may facilitate the recruitment and concentration of the K_{ATP} channels at the ER exit sites where COPII coats bud off vesicles destined for the Golgi. The potential role of the SUR1 export signal in the K_{ATP} channel concentration at the ER exit sites can be tested using the temperature-sensitive mutant of the vesicular stomatitis virus glycoprotein (VSVG) that allows functional visualization of ER exit sites. In addition, the SUR1 export signal may interact either with COPII directly or with an escort receptor. Expressing immobilized SUR1 C-terminus peptides with β -cell lysates and pulling down the putatively interactive proteins may test this. In summary, a possible future direction on this topic would be to determine whether the export signal is essential in the recruitment of K_{ATP} channels at the ER exit sites and the possible identification of the receptor that putatively mediates this recruitment and how this affects K_{ATP} channel cell surface expression.

The folding of SUR1 and Δ F1388.

Deletion of phenylalanine 1388 (Δ F1388) in the SUR1 subunit prevents K_{ATP} channels from reaching the plasma membrane and is a cause of HI. The Δ F1388 mutant channels are retained in the ER suggesting that Δ F1388 is probably misfolded. It is possible to think that the Δ F1388 mutation might generate a defect in the folding kinetics of SUR1 and in this way Δ F1388 may impair the acquisition of a fully folded SUR1 conformation. If this were the situation, the Δ F1388 conformation would not be different from an unfolded conformer of SUR1. In any case, direct evidence of changes in the conformation of Δ F1388 compared with SUR1 may be achieved using comparative limited proteolysis of both Δ F1388 and SUR1 in a native microsomal environment, similar to the experimental approach used for establishing the conformational differences between CFTR and CFTR Δ F508. In addition, F1388X substitutions may be used to dissect SUR1 conformations that let K_{ATP} channel ER export competence but prevent proper functionality of K_{ATP} channels (such as F1388V, F1388I) or vice-versa (such as F1388S, F1388Y) (see Chapter 2).

The MgADP insensitivity of the Δ F1388 mutant.

Inactivation of the RKR retention signal allows partial cell surface expression of K_{ATP} channels bearing the Δ F1388 mutation. However, the mutant channels expressed at the cell surface are insensitive to the activating ligand MgADP. The Δ F1388 channel insensitivity to MgADP may be explained because of the location of the Δ F1388 mutation at the NBF2, which is an essential domain that lead Kir6.2 activation by hydrolyzing MgATP, binding the hydrolytic product MgADP, and by transducing the

hydrolytic cycle to a conformational change that opens Kir6.2. It is possible that the Δ F1388 mutation may affect one or more of these events. The ATPase activity of the mutant and the wild type NBF2 may be compared using fusion constructs (i.e. NBF2-maltose binding protein) and measuring the production of [32 P] Pi from labeled [γ - 32 P] ATP. The binding properties of the mutant and the wild type SUR1 may be addressed using photo-affinity labeling of SUR1 and Δ F1388 with 8-Azido [α - 32 P] ATP. Single channel recordings can determine the coupling between SUR1 and Kir6.2 because SUR1 controls the Kir6.2 interburst duration time. Since Δ F1388 is insensitive to MgADP, it would be useful to take advantage of the F1388X substitutions trying to address whether single channel recordings are affected by F1388X (X= any amino acid) substitutions and correlate those results with the lack of MgADP response observed in the Δ F1388 mutant. In summary, a future direction for this topic would be to determine whether the Δ F1388 mutation determines changes in the normal nucleotide hydrolysis, nucleotide binding, and/or the coupling step. Nevertheless, those quantifications cannot be limited to the Δ F1388 mutant only. The F1388X substitutions would allow taking advantage of their varied MgADP responses that probably are correlated with specific conformational changes. Consequently, the F1388X substitutions would let to a better understanding of the K_{ATP} channel physiology.

The F1388L substitution: Gain of function.

Substitution of the SUR1 F1388 residue by a leucine (F1388L) generated a substantial K_{ATP} channel gain of function. F1388L was more sensitive to MgADP and its Maximal Current was at least two times the Maximal Current of the wild type. Although

somewhat mentioned in the previous paragraph, it would be important to establish whether F1388L may be affecting one or more of the following events: NBFs nucleotide hydrolysis, NBFs nucleotide binding, and/or the coupling step between SUR1 and Kir6.2. In addition, F1388L shifts the pharmacological profile of SUR from wild type SUR1 to wild type SUR2A. It would be interesting to perform the reciprocal mutation in the SUR2A L1388 site changing its leucine by a phenylalanine –the residue present in SUR1, and observe whether this L to F substitution shifts the pharmacological profile of SUR2A towards one closer to SUR1. In this event, the F/L1388 residue would be portrayed as a residue that has major significance in the pharmacological response of each K_{ATP} channel subtype. This may help to understand how SUR actually couples the binding of a pharmacological agent with the activation of Kir6.2.

Specific K_{ATP} channel degradation mediated by signals.

Quality control is based on set of general mechanisms that recognize unfolded and misfolded proteins normally targeted for degradation. Recent studies have begun to delineate selective mechanisms that regulate export of individual protein species or protein families. Moreover, QC specificity may be rendered by target sequences that are present in membrane proteins. It would be important to identify specific sequences on the SUR1 or Kir6.2 subunits that may target them for ER degradation. The identified sequences may be used for further identification of QC factors that may be crucial on K_{ATP} channel biogenesis and delivery to forward compartments.

Appendix

The SUR1 NBF1 shows dissociation between nucleotide response and trafficking competence.

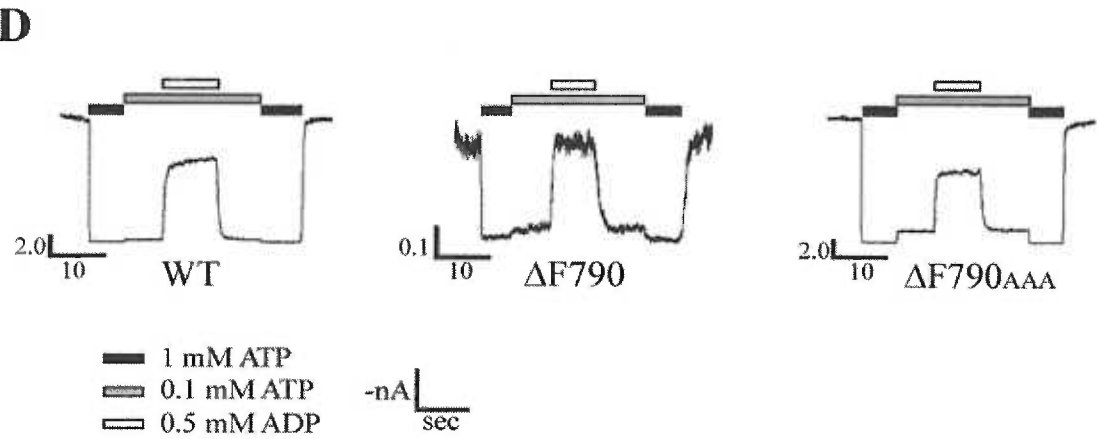
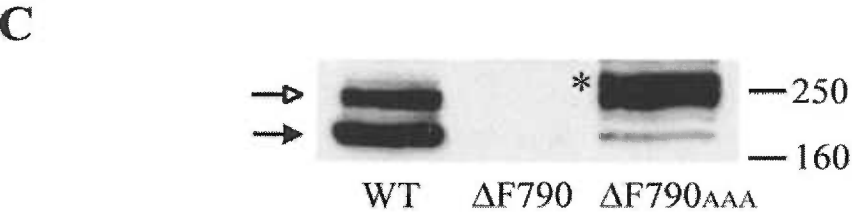
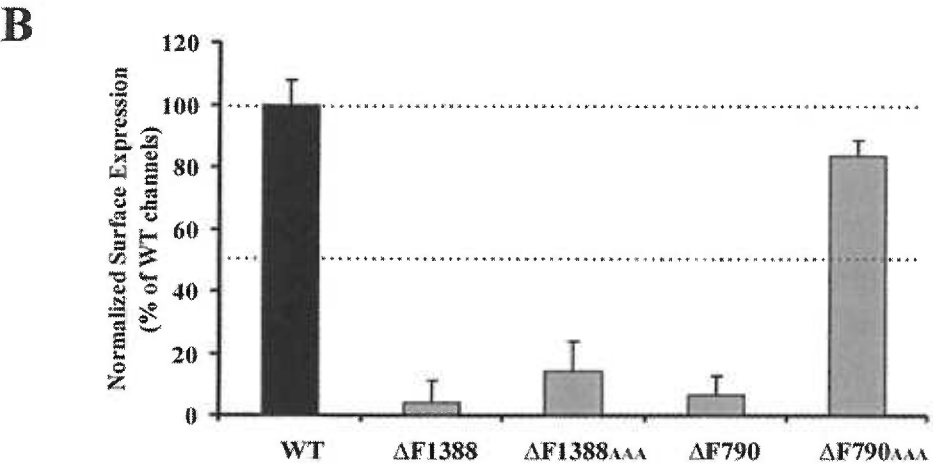


FIGURE 27

(A) Comparison between the CFTR F508 (NBF1) position and its SUR1 homologous, F790 (NBF1).

(B) Surface expression of fSUR1~Kir6.2, fSUR1 Δ F1388~Kir 6.2, and fSUR1 Δ F790~Kir6.2 with (AAA) and without the inactivation of the RKR retention signal. *Note* the prominent increase in the cell surface expression level of fSUR1 Δ F790_{AAA} ~ Kir6.2.

(C) Western blots of fSUR1-WT, fSUR1- Δ F790, fSUR1- Δ F790aaa, co-expressed with Kir6.2. *Note* the different protein expression levels between Δ F790 and Δ F790_{AAA}.

(D) Patch clamp recordings of SUR1 Δ F790 mutant channels. *Note* that there is almost no difference in the amount of MgADP response.

Experimental Procedures

Construction of SUR1 Mutations— Δ F790 mutation of SUR1 was introduced into hamster FLAG-SUR1 cDNA in the pECE plasmid using the QuickChange site-directed mutagenesis kit (Stratagene) as described previously [173]. Epitope tag and mutations were confirmed by DNA sequencing. All SUR1 constructs are in the pECE vector and mouse Kir6.2 cDNA in the pCMV6b vector (a gift from Dr. S. Seino). In immunoblotting experiments, a rat Kir6.2 in pCDNA3 (a gift from Dr. C. Vandenberg) was used for cotransfection. Mutant clones from multiple PCRs were analyzed in all experiments to avoid false results caused by undesired mutations introduced by PCR. In some cases, an additional subcloning step (a restriction fragment of *NotI* and *EcoRI* corresponding to nucleotide positions 4135-4858 of the plasmid) was used to minimize potential PCR-introduced artifacts.

Chemiluminescence Assay-- Surface expression of channels was quantified as described previously [172]. COSm6 cells plated in 35-mm dishes were fixed with 4% paraformaldehyde for 30 min at 4 °C, 48-72 h after transfection. Fixed cells were pre-

blocked in PBS + 0.1% BSA for 30 min or overnight, incubated in M2 anti-FLAG antibody (10 µg/ml) for an hour, washed 4 times for 30 min in PBS + 0.1% BSA, incubated in horseradish peroxidase-conjugated anti-mouse (The Jackson Laboratories, 1:1000 dilution) for 20 min, washed again 4 times for 30 min in PBS + 0.1% BSA, and 2 times for 5 min in PBS. Chemiluminescence signal of each dish was quantified in a TD-20/20 luminometer (Turner Designs) following 15 s of incubation in Power Signal Elisa luminol solution (Pierce). All steps after fixation were carried out at room temperature. Results of each experiment are the average of duplicate or triplicate dishes. For each construct, 3-10 independent experiments were performed.

Immunoblotting-- Immunoblotting analyses were performed using COS-1 instead of COSm6 cells to avoid high background [172]. Although both gave qualitatively similar results, the rat Kir6.2 in pCDNA3 consistently yielded better expression of Kir6.2 than mouse Kir6.2 in pCMV6b when transfected in COS-1 cells; we therefore used rat Kir6.2 for immunoblotting experiments. Cells in 35-mm dishes were transfected with 0.6 µg of SUR1 and 0.4 µg of rat Kir6.2 per dish using FuGENE. Cells were lysed 48-72 h later in 20 mM Hepes, pH 7.0, 5 mM EDTA, 150 mM NaCl, 1% Nonidet P-40 with CompleteTM protease inhibitors (Roche Molecular Biochemicals). Proteins in cell lysates were separated by SDS-PAGE (8%), transferred to nitrocellulose, analyzed by incubation with the M2 anti-FLAG antibody followed by horseradish peroxidase-conjugated anti-mouse secondary antibodies (Amersham Biosciences), and visualized by chemiluminescence (Super Signal West Femto; Pierce).

Patch Clamp Recordings-- COSm6 cells were transfected using FuGENE and plated onto coverslips. The cDNA for the green fluorescent protein was cotransfected with SUR1 and

Kir6.2 to facilitate identification of positively transfected cells. Patch clamp recordings were made 36-72 h post-transfection. All experiments were performed at room temperature as described previously [173]. Micropipettes were pulled from non-heparinized Kimble glass (Fisher) on a horizontal puller (Sutter Instrument, Co., Novato, CA). Electrode resistance was typically 0.5-1 megohms when filled with K-INT solution (below). Inside-out patches were voltage-clamped with an Axopatch 1D amplifier (Axon Inc., Foster City, CA). The standard bath (intracellular) and pipette (extracellular) solution (K-INT) had the following composition: 140 mM KCl, 10 mM K-Hepes, 1 mM K-EGTA, pH 7.3. Data were analyzed using pCLAMP software (Axon Instrument).

Results and discussion

We engineered the homologous $\Delta F508$ mutation of the CFTR in the SUR1 subunit of the K_{ATP} channels that corresponds to the mutation SUR1 $\Delta F790$. Both mutations are located in the NBF1 of either CFTR ($\Delta F508$) or SUR1 ($\Delta F790$) respectively (Fig. 27A). Cell surface expression of the mutant $\Delta F790$ reveals a lack of surface expression similar to the cell surface expression level of $\Delta F1388$ (Fig. 27B). The lack of cell surface expression of the $\Delta F790$ mutant may be explained by the following. First, the SUR1 $\Delta F790$ mutation may cause misfolding and retention of the K_{ATP} channels, probably at the ER level. And second, the $\Delta F790$ mutant may be prone to very fast degradation since its steady-state protein level is significantly reduced (Fig. 27C). The latter is in clear contrast with the $\Delta F1388$ mutant that does not show a major difference in the steady-state protein level when compared with the SUR1 wild type (Fig.

10).

The inactivation of the RKR retention signal on the SUR1 $\Delta F790$ channels ($\Delta F790_{AAA}$) allows them to achieve a cell surface expression level similar to the wild type channels and correlates with a significant increase in the $\Delta F790_{AAA}$ steady-state protein level (Fig. 27C). This suggests that once the $\Delta F790_{AAA}$ mutant channels have left the ER they are no longer targeted for rapid degradation (Fig. 27C). Moreover, the $\Delta F790_{AAA}$ channel export out of the ER seems to be more efficient than the wild type channel since almost all $\Delta F790_{AAA}$ appears as a mature band.

Although the $\Delta F790$ channel biogenesis seems to show clear differences with the wild type channel biogenesis, when $\Delta F790$ mutant channels are expressed at the cell surface they do not show differences on their MgADP response when compared with the MgADP response of the wild type channels (Fig. 27D).

These results suggest that SUR1-NBF1, as well as SUR1-NBF2, show dissociation between trafficking competence and functional competence. Moreover, mutations on either the SUR1-NBF1 or the SUR1-NBF2 seem to be recognized differentially by the QC system. Consequently, the NBF1 $\Delta F790$ mutant appears to be rapidly degraded probably by ERAD since its steady-state protein level is significantly lower than SUR1 wild type. However, the $\Delta F790$ protein expression is significantly increased when its RKR signal is inactivated — $\Delta F790_{AAA}$, and is able to leave the ER. This suggests that the exposed RKR signal may play a key role in the recognition and retention of unfolded or misfolded K_{ATP} channel subunits (Fig. 27C). Furthermore, the RKR signal may be involved in targeting K_{ATP} channel subunits to ERAD through its interaction with proteins of the QC system.

REFERENCES

1. Ashcroft, F.M., D.E. Harrison, and S.J. Ashcroft, *Glucose induces closure of single potassium channels in isolated rat pancreatic beta-cells*. *Nature*, 1984. **312**(5993): p. 446-8.
2. Cook, D.L. and C.N. Hales, *Intracellular ATP directly blocks K⁺ channels in pancreatic B-cells*. *Nature*, 1984. **311**(5983): p. 271-3.
3. Ashcroft, F.M., *Adenosine 5'-triphosphate-sensitive potassium channels*. *Annu Rev Neurosci*, 1988. **11**: p. 97-118.
4. Babenko, A.P., L. Aguilar-Bryan, and J. Bryan, *A view of sur/KIR6.X, KATP channels*. *Annu Rev Physiol*, 1998. **60**: p. 667-87.
5. Aguilar-Bryan, L., et al., *Toward understanding the assembly and structure of KATP channels*. *Physiol Rev*, 1998. **78**(1): p. 227-45.
6. Aguilar-Bryan, L. and J. Bryan, *Molecular biology of adenosine triphosphate-sensitive potassium channels*. *Endocr Rev*, 1999. **20**(2): p. 101-35.
7. Seino, S., *ATP-sensitive potassium channels: a model of heteromultimeric potassium channel/receptor assemblies*. *Annu Rev Physiol*, 1999. **61**: p. 337-62.
8. Inagaki, N., et al., *Cloning and functional characterization of a novel ATP-sensitive potassium channel ubiquitously expressed in rat tissues, including pancreatic islets, pituitary, skeletal muscle, and heart*. *J Biol Chem*, 1995. **270**(11): p. 5691-4.
9. Aguilar-Bryan, L., et al., *Cloning of the beta cell high-affinity sulfonylurea receptor: a regulator of insulin secretion*. *Science*, 1995. **268**(5209): p. 423-6.
10. Inagaki, N., et al., *A family of sulfonylurea receptors determines the pharmacological properties of ATP-sensitive K⁺ channels*. *Neuron*, 1996. **16**(5): p. 1011-7.
11. Isomoto, S., et al., *A novel sulfonylurea receptor forms with BIR (Kir6.2) a smooth muscle type ATP-sensitive K⁺ channel*. *J Biol Chem*, 1996. **271**(40): p. 24321-4.
12. Zerangue, N., et al., *A new ER trafficking signal regulates the subunit stoichiometry of plasma membrane K(ATP) channels*. *Neuron*, 1999. **22**(3): p. 537-48.
13. Jan, L.Y. and Y.N. Jan, *Cloned potassium channels from eukaryotes and prokaryotes*. *Annu Rev Neurosci*, 1997. **20**: p. 91-123.
14. Bichet, D., F.A. Haass, and L.Y. Jan, *Merging functional studies with structures of inward-rectifier K(+) channels*. *Nat Rev Neurosci*, 2003. **4**(12): p. 957-67.
15. Inagaki, N., et al., *Reconstitution of IKATP: an inward rectifier subunit plus the sulfonylurea receptor*. *Science*, 1995. **270**(5239): p. 1166-70.
16. Kuo, A., et al., *Crystal structure of the potassium channel KirBac1.1 in the closed state*. *Science*, 2003. **300**(5627): p. 1922-6.
17. Nishida, M. and R. MacKinnon, *Structural Basis of Inward Rectification. Cytoplasmic Pore of the G Protein-Gated Inward Rectifier GIRK1 at 1.8 Å Resolution*. *Cell*, 2002. **111**(7): p. 957-65.

18. Doyle D., C.J., Pfuetzner R., Kuo A., Gulbis JM., Cohen S., Chait B., Mackinnon R., *The structure of the Potassium Channel: Molecular Basis of K⁺ Conduction and Selectivity*. Science, 1998. **280**: p. 69-77.
19. Enkvetchakul, D., et al., *The kinetic and physical basis of K(ATP) channel gating: toward a unified molecular understanding*. Biophys J, 2000. **78**(5): p. 2334-48.
20. S., C., *Potassium channel structures*. Nature Rev. Neurosci., 2002. **3**: p. 115-121.
21. Yang, J., et al., *Stabilization of ion selectivity filter by pore loop ion pairs in an inwardly rectifying potassium channel*. Proc Natl Acad Sci U S A, 1997. **94**(4): p. 1568-72.
22. Higgins, C.F., *The ABC of channel regulation*. Cell, 1995. **82**(5): p. 693-6.
23. Conti, L.R., et al., *Transmembrane topology of the sulfonylurea receptor SUR1*. J Biol Chem, 2001. **276**(44): p. 41270-8.
24. Clement, J.P.t., et al., *Association and stoichiometry of K(ATP) channel subunits*. Neuron, 1997. **18**(5): p. 827-38.
25. Schwappach, B., et al., *Molecular basis for K(ATP) assembly: transmembrane interactions mediate association of a K⁺ channel with an ABC transporter*. Neuron, 2000. **26**(1): p. 155-67.
26. Chan, K.W., H. Zhang, and D.E. Logothetis, *N-terminal transmembrane domain of the SUR controls trafficking and gating of Kir6 channel subunits*. Embo J, 2003. **22**(15): p. 3833-43.
27. Ashcroft, F.M. and F.M. Gribble, *Correlating structure and function in ATP-sensitive K⁺ channels*. Trends Neurosci, 1998. **21**(7): p. 288-94.
28. Tucker, S.J., et al., *Truncation of Kir6.2 produces ATP-sensitive K⁺ channels in the absence of the sulphonylurea receptor*. Nature, 1997. **387**(6629): p. 179-83.
29. Tucker, S.J. and F.M. Ashcroft, *A touching case of channel regulation: the ATP-sensitive K⁺ channel*. Curr Opin Neurobiol, 1998. **8**(3): p. 316-20.
30. Trapp, S., et al., *Identification of residues contributing to the ATP binding site of Kir6.2*. Embo J, 2003. **22**(12): p. 2903-12.
31. Tucker, S.J. and F.M. Ashcroft, *Mapping of the physical interaction between the intracellular domains of an inwardly rectifying potassium channel, Kir6.2*. J Biol Chem, 1999. **274**(47): p. 33393-7.
32. Tucker, S.J., et al., *Molecular determinants of KATP channel inhibition by ATP*. Embo J, 1998. **17**(12): p. 3290-6.
33. Proks, P., et al., *Involvement of the N-terminus of Kir6.2 in the inhibition of the KATP channel by ATP*. J Physiol, 1999. **514**(Pt 1): p. 19-25.
34. Reimann, F., et al., *The role of lysine 185 in the kir6.2 subunit of the ATP-sensitive channel in channel inhibition by ATP*. J Physiol, 1999. **520**(Pt 3): p. 661-9.
35. Li, L., J. Wang, and P. Drain, *The I182 region of k(ir)6.2 is closely associated with ligand binding in K(ATP) channel inhibition by ATP*. Biophys J, 2000. **79**(2): p. 841-52.
36. Drain, P., L. Li, and J. Wang, *KATP channel inhibition by ATP requires distinct functional domains of the cytoplasmic C terminus of the pore-forming subunit*. Proc Natl Acad Sci U S A, 1998. **95**(23): p. 13953-8.

37. Trapp , S.H.S., Jones P., Samson M., and Ashcroft F., *Identification of residues contributing to the ATP binding site of Kir6.2*. EMBO J, 2003. **22**(12): p. 2903-2912.
38. Shyng, S.L., et al., *Structural determinants of PIP(2) regulation of inward rectifier K(ATP) channels*. J Gen Physiol, 2000. **116**(5): p. 599-608.
39. MacGregor, G.G., et al., *Nucleotides and phospholipids compete for binding to the C terminus of KATP channels*. Proc Natl Acad Sci U S A, 2002. **99**(5): p. 2726-31.
40. Baukrowitz, T.a.F.B., *KATP channels gated by intracellular nucleotides and phospholipids*. Eur. J. Biochem., 2000. **267**: p. 5842-5848.
41. Baukrowitz, T. and B. Fakler, *K(ATP) channels: linker between phospholipid metabolism and excitability*. Biochem Pharmacol, 2000. **60**(6): p. 735-40.
42. Hilgemann, D.W., S. Feng, and C. Nasuhoglu, *The complex and intriguing lives of PIP2 with ion channels and transporters*. Sci STKE, 2001. **2001**(111): p. RE19.
43. Shyng, S.L. and C.G. Nichols, *Membrane phospholipid control of nucleotide sensitivity of KATP channels*. Science, 1998. **282**(5391): p. 1138-41.
44. Baukrowitz, T., et al., *PIP2 and PIP as determinants for ATP inhibition of KATP channels*. Science, 1998. **282**(5391): p. 1141-4.
45. Ashcroft, F.M., *Exciting times for PIP2*. Science, 1998. **282**(5391): p. 1059-60.
46. Shyng, S.L., et al., *Modulation of nucleotide sensitivity of ATP-sensitive potassium channels by phosphatidylinositol-4-phosphate 5-kinase*. Proc Natl Acad Sci U S A, 2000. **97**(2): p. 937-41.
47. Cukras C., J.I.a.N.C., *Structural and Functional Determinants of Conserved Lipid Interaction Domains of Inward Rectifying Kir6.2 Channels*. J. Gen. Physiol., 2002. **119**: p. 581-591.
48. Cukras, C., Jeliaskova I. and Nichols CG, *The Role of NH₂-terminal Positive Charges in the Activity of Inward Rectifier K_{ATP} Channels*. J. Gen. Physiol., 2002. **120**: p. 437-446.
49. Gribble, F.M., S.J. Tucker, and F.M. Ashcroft, *The essential role of the Walker A motifs of SUR1 in K-ATP channel activation by Mg-ADP and diazoxide*. Embo J, 1997. **16**(6): p. 1145-52.
50. Matsuo, M., et al., *Mutations in the linker domain of NBD2 of SUR inhibit transduction but not nucleotide binding*. Embo J, 2002. **21**(16): p. 4250-8.
51. Shyng, S., T. Ferrigni, and C.G. Nichols, *Regulation of KATP channel activity by diazoxide and MgADP. Distinct functions of the two nucleotide binding folds of the sulfonylurea receptor*. J Gen Physiol, 1997. **110**(6): p. 643-54.
52. Matsuo, M., et al., *Functional analysis of a mutant sulfonylurea receptor, SUR1-R1420C, that is responsible for persistent hyperinsulinemic hypoglycemia of infancy*. J Biol Chem, 2000. **275**(52): p. 41184-91.
53. Matsuo, M., et al., *Different binding properties and affinities for ATP and ADP among sulfonylurea receptor subtypes, SUR1, SUR2A, and SUR2B*. J Biol Chem, 2000. **275**(37): p. 28757-63.
54. Matsuo, M., et al., *ATP Binding Properties of the Nucleotide-binding Folds of SUR1*. J. Biol. Chem., 1999. **274**(52): p. 37479-37482.

55. Ueda, K., N. Inagaki, and S. Seino, *MgADP antagonism to Mg²⁺-independent ATP binding of the sulfonylurea receptor SUR1*. *J Biol Chem*, 1997. **272**(37): p. 22983-6.
56. Ueda, K., et al., *Cooperative binding of ATP and MgADP in the sulfonylurea receptor is modulated by glibenclamide*. *Proc Natl Acad Sci U S A*, 1999. **96**(4): p. 1268-72.
57. Ueda, K., et al., *Comparative aspects of the function and mechanism of SUR1 and MDR1 proteins*. *Biochim Biophys Acta*, 1999. **1461**(2): p. 305-13.
58. Zingman, L.V., et al., *Tandem function of nucleotide binding domains confers competence to sulfonylurea receptor in gating ATP-sensitive K⁺ channels*. *J Biol Chem*, 2002. **277**(16): p. 14206-10.
59. Zingman, L.V., et al., *Signaling in channel/enzyme multimers: ATPase transitions in SUR module gate ATP-sensitive K⁺ conductance*. *Neuron*, 2001. **31**(2): p. 233-45.
60. Bienengraeber, M., et al., *ATPase activity of the sulfonylurea receptor: a catalytic function for the K(ATP) channel complex*. *Faseb J*, 2000. **14**(13): p. 1943-52.
61. Carrasco, A.J., et al., *Adenylate kinase phosphotransfer communicates cellular energetic signals to ATP-sensitive potassium channels*. *Proc Natl Acad Sci U S A*, 2001. **98**(13): p. 7623-8.
62. Crawford, R.M., et al., *Creatine kinase is physically associated with the cardiac ATP-sensitive K⁺ channel in vivo*. *Faseb J*, 2002. **16**(1): p. 102-4.
63. Dzeja, P.P. and A. Terzic, *Phosphotransfer networks and cellular energetics*. *J Exp Biol*, 2003. **206**(Pt 12): p. 2039-47.
64. Proks, P., et al., *Sulfonylurea stimulation of insulin secretion*. *Diabetes*, 2002. **51 Suppl 3**: p. S368-76.
65. Bryan, J. and L. Aguilar-Bryan, *Sulfonylurea receptors: ABC transporters that regulate ATP-sensitive K(+) channels*. *Biochim Biophys Acta*, 1999. **1461**(2): p. 285-303.
66. Ashfield, R., et al., *Identification of the high-affinity tolbutamide site on the SUR1 subunit of the K(ATP) channel*. *Diabetes*, 1999. **48**(6): p. 1341-7.
67. Babenko, A.P., G. Gonzalez, and J. Bryan, *The tolbutamide site of SUR1 and a mechanism for its functional coupling to K(ATP) channel closure*. *FEBS Lett*, 1999. **459**(3): p. 367-76.
68. Hambrook, A., et al., *ATP-Sensitive K⁺ channel modulator binding to sulfonylurea receptors SUR2A and SUR2B: opposite effects of MgADP*. *Mol Pharmacol*, 1999. **55**(5): p. 832-40.
69. Ashcroft, F.M. and F.M. Gribble, *New windows on the mechanism of action of K(ATP) channel openers*. *Trends Pharmacol Sci*, 2000. **21**(11): p. 439-45.
70. Gribble, F.M. and F. Reimann, *Pharmacological modulation of K(ATP) channels*. *Biochem Soc Trans*, 2002. **30**(2): p. 333-9.
71. Schwanstecher, M., et al., *Potassium channel openers require ATP to bind to and act through sulfonylurea receptors*. *EMBO Journal*, 1998. **17**(19): p. 5529-35.
72. Uhde, I., et al., *Identification of the potassium channel opener site on sulfonylurea receptors*. *J Biol Chem*, 1999. **274**(40): p. 28079-82.
73. Babenko, A.P., G. Gonzalez, and J. Bryan, *Pharmaco-topology of sulfonylurea receptors. Separate domains of the regulatory subunits of K(ATP) channel*

- isoforms are required for selective interaction with K(+) channel openers.* J Biol Chem, 2000. **275**(2): p. 717-20.
74. Moreau, C., et al., *The molecular basis of the specificity of action of K(ATP) channel openers.* Embo J, 2000. **19**(24): p. 6644-51.
 75. Huopio, H., et al., *K(ATP) channels and insulin secretion disorders.* Am J Physiol Endocrinol Metab, 2002. **283**(2): p. E207-16.
 76. Nichols, C.G., et al., *Adenosine diphosphate as an intracellular regulator of insulin secretion.* Science, 1996. **272**(5269): p. 1785-7.
 77. Thomas, P., Y. Ye , and L. E., *Mutations of the pancreatic islet inward rectifier also lead to familial persistent hyperinsulinemic hypoglycemia of infancy.* Hum. Mol. Genet., 1996. **5**: p. 1809-1812.
 78. Nestorowicz, A., et al., *A nonsense mutation in the inward rectifier potassium channel gene, Kir6.2, is associated with familial hyperinsulinism.* Diabetes, 1997. **46**(11): p. 1743-8.
 79. Thomas, P.M., et al., *Mutations in the sulfonylurea receptor gene in familial persistent hyperinsulinemic hypoglycemia of infancy.* Science, 1995. **268**(5209): p. 426-9.
 80. Sakura, H., et al., *Altered functional properties of KATP channel conferred by a novel splice variant of SUR1.* J Physiol, 1999. **521 Pt 2**: p. 337-50.
 81. Miki, T., et al., *Abnormalities of pancreatic islets by targeted expression of a dominant-negative KATP channel.* Proc Natl Acad Sci U S A, 1997. **94**(22): p. 11969-73.
 82. Miki, T., et al., *Defective insulin secretion and enhanced insulin action in KATP channel-deficient mice.* Proc Natl Acad Sci U S A, 1998. **95**(18): p. 10402-6.
 83. Seghers, V., et al., *Sur1 knockout mice. A model for K(ATP) channel-independent regulation of insulin secretion.* J Biol Chem, 2000. **275**(13): p. 9270-7.
 84. Nestorowicz, A., et al., *Mutations in the sulfonylurea receptor gene are associated with familial hyperinsulinism in Ashkenazi Jews.* Hum Mol Genet, 1996. **5**(11): p. 1813-22.
 85. Cheng, S.H., et al., *Defective intracellular transport and processing of CFTR is the molecular basis of most cystic fibrosis.* Cell, 1990. **63**(4): p. 827-34.
 86. Ward, C.L. and R.R. Kopito, *Intracellular turnover of cystic fibrosis transmembrane conductance regulator. Inefficient processing and rapid degradation of wild-type and mutant proteins.* J Biol Chem, 1994. **269**(41): p. 25710-8.
 87. Ward, C.L., S. Omura, and R.R. Kopito, *Degradation of CFTR by the ubiquitin-proteasome pathway.* Cell, 1995. **83**(1): p. 121-7.
 88. Ellgaard , L., Helenius , A., *Quality Control in the Endoplasmic Reticulum.* Nature Rev. Mol.Cell Biol., 2003. **4**: p. 181-191.
 89. Ellgaard L, M.M., Helenius A, *Setting the Standards: Quality Control in the Secretory Pathway.* Science, 1999. **286**: p. 1882-1888.
 90. Wickner S., M.M., Gottesman S., *Posttranslational Quality Control: Folding, Refolding, and Degrading Proteins.* Science, 1999. **286**: p. 1888-1893.
 91. Tsai , B.Y.Y.a.R.T., *Retro-translocation of Proteins from the Endoplasmic Reticulum into the Cytosol.* Nat.Rev. Mol Cell Bio., 2002. **3**: p. 246-255.

92. Jarosch, E.G.-F.R., Meusser B., Walter J., and Sommer T., *Protein Dislocation from the Endoplasmic Reticulum- Pulling Out the Suspect*. Traffic, 2002. **3**: p. 530-536.
93. Kostova, Z.a.W.D., *For whom the bell tolls: protein quality control of the endoplasmic reticulum and the ubiquitin-proteasome connection*. EMBO J, 2003. **22**(10): p. 2309-2317.
94. Green, N.W., *Ion Channel Assembly: Creating Structures that Function*. J. Gen. Physiol., 1999. **113**: p. 163-169.
95. Wanamaker, C.C., J.; Green W., *Regulation of Nicotinic Acetylcholine Receptor Assembly*. Ann N Y Acad Sci., 2003. **998**: p. 66-80.
96. Kopito, R.R., *Biosynthesis and degradation of CFTR*. Physiol Rev, 1999. **79**(1 Suppl): p. S167-73.
97. Kopito, R.R., *ER quality control: the cytoplasmic connection*. Cell, 1997. **88**(4): p. 427-30.
98. Ma, D. and L.Y. Jan, *ER transport signals and trafficking of potassium channels and receptors*. Curr Opin Neurobiol, 2002. **12**(3): p. 287-92.
99. Zerangue, N., et al., *Analysis of endoplasmic reticulum trafficking signals by combinatorial screening in mammalian cells*. Proc Natl Acad Sci U S A, 2001. **98**(5): p. 2431-6.
100. Teasdale R., J.M., *Signal-Mediated Sorting of Membrane Proteins Between the Endoplasmic Reticulum and the Golgi Apparatus*. Ann Rev.Cell Dev. Biol., 1996. **12**: p. 27-54.
101. Nufer O., G.S., DEgen M., Kappeler F., Paccaud J-P., Tani K. and Hauri H-P., *Role of cytoplasmic C-terminal amino acids of membrane proteins in ER export*. Journ of Cell Science, 2001. **115**: p. 619-628.
102. Yuan, H., K. Michelsen, and B. Schwappach, *14-3-3 dimers probe the assembly status of multimeric membrane proteins*. Curr Biol, 2003. **13**(8): p. 638-46.
103. O'Kelly, I., et al., *Forward transport. 14-3-3 binding overcomes retention in endoplasmic reticulum by dibasic signals*. Cell, 2002. **111**(4): p. 577-88.
104. Margenta-Mitrovic M., J.Y.-N., Jan LY, *A Trafficking Checkpoint Controls GABA_B Receptor Heterodimerization*. Neuron, 2000. **27**: p. 97-106.
105. Standley, S.R.K., McCallum J., Sans N., and Wenthold, *PDZ Domain Suppression of an ER Retention Signal in NMDA Receptor NR1 Splice Variants*. Neuron, 2000. **28**: p. 887-898.
106. Scott, D.B., et al., *An NMDA receptor ER retention signal regulated by phosphorylation and alternative splicing*. J Neurosci, 2001. **21**(9): p. 3063-72.
107. Chang, H.Y., *The involvement of ATP-sensitive potassium channels in beta 2-adrenoceptor agonist-induced vasodilatation on rat diaphragmatic microcirculation*. Br J Pharmacol, 1997. **121**(5): p. 1024-30.
108. Bichet, D., Cornet V., Geib S., Carlier D., Volsen S., Toshi H., Mori Y., De Waard M, *The I-II Loop of the Ca²⁺ Channel $\alpha 1$ Subunit Contains an Endoplasmic Reticulum Retention Signal Antagonized by the β subunit*. Neuron, 2000. **25**: p. 177-190.
109. Greger I., K.L., Ziff E, *RNA Editing at Arg607 Controls AMPA Receptor Exit from the Endoplasmic Reticulum*. Neuron, 2002. **34**: p. 759-772.

110. Greger I., K.L., Kong X., Ziff E, *AMPA Receptor Tetramerization is mediated by Q/R editing*. *Neuron*, 2003. **40**: p. 763-774.
111. Ren Z., R.N., Garcia E., Sanders J., Swanson G. and Marshall J., *Multiple Trafficking Signals Regulate Kainate Receptor KA2 Subunit Surface Expression*. *J. Neuroscience*, 2003. **23**(16): p. 6608-6616.
112. Yan S., S.J., Xu J., Zhu Y., Contractor A., and Swanson G., *A C-terminal Determinant of GluR6 Kainate Receptor Trafficking*. *J. Neuroscience*, 2004. **24**(3): p. 679-691.
113. Ren Z, R.N., Needleman LA, Sanders JM, Swanson GT, Marshall J., *Cell surface expression of GluR5 kainate receptors is regulated by an endoplasmic reticulum retention signal*. *J. Biol. Chem.*, 2003. **278**(52): p. 52700-9.
114. Wang , J.-M.Z.L., Yao Y., Viroonchatapan N., Rothe E. and Wang Z-Z, *A transmembrane motif governs the surface trafficking of nicotinic acetylcholine receptors*. *Nature Neuroscience*, 2002. **5**(10): p. 963-970.
115. Barlowe, C., *Traffic COPs of the Early Secretory Pathway*. *Traffic*, 2000. **1**: p. 371-377.
116. Barlowe, C., *COPII- dependent transport from the endoplasmic reticulum*. *Curr.Opin. in Cell Biol.*, 2002. **14**: p. 417-422.
117. Barlowe, C., *Signals for COPII-dependent export from the ER: what's the ticket out?* *Trends Cell Biol*, 2003. **13**(6): p. 295-300.
118. Kirchhausen, T., *Three ways to make a vesicle*. *Nat Reviews Molec.Cell Biol.*, 2000. **1**(Dec).
119. Gorelick F., S.C., *Exiting the endoplasmic reticulum*. *Mol. Cell. Endocrinol.*, 2001. **177**: p. 13-18.
120. Nishimura, N. and W.E. Balch, *A Di-Acidic Signal Required for Selective Export from the Endoplasmic Reticulum*. *Science*, 1997. **277**: p. 556-558.
121. Ma, D., et al., *Diverse trafficking patterns due to multiple traffic motifs in G protein-activated inwardly rectifying potassium channels from brain and heart*. *Neuron*, 2002. **33**(5): p. 715-29.
122. Ma, D., et al., *Role of ER export signals in controlling surface potassium channel numbers*. *Science*, 2001. **291**(5502): p. 316-9.
123. Sharma, N., et al., *The C terminus of SUR1 is required for trafficking of KATP channels*. *J Biol Chem*, 1999. **274**(29): p. 20628-32.
124. Mu, Y., et al., *Activity-dependent mRNA splicing controls ER export and synaptic delivery of NMDA receptors*. *Neuron*, 2003. **40**(3): p. 581-94.
125. Manganas LN., W.Q., Scannevin RH.,Antonucci DE., Rhodes K.,and Trimmer J., *Identification of trafficking determinant localized to the Kv1 channel pore*. *Proc Natl Acad Sci U S A*, 2001. **98**(24): p. 14055-14059.
126. Li , D., K. Takimoto, and E.S. Levitan, *Surface Expression of Kv1 Channels Is Governed by a C-terminal Motif*. *J. Biol. Chem.*, 2000. **275**(16): p. 11597-11602.
127. Scott, D.B., T.A. Blanpied, and M.D. Ehlers, *Coordinated PKA and PKC phosphorylation suppresses RXR-mediated ER retention and regulates the surface delivery of NMDA receptors*. *Neuropharmacology*, 2003. **45**(6): p. 755-67.
128. Kowalski, J., et al., *Protein folding stability can determine the efficiency of scape from endoplasmic quality control*. *J. Biol. Chem.*, 1998. **273**: p. 19453-19458.

129. Zhang, F., N. Kartner, and G. Lukacs, *Limited proteolysis as a proeb for arrested conformational maturation of $\Delta F508$ CFTR*. *Nature Struct. Biol.*, 1998. **5**(3): p. 180-183.
130. Schubert, U.A., L. Gibbs, J. Norbury C., Yewdell J., Bennink J, *Rapid degradation of a large fraction of newly synthesized proteins by proteasomes*. *Nature*, 2000. **404**: p. 770-774.
131. Shi G., N.K., Hammond S., Rhodes K., Schechter L. and Trimmer J., *β subunits promote K^+ channel surface expression through effects early in biosynthesis*. *Neuron*, 1996. **16**: p. 843-852.
132. Lukacs, G., et al., *Conformational Maturation of CFTR but not its mutant counterpart ($\Delta F508$) occurs in the endoplasmic reticulum and requires ATP*. *Embo J*, 1994. **13**: p. 6076-6086.
133. Petaja-Repo, U.H., M. Lapierriere, Bahlla S., A. Walker, P. and and B. M., *Newly Synthesized Human δ Opiod Receptors Retained in the Endoplasmic Reticulum Are Retrotranslocated to the Cytosol, Deglycosylated, Ubiquitinated, and Degraded by the Proteasome*. *J. Biol. Chem.*, 2001. **276**(6): p. 4416-4423.
134. Petaja-Repo, U.E., et al., *Ligands act as pharmacological chaperones and increase the efficiency of delta opioid receptor maturation*. *Embo J*, 2002. **21**(7): p. 1628-37.
135. Petaja-Repo, U., et al., *Export from the endoplasmic reticulum represents the limiting step in the maturation and cell surface expression on the human δ opioid receptor*. *J. Biol. Chem.*, 2000. **275**: p. 13727-13736.
136. Huh, K.-H. and R. Wenthold, *Turover Analysis of Glutamate Receptors Identifies a Rapidly Degraded Pool of the N-Methyl-D-Aspartate Receptor Subunit, NR1, in Cultured Cerebellar Granule Cells*. *J. Biol. Chem.*, 1999. **274**(1): p. 151-157.
137. Bonifacino, J.S. and A.M. Weissman, *Ubiquitin and the control of protein fate in the secretory and endocytic pathways*. *Annu Rev Cell Dev Biol*, 1998. **14**: p. 19-57.
138. Johnston, J.A., C.L. Ward, and R.R. Kopito, *Aggresomes: a cellular response to misfolded proteins*. *J Cell Biol*, 1998. **143**(7): p. 1883-98.
139. Musil, L.S., et al., *Regulation of connexin degradation as a mechanism to increase gap junction assembly and function*. *J Biol Chem*, 2000. **275**(33): p. 25207-15.
140. Leithch, V., P. Agre, and L. King, *Altered ubiquitination and stability of aquaporin-1 in hypertonic stress*. *Proc Natl Acad Sci U S A*, 2001. **98**: p. 2894-2898.
141. Ashcroft, S.J. and F.M. Ashcroft, *Properties and functions of ATP-sensitive K-channels*. *Cell Signal*, 1990. **2**(3): p. 197-214.
142. Nichols, C.G. and W.J. Lederer, *Adenosine triphosphate-sensitive potassium channels in the cardiovascular system*. *Am J Physiol*, 1991. **261**(6 Pt 2): p. H1675-86.
143. Terzic, A., A. Jahangir, and Y. Kurachi, *Cardiac ATP-sensitive K^+ channels: regulation by intracellular nucleotides and K^+ channel-opening drugs*. *Am J Physiol*, 1995. **269**(3 Pt 1): p. C525-45.
144. Inagaki, N., T. Gono, and S. Seino, *Subunit stoichiometry of the pancreatic beta-cell ATP-sensitive K^+ channel*. *FEBS Lett*, 1997. **409**(2): p. 232-6.

145. Shyng, S. and C.G. Nichols, *Octameric stoichiometry of the KATP channel complex*. J Gen Physiol, 1997. **110**(6): p. 655-64.
146. Dunne, M.J. and O.H. Petersen, *Intracellular ADP activates K⁺ channels that are inhibited by ATP in an insulin-secreting cell line*. FEBS Lett, 1986. **208**(1): p. 59-62.
147. Aynsley-Green, A., et al., *Nesidioblastosis of the pancreas: definition of the syndrome and the management of the severe neonatal hyperinsulinaemic hypoglycaemia*. Arch Dis Child, 1981. **56**(7): p. 496-508.
148. Landau, H., and M. Schiller, eds., *Pediatric Surgery of the Liver, Pancreas and Spleen*. (Saunders, Philadelphia), 1991: p. 187-201.
149. Permutt, M.A., et al., *Genetics of type II diabetes*. Recent Prog Horm Res, 1998. **53**: p. 201-16.
150. Sharma, N., et al., *Familial hyperinsulinism and pancreatic beta-cell ATP-sensitive potassium channels*. Kidney Int, 2000. **57**(3): p. 803-8.
151. Dunne, M.J., et al., *Familial persistent hyperinsulinemic hypoglycemia of infancy and mutations in the sulfonylurea receptor*. New England Journal of Medicine, 1997. **336**(10): p. 703-6.
152. Shyng, S.L., et al., *Functional analyses of novel mutations in the sulfonylurea receptor 1 associated with persistent hyperinsulinemic hypoglycemia of infancy*. Diabetes, 1998. **47**(7): p. 1145-51.
153. Kane, C., et al., *Loss of functional KATP channels in pancreatic beta-cells causes persistent hyperinsulinemic hypoglycemia of infancy*. Nat Med, 1996. **2**(12): p. 1344-7.
154. Nestorowicz, A., et al., *Genetic heterogeneity in familial hyperinsulinism*. Hum Mol Genet, 1998. **7**(7): p. 1119-28.
155. Tusnady, G.E., et al., *Membrane topology distinguishes a subfamily of the ATP-binding cassette (ABC) transporters*. FEBS Lett, 1997. **402**(1): p. 1-3.
156. Raab-Graham, K.F., et al., *Membrane topology of the amino-terminal region of the sulfonylurea receptor*. J Biol Chem, 1999. **274**(41): p. 29122-9.
157. Chang X-B., C.L., Hou Y-X., Jensen T., Aleksandrov AA., Mengos A., and Riordan J, *Removal of Multiple Arginine-Framed Trafficking Signals Overcomes Misprocessing of $\Delta F508$ CFTR Present in Most Patients with Cystic Fibrosis*. Molecular Cell, 1999. **4**: p. 137-142.
158. Shyng, S., T. Ferrigni, and C.G. Nichols, *Control of rectification and gating of cloned KATP channels by the Kir6.2 subunit*. J Gen Physiol, 1997. **110**(2): p. 141-53.
159. Zhou, Z., et al., *Properties of HERG channels stably expressed in HEK 293 cells studied at physiological temperature*. Biophys J, 1998. **74**(1): p. 230-41.
160. Denning GM, A.M., Amara JF, Marshall J, Smith AE, Welsh MJ., *Processing of mutant cystic fibrosis transmembrane conductance regulator is temperature-sensitive*. Nature, 1992. **358**.
161. Qu, B.H., E. Strickland, and P.J. Thomas, *Cystic fibrosis: a disease of altered protein folding*. J Bioenerg Biomembr, 1997. **29**(5): p. 483-90.
162. Jensen TJ, L.M., Pind S, Williams DB, Goldberg AL, Riordan JR., *Multiple proteolytic systems, including the proteasome, contribute to CFTR processing*. Cell, 1995. **83**(1): p. 129-35.

163. Sato, S., C.L. Ward, and R.R. Kopito, *Cotranslational ubiquitination of cystic fibrosis transmembrane conductance regulator in vitro*. J Biol Chem, 1998. **273**(13): p. 7189-92.
164. Loo, T.W. and D.M. Clarke, *Drug-stimulated ATPase activity of human P-glycoprotein requires movement between transmembrane segments 6 and 12*. J Biol Chem, 1997. **272**(34): p. 20986-9.
165. Brown CR, H.-B.L., Biwersi J, Verkman AS, Welch WJ., *Chemical chaperones correct the mutant phenotype of the delta F508 cystic fibrosis transmembrane conductance regulator protein*. Cell Stress Chaperones, 1996. **1**(2): p. 109-15.
166. Zhou, Z., et al., *Block of HERG potassium channels by the antihistamine astemizole and its metabolites desmethylastemizole and norastemizole*. J Cardiovasc Electrophysiol, 1999. **10**(6): p. 836-43.
167. Dalemans W, B.P., Champigny G, Jallat S, Dott K, Dreyer D, Crystal RG, Pavirani A, Lecocq JP, Lazdunski M., *Altered chloride ion channel kinetics associated with the delta F508 cystic fibrosis mutation*. Nature, 1991. **354**: p. 503-4.
168. Chutkow, W.A., et al., *Cloning, tissue expression, and chromosomal localization of SUR2, the putative drug-binding subunit of cardiac, skeletal muscle, and vascular KATP channels*. Diabetes, 1996. **45**(10): p. 1439-45.
169. Isomoto, S. and Y. Kurachi, *Function, regulation, pharmacology, and molecular structure of ATP-sensitive K⁺ channels in the cardiovascular system*. J Cardiovasc Electrophysiol, 1997. **8**(12): p. 1431-46.
170. Zingman, L.V., et al., *Kir6.2 is required for adaptation to stress*. Proc Natl Acad Sci U S A, 2002. **99**(20): p. 13278-83.
171. Partridge, C.J., D.J. Beech, and A. Sivaprasadarao, *Identification and pharmacological correction of a membrane trafficking defect associated with a mutation in the sulfonylurea receptor causing familial hyperinsulinism*. J Biol Chem, 2001. **276**(38): p. 35947-52.
172. Taschenberger G, M.A., Shen S, Lester LB, LaFranchi S, Shyng SL., *Identification of a familial hyperinsulinism-causing mutation in the sulfonylurea receptor 1 that prevents normal trafficking and function of KATP channels*. J Biol Chem., 2002. **277**(19): p. 17139-46.
173. Cartier, E.A., et al., *Defective trafficking and function of KATP channels caused by a sulfonylurea receptor 1 mutation associated with persistent hyperinsulinemic hypoglycemia of infancy*. Proc Natl Acad Sci U S A, 2001. **98**(5): p. 2882-7.
174. Conti, L.R., C.M. Radeke, and C.A. Vandenberg, *Membrane Targeting of ATP-sensitive Potassium Channel. EFFECTS OF GLYCOSYLATION ON SURFACE EXPRESSION*. J Biol Chem, 2002. **277**(28): p. 25416-22.
175. Quayle, J.M., M.T. Nelson, and N.B. Standen, *ATP-sensitive and inwardly rectifying potassium channels in smooth muscle*. Physiol Rev, 1997. **77**(4): p. 1165-232.
176. D'hahan N., M.C., Prost A-L., Jacquet H., Alekseev A., Terzic A., and Vivandou M., *Pharmacological plasticity of cardiac ATP-sensitive potassium channels toward diazoxide revealed by ADP*. Proc Natl Acad Sci U S A, 1999. **96**(21): p. 12162-12167.

177. Diederichs, K., et al., *Crystal structure of MalK, the ATPase subunit of the trehalose/maltose ABC transporter of the archaeon Thermococcus litoralis*. *Embo J*, 2000. **19**(22): p. 5951-61.
178. Locher, K.P., A.T. Lee, and D.C. Rees, *The E. coli BtuCD structure: a framework for ABC transporter architecture and mechanism*. *Science*, 2002. **296**(5570): p. 1091-8.
179. Yuan, Y.R., et al., *The crystal structure of the MJ0796 ATP-binding cassette. Implications for the structural consequences of ATP hydrolysis in the active site of an ABC transporter*. *J Biol Chem*, 2001. **276**(34): p. 32313-21.
180. Karpowich, N., et al., *Crystal structures of the MJ1267 ATP binding cassette reveal an induced-fit effect at the ATPase active site of an ABC transporter*. *Structure (Camb)*, 2001. **9**(7): p. 571-86.
181. Babenko, A.P., G. Gonzalez, and J. Bryan, *Two regions of sulfonylurea receptor specify the spontaneous bursting and ATP inhibition of KATP channel isoforms*. *J Biol Chem*, 1999. **274**(17): p. 11587-92.
182. Matsuoka, T., et al., *C-terminal tails of sulfonylurea receptors control ADP-induced activation and diazoxide modulation of ATP-sensitive K(+) channels*. *Circ Res*, 2000. **87**(10): p. 873-80.
183. Gribble, F.M., et al., *Properties of cloned ATP-sensitive K+ currents expressed in Xenopus oocytes*. *J Physiol*, 1997. **498**(Pt 1): p. 87-98.
184. Hambrook, A., C. Loffler-Walz, and U. Quast, *Glibenclamide binding to sulphonylurea receptor subtypes: dependence on adenine nucleotides*. *Br J Pharmacol*, 2002. **136**(7): p. 995-1004.
185. D'Hahan, N., et al., *A transmembrane domain of the sulfonylurea receptor mediates activation of ATP-sensitive K(+) channels by K(+) channel openers*. *Mol Pharmacol*, 1999. **56**(2): p. 308-15.
186. D'Hahan, N., et al., *Pharmacological plasticity of cardiac ATP-sensitive potassium channels toward diazoxide revealed by ADP*. *Proc Natl Acad Sci U S A*, 1999. **96**(21): p. 12162-7.
187. Dickinson, K.E., et al., *Nucleotide regulation and characteristics of potassium channel opener binding to skeletal muscle membranes*. *Mol Pharmacol*, 1997. **52**(3): p. 473-81.
188. Reimann, F., F.M. Gribble, and F.M. Ashcroft, *Differential response of K(ATP) channels containing SUR2A or SUR2B subunits to nucleotides and pinacidil*. *Mol Pharmacol*, 2000. **58**(6): p. 1318-25.
189. Aguilar-Bryan, L., J.P.t. Clement, and D.A. Nelson, *Sulfonylurea receptors and ATP-sensitive potassium ion channels*. *Methods Enzymol*, 1998. **292**: p. 732-44.
190. Cartier, E.A., S. Shen, and S.L. Shyng, *Modulation of the trafficking efficiency and functional properties of ATP-sensitive potassium channels through a single amino acid in the sulfonylurea receptor*. *J Biol Chem*, 2003. **278**(9): p. 7081-90.
191. Crane, A. and L. Aguilar-Bryan, *Assembly, maturation, and turnover of KATP channel subunits*. *J Biol Chem*, 2003. **279**(10): p. 9080-9090.
192. Yan, F., et al., *Sulfonylureas correct trafficking defects of ATP-sensitive potassium channels caused by mutations in the sulfonylurea receptor*. *J Biol Chem*, 2004.

193. Loo, T.W. and D.M. Clarke, *Quality control by proteases in the endoplasmic reticulum. Removal of a protease-sensitive site enhances expression of human P-glycoprotein.* J Biol Chem, 1998. **273**(49): p. 32373-6.
194. Shi, S.H., L.Y. Jan, and Y.N. Jan, *Hippocampal neuronal polarity specified by spatially localized mPar3/mPar6 and PI 3-kinase activity.* Cell, 2003. **112**(1): p. 63-75.
195. Minami, Y., Weissman, A., Samuelson, L., Klausner, R., *Building a multichain receptor: Synthesis, degradation, and assembly of the T-cell antigen receptor.* Proc Natl Acad Sci U S A, 1987. **84**: p. 2688-2692.
196. Junn E., L.S., Suhr U., and Mouradian M., *Parkin Accumulation in Aggregates Due to Proteasome Impairment.* J.Biol.Chem., 2002. **277**(49): p. 47870-47877.
197. Herrmann J., M.P.a.S.R., *Out of the ER-outfitters, escorts and guides.* Trends Cell Biol, 1999. **9**: p. 5-7.
198. Meacham G., P.C., Wenyue Z., Younger MJ. and Cyr DM, *The Hsc70 co-chaperone CHIP targets immature CFTR for proteasomal degradation.* Nature Cell Biology, 2000. **3**: p. 100-105.
199. Wang, C., et al., *Compromised ATP binding as a mechanism of phosphoinositide modulation of ATP-sensitive K(+) channels.* FEBS Lett, 2002. **532**(1-2): p. 177-82.